The design of ultrasonic resonators with wide output cross-sections

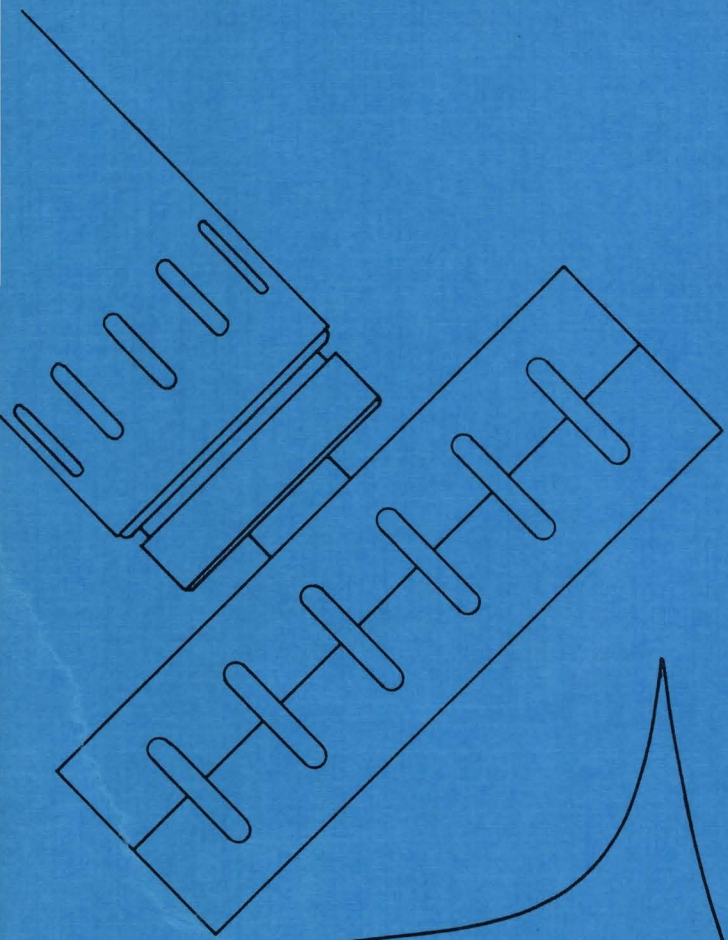

PLLM Derks

THE DESIGN OF ULTRASONIC RESONATORS WITH WIDE OUTPUT CROSS-SECTIONS

THE DESIGN OF ULTRASONIC RESONATORS WITH WIDE OUTPUT CROSS-SECTIONS

PROEFSCHRIFT

ter verkrijging van de graad van doctor in de technische wetenschappen aan de Technische Hogeschool Eindhoven, op gezag van de rector magnificus, prof. dr. S.T.M. Ackermans, voor een commissie aangewezen door het college van dekanen in het openbaar te verdedigen op vrijdag 16 november 1984 te 14.00 uur.

door

PIERRE LOUIS LEONARD MARIE DERKS

geboren te Saint Setiers (Frankrijk)

Dit proefschrift is goedgekeurd door de promotoren

PROF. DR. IR. J.D. JANSSEN

en

PROF. IR. F. DOORSCHOT

Mens agitat molem;
sed vibrantes sententiae
momentum leviunt

CONTENTS

page

LIST OF SYMBOLS

1. INTRODUCTION 1
   1.1 Historical aspects 1
   1.2 Principles of ultrasonic plastic welding equipment 1
   1.3 Aim of the present work 4

2. HALF-WAVELENGTH RESONATORS AND VIBRATION ANALYSIS 7
   2.1 Resonating tools 7
   2.2 Resonator materials 10
   2.3 Vibration analysis 13

3. OBSERVATION ON A RANGE OF RESONATORS 14
   3.1 General design requirements 14
   3.2 Classification of resonator shapes 14
   3.3 Analysis of some resonators 19

4. SURVEY OF PATENT LITERATURE (patents and patent applications) ON RESONATORS WITH WIDE OUTPUT CROSS-SECTIONS 26
   4.1 Introduction 26
   4.2 Design principles 26
   4.3 Influencing the output vibration amplitude 28
   4.4 Coupling of resonators to a multiple resonator system 31
   4.5 Some remarks 34

5. SOLID CYLINDRICAL RESONATORS 35
   5.1 Introduction 35
   5.2 Literature review 35
   5.3 Cylinder dimensions of interest 36
   5.4 Experimental studies of the vibrations of solid cylinders by McMahon (1964) 36
   5.5 Rayleigh's correction to the wave propagation velocity 38
   5.6 Approximate theory for the calculation of the resonance frequency of the longitudinal mode 41
   5.7 Resonance frequency measurement of five cylinders 45
   5.8 The effect of coupling to a transducer and spurious modes 47
   5.9 Amplitude measurements 49
   5.10 Other modes of vibration 53
   5.11 Conclusions 53

6. SOLID RECTANGULAR RESONATORS 54
   6.1 Introduction 54
   6.2 Literature review 54
   6.3 Corrections to the wave-propagation velocity 55
   6.4 Apparent elasticity method 56
   6.5 Resonance conditions according to Stepanenko 59
   6.6 Rayleigh-Ritz method to determine the resonance frequency and mode of vibration 60
   6.7 Dimensioning of rectangular resonators 63

6.8 Comparison with measurements 63
6.9 Conclusions 66

7. OPTIMIZATION OF A RESONATOR: EXPERIMENTALLY AND WITH FINITE ELEMENT ANALYSIS 68
7.1 Introduction 68
7.2 Description of the resonator shape 68
7.3 Optimization on an experimental approach 70
7.4 Finite element analysis 72
7.5 Experimental verification of the computer calculations 74
7.6 Final optimization of the resonator 74
7.7 Conclusions 78

8. A SIMPLIFIED MODEL TO CALCULATE THE RESONANCE CONDITIONS FOR THE LONGITUDINAL VIBRATIONAL MODE IN WIDE RESONATORS 80
8.1 Introduction 80
8.2 The blade-like resonator 82
8.3 The block-like resonator 86
8.4 The cylindrical-type resonator 89
8.5 Conclusions 90

9. FINITE ELEMENT ANALYSIS OF THE EFFECT OF SHAPE VARIATIONS FOR SOME RESONATORS 92
9.1 Introduction 92
9.2 Two types of slots in a blade-like resonator 92
9.3 Finite element analysis 92
9.4 Variation of the slotlength of type A (figure 9.1) 95
9.5 Variation of the slotlength of type B (figure 9.2) 102
9.6 Stress analysis 106
9.7 Conclusions 107

10. MULTIRESONATOR SYSTEM FOR ULTRASONIC PLASTIC ASSEMBLY 109
10.1 Introduction 109
10.2 The funnel shaped resonator 111
10.3 Frequency equation, amplitude gain and shape factor 112
10.4 Dimensioning of funnel-shaped resonators 115
10.5 Experimental verifications 116
10.6 Additional tuning of the resonators 119
10.7 Conclusions 120

SUMMARY 121
SAMENVATTING 123

Appendix 1 : The design of a block-like resonator 126
Appendix 2 : Rayleigh's correction to the wave propagation velocity 132
Appendix 3 : Wide output resonator according to Stepanenko (1979) 135

REFERENCES 136

LIST OF SYMBOLS

a_i	constant number i (chapter 6)	(–)
a_i	constant number i (chapter 10)	
A	area (cross-section)	(m^2)
A_i	constant number i	
b	width	(m)
B	width	(m)
c	wave propagation velocity	(ms^{-1})
c'	corrected value of c	(ms^{-1})
d	diameter, thickness (chapter 6)	(m)
D	diameter	(m)
E	Young's modulus	(Nm^{-2})
E'	apparent elastic modulus (chapter 5 and 6)	(Nm^{-2})
f	frequency	(s^{-1})
F	force	(N)
h	height	(m)
J_0, J_1	Bessel function	(–)
j	$\sqrt{-1}$	(–)
k	wave number	(m^{-1})
K	radius of gyration	(m)
l	length	(m)
L	length	(m)
m	factor (chapter 10)	(m^{-1})
m	degree of wave coupling (chapter 5 and 6)	(–)
M	amplitude gain	(–)
n	order of symmetry (chapter 5)	(–)
n	number of slots	(–)
N	diameter ratio	(–)
P_{loss}	power dissipation	(Nms^{-1})
Q	quality factor	(–)
r	radius	(m)
R	thickness	(m)
s	thickness of bridging element	(m)
t	time	(s)
t	slotwidth	(m)
u, u_e, u_o, $\tilde{u}$	displacement, amplitude	(m)
$\dot{u}$	time derivative of u	(ms^{-1})
U_p	potential energy	(Nm)
U_k	kinetic energy	(Nm)
v	displacement	(m)
V	volume	(m^3)
w, w_e, w_o, $\tilde{w}$	displacement, amplitude	(m)
$\dot{w}$	time derivative of w	(ms^{-1})
x	coordinate	(m)
x	dimension of section (chapter 8)	(m)
y	coordinate	(m)
y	length (chapter 8)	(m)
z	coordinate	(m)
Z	mechanical impedance	(Nsm^{-1})

a	constant (chapter 5)	(–)
a	ratio l/b (chapter 6)	(–)
γ	shear angle	(–)
δ_m	mechanical loss factor	(–)
ϵ	strain	(–)
η	amplitude ratio (chapter 6)	(–)
θ	angle	(–)
λ	wave length	(m)
ν	Poisson's ratio	(–)
ρ	specific mass	($kg\ m^{-3}$)
$\sigma, \bar{\sigma}$	stress	(Nm^{-2})
τ	shear stress	(Nm^{-2})
$\bar{\varphi}$	shape factor (chapter 10)	(–)
ω	angular frequency	(s^{-1})
ω'	corrected value of ω	(s^{-1})

1. INTRODUCTION

1.1. Historical aspects

The high-power uses of ultrasonics are generally believed to be rooted to the invention of sonar in 1917 (Langevin). The spectacular effects of high-power ultrasonics on various processes as first described by Wood and Loomis in 1927, induced many scientific research activities on dispersion, coagulation action, chemical and biological effects and cavitation. Not until 1950 did a burst of activity in high-power ultrasonics, such as cleaning and machining, advance from laboratory phenomena to industrial applications (Graff (1977)). A great breakthrough was made possible by the development of piezo-electrical crystals and of the modern efficient transducer which converts electrical power into mechanical power (the prestressed sandwich transducers). Another major advancement was the use of tapered halfwavelength resonators for the magnification of the amplitude of vibrations of the piezo-electric transducers. The most important applications of high-intensity ultrasonics that came in accelerated development for industrial use since then, are drilling, cleaining, soldering, metal welding and plastic welding.

High-power ultrasonics extend from somewhat above the range of human hearing into the megahertz range. Most industrial applications have an operating frequency between 20 and 60 kHz with power densities at the output surface ranging from a few W/cm^2 to several thousands of W/cm^2. At the output surface the vibrational amplitudes are between 1 and 50 μm (Hulst (1973), Thews (1975)).

Some examples: cleaning is done at 0.5 to 3 W/cm^2, plastic welding at 10 to 50 W/cm^2, drilling at 10 to 100 W/cm^2, and metal welding at 600 to 6000 W/cm^2.

Power ultrasonics has grown in terms of commercial use by the seventies, although it was still mainly restricted to a few processes. Ultrasonic cleaning has become the major application (Graff (1977)). Unheralded by scientific publications ultrasonic plastic welding has become a large-scale industrial process, whereas the considerably researched metallurgical and metal working processes have resulted in little (Shoh (1975); Fitzgerald (1980)).

The basic studies on ultrasonic cleaning were published between 1940 and 1950. With respect to the widespread industrial use nowadays, it is hard to envision any breakthroughs in this field (Shoh (1975)). Basic research on plastic welding has hardly been published until 1970 (Potente (1971)). Since then there appears to be a general lack of interest in academic research on these applications of high power ultrasonics. One of the reasons was that industry lived very well with the stand of technology. It can be observed in the last five years that the continuing technological developments are reaching the boundaries of the potentials of the ultrasonic techniques as they have been available up to now. There is need for more basical understanding of the processes and the operation of the equipment to fulfill the requirements of today.

1.2. Principles of ultrasonic plastic welding equipment

The essential elements of an ultrasonic welding apparatus can be seen in Fig. 1.1. These are: a generator, the welding press, the transducer, the booster and the resonator ("horn" or "sonotrode"). The generator, or power supply, converts electrical energy into mechanical vibratory energy at an ultrasonic frequency by means of piezo-electric

elements, rigidly clamped between two metal parts in a sandwich construction. This type of modern transducer is well described in literature (Hulst (1972); Neppiras (1973); Maropis (1969)). The transducer is driven in a resonance frequency and the vibrations are generated in the length direction. The transducer is designed to vibrate in the fundamental longitudinal mode, the half-wavelength mode ($\lambda/2$) (this mode will be described in chapter 2). The piezo-electric elements are located adjacent the nodal plane where the amplitudes of motion are minimum. For welding applications the amplitudes of vibrations of the transducer are far too low (about 1 to 5 μm). A booster is used to produce an amplification of the amplitudes, the amount of which is determined by its shape (mostly the amplitude gain is between 1 and 4). The booster also is designed to vibrate in the fundamental longitudinal mode (half-wavelength) at the same frequency as the transducer. They are coupled mechanically. The booster is fitted with a special support means at the nodal plane to allow a clamping of the resonating system to the welding press with minimum losses (the vibrations in the system are not hindered by the fact that it is supported). Once the resonance frequency is chosen, the dimensions of the transducer and booster are fixed and so the location of the nodal plane.

The resonance frequencies of ultrasonic welding systems have been standardized to obtain a limited range of resonating systems according to their dimensions and the power capability. For powers up to 3000 W the 20 kHz range is used (frequency some value between 19 and 22 kHz). For powers between 50 and 500 W the 40 kHz range is used (frequency between 35 and 40 kHz). For low power applications of 0.1 to 5 W the 60 kHz range is suited (frequency between 58 and 62 kHz). A commercial ultrasonic welding system will be provided with a resonating system of one of these ranges and the exact resonance frequency will depend on the suppliers choice.

The mechanical vibratory energy is transmitted from the booster to the products to be welded by means of the resonator. It is shaped and profiled such as to amplify and concentrate the mechanical energy, and transmit it to the product parts in such a way that energy absorption in the plastic is optimised. This resonator is designed for each application individually according to the product shape. It is clamped to the booster by mechanical means (steel bolt) and can be exchanged easily. The resonator also is driven in a resonance mode. Its resonance frequency must fairly well coincide with that of the transducer-booster assembly. If not, the resonance frequency of the complete system will change and the support of the booster will no longer be located in the nodal plane and vibrations will be induced into the welding press (in practice a frequency shift of 1% can be tolerated). The design of these resonators is the subject of the present work.

The resonating system is fixed in the welding press. A pneumatically controlled carriage system applies the resonator with some predetermined pressure to the parts to be welded, which are positioned into a jig or fixture. The design of adequate jigs greatly determines weld quality. After the pressure is applied (depending on the application some value between 10 and 2000 N), ultrasonic energy is generated during a fixed welding time, in which the thermoplastic is heated in the weld area (generally 0.1 to 1.5 sec.). After this the parts are held together during the hold time to allow solidification of the plastic (about 0.3-1 sec.).

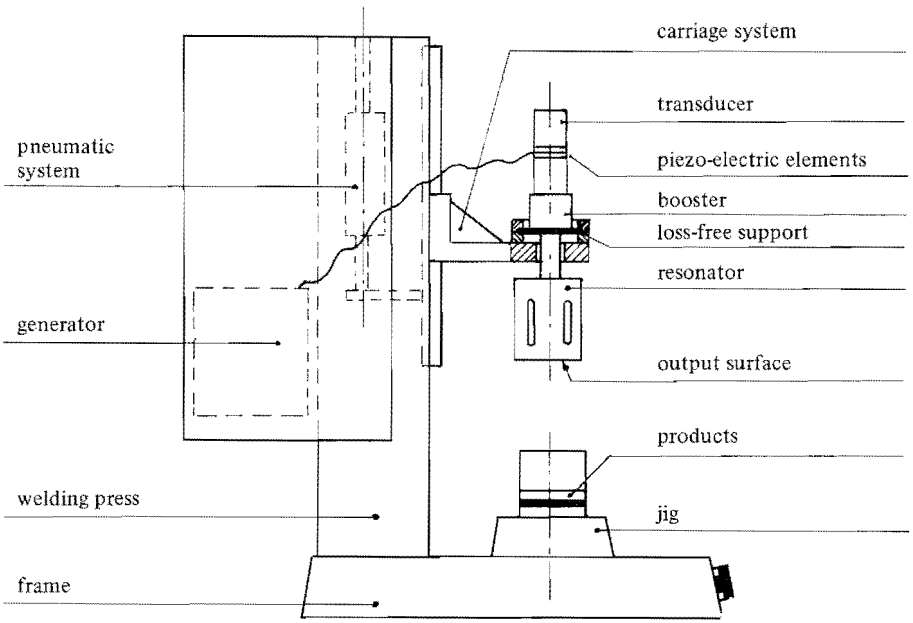

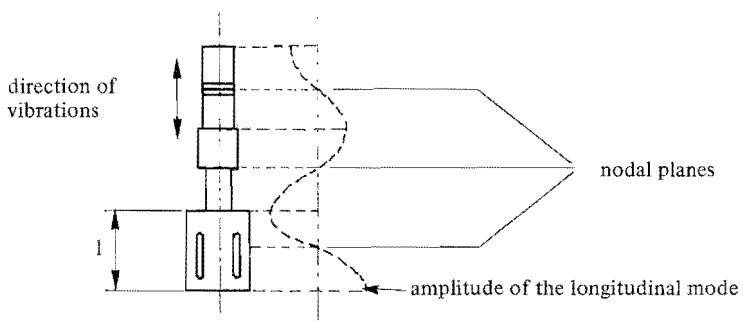

Fig. 1.1 Elements of an ultrasonic welding system (scale about **1:10***); the lower drawing shows the projection of the longitudinal vibrational mode in the resonating systems and the location of nodal planes; the resonator length is l.*

The absorption of energy in the plastics is proportional to the square of the vibrational amplitude at the output area of the resonator (Potente (1971); Becker (1973)). Therefore at all places where the resonator is in contact with the plastic parts, the amplitude should be as equal as possible to guarantee a uniform energy absorption (deviations of maximum 10% are found acceptable). The amplitude largely determines the welding time needed, and it is therefore of economical interest to have large amplitudes. The basical problem in the present work is to design resonators producing uniform output amplitudes along the output surface.

The pressure has only a small influence on the welding time, but rather determines the coupling between resonator and product, and so the effectiveness of energy transmission (Kröbe (1980); Denys (1967)).

The energy absorption in the thermoplastic parts is proportional to the frequency of the generated vibrations (Potente (1971)). Once a welding system has been chosen out of the range 20, 40 or 60 kHz, the frequency is within a 10% range about these values. Therefore the actual resonance frequency is not a critical design parameter for the welding process.

As a conclusion, the design of resonators is concerned with the vibrational mode from the point of view of the welding process and energy transmission, and with the resonance frequency from the point of view of a loss-free coupling of the vibrating system to the welding press through the support of the booster.

1.3. Aim of the present work

In ultrasonic plastic welding the most vital part is the welding tool (often called resonator, horn, sonotrode or velocity transformer). Each tool is designed specifically, based on the required application. The design of half-wavelength resonating tools has been extensively described in literature up to now, as far as the lateral dimensions are small as compared to the length which is determined by the wavelength in that specific material (see Figure 1.1) (Merkulov (1957); Neppiras (1977) (1963); Coy (1974)). One of the problems encountered in tool design is the occurrance of unwanted supurious vibrational modes when any of the lateral dimensions exceeds the half-wavelength ($\lambda/2$) (Crawford (1969); Stafford (1979)).

In the present work all resonators having at least one of the lateral dimensions (more specifically the dimensions of the output surface) exceeding one third of the wavelength ($\lambda/3$), will be called resonators with wide output cross-sections.

The design of resonators with wide output cross-sections is hardly described in literature. An attempt was made by Stepanenko (1979) to calculate the resonance condition for a set of mechanically coupled resonators, producing thus very wide output cross-sections (output surface of 8100 mm width). It is, however, not generally applicable for designing ultrasonic resonators, because the theory is not based on the requirements as to obtain a uniform output-amplitude (the measured difference between minimum and maximum amplitude was 30%) (see appendix 3).

Although widely used in plastic welding applications, the design of these tools remains the domain of a few very experienced people, resulting in statements like in Jakubowski's paper "Translating an art into sound design principles" (1972).

Shoh (1975) stated that further developments in ultrasonic plastic welding were to be expected in the area of horn improvement to expand size and wear.

Problems that are often met in resonator design are:
- improper welding or poor energy transmission to the process;
- short tool life (failure due to fatigue);
- noise produced during welding is unacceptable;
- the lack of thorough knowledge of design principles turns the devicing of resonators into a very expensive business.

The present study is based on the conviction that ultrasonic plastic welding is still a very promising technology and will remain so for a long time. Integration of it in modern manufacturing processes can only tally with quality improvement programs when there is sufficient knowledge of the process itself and of all aspects of tool design.

The aim of this study is the description of the problems encountered in tool design and elaboration of the design principles that will take away the limitations which prevent full exploitation of the technology.

In all papers on resonator design, the vibrations in the resonator are studied for the case where there is no load applied (the freely vibrating resonator). Under welding conditions the vibrations are damped due to the load of the welding process. There is, however no realistic model available to describe the complex situation under load. From own experiments on the measurement of the amplitudes of vibrations in a resonator under welding conditions, it is observed that the amplitude sometimes can decrease (it also depends on the power supply that is used). However, the mode of the vibrations of the resonator does not change, so that it can be considered identical to that of the freely vibrating resonator. In the next only freely vibrating resonators will be analyzed.

In chapter 2 the basic theory of half-wavelength resonators will be discussed and some remarks are made to the analysis of ultrasonic vibrations.

In chapter 3 the dimensions and shapes of resonators that are currently used will be classified. Based on own experiences, an analysis of the problems encountered when designing resonating tools is set up in terms of the vibrational modes and resonance frequencies.

The information on the design principles for wide output resonators that is available from patent literature is summarized in chapter 4. Of interest is to learn what kind of geometry changes can be used to improve the performance of a resonator.

In chapter 5 and 6 the applicability of solid cylindrical and rectangular resonators is studied extensively. It is investigated both analytically and experimentally up to what dimensions resonators of these basical shapes can be used for welding applications without providing slots, cut-outs etc. The literature on the vibrations in cylindrical and rectangular resonators will be reviewed and formula will be derived from it to calculate the resonance conditions for the fundamental longitudinal mode.

Above certain dimensions the resonators have to be slotted or provided with cut-outs to obtain a vibrational mode with a constant output amplitude. In chapter 7 the optimization of a specific resonator will be discussed. The overall dimensions were determined from the information available from the slender rod resonators and the patent literature. First, the geometry will be optimised on an experimental approach by providing various cut-outs based on the interpretation of the vibrational modes and frequencies as measured. Secondly a finite element analysis is used to study the vibrational characteristics of the same resonator and it will be shown that at other dimensions a resonator can be designed which shows a constant output amplitude without providing additional cut-outs.

In chapter 8 a model will be presented to calculate the overall dimensions for wide output resonators of blade-like, block-like and cylindrical shape, which are provided with slots. The model is set up to predict the resonance condition in these resonators for which a vibrational mode can be expected with a constant output amplitude. The predictions of the model are found to be in good agreement with the experiments.

The possibility to predict the optimum geometry to obtain the desired mode at a given resonance frequency, does not imply that all problems have been overcome. In a wide output resonator many resonance modes are possible, and sometimes they do interfere with the desired mode. The complex shape of slotted resonators does not allow an analytical analysis of all modes. In chapter 9 a finite element analysis is used to derive mode charts for one resonator type with various slotlengths. These charts show the resonance frequencies of various vibrational modes as function of the slotlength. They allow to predict critical dimensions at which modes do interfere. Interpretation of the calculated modes reveals that for some slotlengths no mode with a constant output amplitude can be obtained.

Finally, in chapter 10 the design of multiple resonator systems is discussed. Wide output resonators often are successfully used to transmit vibratory energy to several half-wavelength resonators which are coupled to its output surface. They are used for welding products of complex shape in which great differences in height levels of the weld area are present and where different amplitude levels of the resonator may be needed. The so-called funnel-shaped resonator will be investigated to explore its capability to serve as half-wavelength resonator of prescribed length and prescribed amplitude gain.

2. HALF-WAVELENGTH RESONATORS AND VIBRATION ANALYSIS

2.1. Resonating tools

In ultrasonic engineering tools are designed to vibrate in a resonance condition. For the main part of the applications the tools are resonating in the fundamental longitudinal mode (half-wave). There are a number of design requirements to take into account. The desired frequency and the resonator material determine the overall dimension such as the length. The stress-distributions along the resonator must be directed such as to guarantee a reasonable life expectancy. For most applications an amplitude amplification is desired.
Generally, bar-type resonators are used with a variable cross-section along the length. Such a tapered resonator will produce an amplitude gain towards the smaller end-portion (the standing wave of the longitudinal vibration has an output amplitude (u_2) higher than the input amplitude (u_1) : $u_2 > u_1$). See figure 2.1.

As long as the lateral dimensions are small as compared to the wavelength, the problem is governed by the one dimensional wave equation for the propagation of longitudinal waves in the bar and solutions are available for some resonator profiles.

Analytical solutions have been derived for exponential, conical, Gaussian-shaped resonators e.o. A large number of papers on this subjects has been published. (Merkulov (1957); Neppiras (1963); Vetter (1966-1968); Makarov (1964)). For most shapes, however, no analytical solutions can be found and numerical procedures are used (Eisner (1963); Kleesattel (1970); Scheibener (1971)).

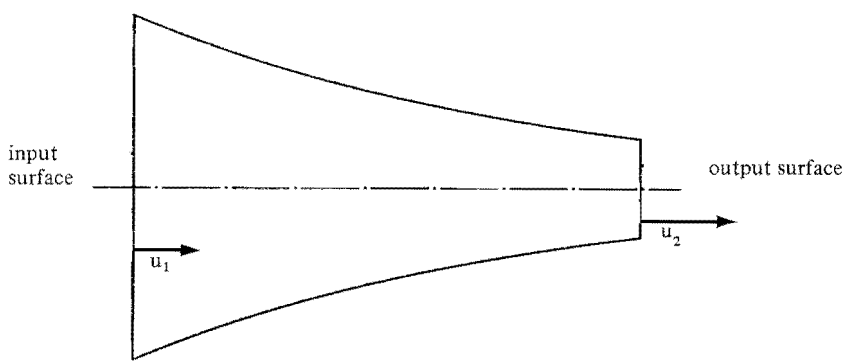

Fig. 2.1 Half-wavelength resonator with a tapered shape towards the output end. (cylindrical cross-section); input amplitude u_1 and output amplitude u_2.

As an example the bar-type resonator with constant cross-section as shown in figure 2.2 will be explained. The material is isotropic and the wavepropagation is uniform in a cross-section of the resonator, it is loss-free and linear elastic. The wave equation for longitudinal waves propagating in the axial direction is:

$$\frac{\partial^2 \tilde{u}}{\partial t^2} = c^2 \frac{\partial^2 \tilde{u}}{\partial x^2} \qquad (2.1)$$

where $\tilde{u}$ is the displacement in the x-direction; it is a function of both time t and coordinate x; c is the propagation velocity for longitudinal waves in slender rods. The solutions of equation (2.1) for harmonic vibrations are as follows:

$$\tilde{u} = (A_1 e^{-jkx} + A_2 e^{+jkx}) e^{j\omega t} = u(x)\, e^{j\omega t} \tag{2.2}$$

where A_1 and A_2 are constants; ω is the angular frequency of the vibrations and k is the wave number:

$$k = \frac{\omega}{c} \tag{2.3}$$

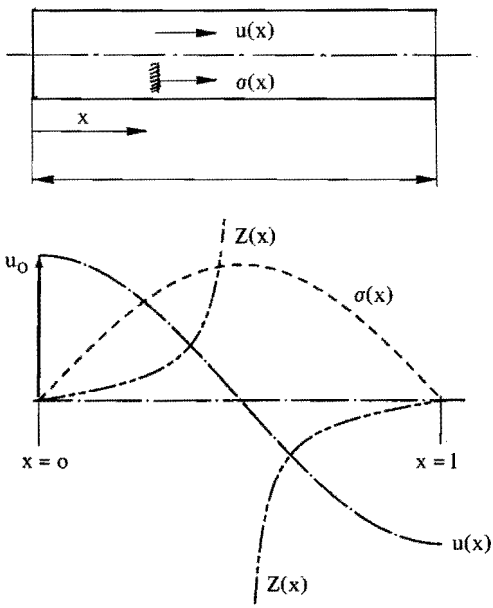

Fig. 2.2 Half-wavelength resonator of length l with a constant cross-section; definition of the displacement u(x), stress σ(x) and the modulus of the mechanical impedance Z(x).

We will only consider the time-independent part of the solution of equation (2.2): the displacement function u(x). For the half-wave length resonator as shown in figure 2.2 the boundary conditions follow from the requirements that the ends are stress-free:

$$\left.\frac{du(x)}{dx}\right|_{x=o} = 0$$

$$\left.\frac{du(x)}{dx}\right|_{x=l} = 0 \tag{2.3}$$

Therefore the displacement function u(x) can be written as follows:

$$u(x) = u_0 \cos(kx) \tag{2.4}$$

where u_0 is the maximum amplitude of motion at the ends. This vibration mode is called the fundamental longitudinal mode.
From equations (2.3) and (2.4) also follows that:

$$kl = \pi \text{ or } l = \frac{\pi}{k} \tag{2.5}$$

This frequency equation relates the resonator length l to the resonance frequency f by

$$l = \frac{\pi}{k} = \frac{\pi c}{\omega} = \frac{c}{2f} \tag{2.6}$$

(where $\omega = 2\pi f$). The length l is very often presented as $\lambda/2$ (half-wavelength).
The mechanical stress in the x-direction $\sigma(x)$ is related to the strain $\epsilon(x)$ and the displacement u(x) as follows:

$$\sigma(x) = E\,\epsilon(x) = E\,\frac{du(x)}{dx} \tag{2.7}$$

Using $c = \sqrt{\frac{E}{\rho}}$, where ρ is the specific mass of the resonator material and E is Young's modulus, equation (2.7) gives:

$$\sigma(x) = -\omega\rho c\, u_0 \sin(kx) \tag{2.8}$$

The stress-function is shown in figure 2.2. It is maximum in the midplane of the resonator where the amplitude is zero (this is called the nodal plane). The maximum stress in a resonator is determined by the frequency, the material properties and the maximum amplitude. At distance x in the resonator, the particle velocity $\dot{u}$ in the x-direction follows:

$$\dot{u} = \frac{\partial \tilde{u}}{\partial t} = \dot{u}(x)\, e^{j\omega t} \tag{2.9}$$

As we only consider time-independent solutions, the particle velocity $\dot{u}(x)$ is calculated from equations (2.2), (2.4) and (2.9):

$$\dot{u}(x) = j\omega u_0 \cos(kx) \tag{2.10}$$

At distance x the axial tensile force F(x) is defined as (A is the cross-sectional area):

$$F(x) = A\,\sigma(x) \tag{2.11}$$

A quantiy that is essential to wave phenomena in solid materials is the mechanical impedance Z(x), which is defined as the quotient of the force F(x) and the particle velocity $\dot{u}(x)$ for a given cross-section:

$$Z(x) = \frac{F(x)}{\dot{u}(x)} \tag{2.12}$$

Using equations (2.10) and (2.11) Z(x) becomes:

$$Z(x) = -j\, A\rho c \tan(kx) \tag{2.13}$$

The modulus of Z(x) is shown in figure 2.2.
It is zero at the ends (F(x) = 0 for x = 0 and x = l) and becomes infinite in the nodal plane $\dot{u}(x) = 0$ at x = l/2). The quantity Z(x) will be used later on to calculate the effect of variations in the cross sections on the wave propagation.

The theory presented here is only valid as long as the displacement is uniform along a cross-section. When the wavelength is no longer large as compared to the dimensions of the cross-section, the wave propagation is distorted by the effect of lateral motions (perpendicular to the wave propagation) on account of the Poisson constant ν (see chapter 5 and 6). It will result in a non-uniform output amplitude.

2.2. Resonator materials

In selecting materials for resonators there are several facts to bear in mind.
As they are driven in a resonance condition, there is the mechanical stress level that determines the failure rate due to fatigue. The mechanical stress is determined by the resonator characteristics such as shape, the material properties (density, Young's modulus) the amplitude of motion and frequency (see equation 2.8). Limitations in high power ultrasonics are also found for reasons of the elastic loss in the resonator. The power dissipation strongly dictates the material choice, because it will decrease the fatigue stress. A third fact, that is related to each application involved, is the wear resistance of the material.
The mechanical damping factor of the material is a very important parameter. It can be described as hysteresis loss or internal friction. Excessive heat built-up in the resonating parts of an ultrasonic system can be a result of it.

The power dissipation in a resonating rod (as shown in figure 2.2) is determined by the mechanical loss-factor δ_m of the material. The mechanical loss-factor is defined as the quotient of the dissipated energy in a volume element per period of vibration and 2π times the maximum stored potential energy of the vibrating rod in the same volume element. (Skimin (1964)):

$$\delta_m = \frac{\text{(dissipated energy) in one period}}{2\pi * \text{(max. stored energy)}} \tag{2.14}$$

The reciproke of δ_m is also known as the mechanical quality factor Q.

The stored potential energy U_p which is a function of time can be calculated from the local stress and strain in the resonator:

$$U_p = \int \bar{\sigma} d\bar{\varepsilon} \tag{2.15}$$

By using equations (2.7) and (2.8) the maximum stored energy $\hat{U}_p$ in one period in a volume element at distance x becomes:

$$\hat{U}_p = \frac{1}{2} E k^2 u_o^2 \cos^2(kx) \tag{2.16}$$

To get from energy to power, equation (2.16) has to be multiplied by the frequency f. Re-writing equation (2.16) it follows with equation (2.8) and equation (2.14) for the power dissipation per unit volume $P_{loss}(x)$:

$$P_{loss}(x) = \frac{1}{2} \frac{\omega}{E} \sigma^2(x) \delta_m \tag{2.17}$$

The power dissipation in a resonator is not constant over the length and is concentrated in the nodal plane. It is proportional to the square of the stress. In order to evaluate the power dissipation in a half-wavelength resonator equation (2.17) has to be integrated. For a resonator of cross-sectional area A, the power loss $P_{loss}(\lambda/2)$ becomes:

$$P_{loss}(\lambda/2) = \frac{\pi}{4} \rho c \omega^2 A u_o^2 \delta_m \qquad (2.18)$$

Typically for an aluminium 20 kHz resonator of diameter d = 50 mm, vibrating at an amplitude u_o = 30 μm the power dissipation becomes ($\delta_m = 5 10^{-5}$, ρ = 2700 kg/m^3, c = 5200 m/s):

$$P_{loss}(\lambda/2) = 15{,}3 \text{ W} \qquad (2.14)$$

For general applications at 20 kHz at amplitude levels of 30 μm, the power dissipation in a half-wavelength resonator of cylindrical cross-section is in the order of 10-30 W. For reason of a lower δ_m, alloys of aluminium and titanium are widely used in ultrasonic engineering ($\delta_m < 5\ 10^{-5}$). .
For chromium steels δ_m can be as high as 100.10^{-5}. Usually, steels or alloys of it are rarely used, especially not at high stress levels.

In general δ_m is not easily measured. Measurements of actual ultrasonic resonators activited at high amplitude levels show that δ_m is not only a material constant, but increases with the stress level (Hulst (1975)).

Of great importance is also the machineability of the material. Resonators with wide output cross-sections, with dimensions above 80 mm (at 20 kHz) are mainly made of aluminium alloys, and very occasionally of titanium alloys. In the present work the main part of the resonators is made of a Duraluminium. The material properties have been analyzed and are summarized in table 2-1 (accuracy for the elastic properties ± 0,5%).

	ρ (kg/m^3)	E (N/m^2)	c (m/s)	ν (–)	σfatique (N/m^2)
Al	$2.71\ 10^3$	$0.73\ 10^{11}$	5200	0.335	$\sim 120\ 10^6$
Ti	$4.41\ 10^3$	$1.08\ 10^{11}$	4930	0.305	$\sim 200\ 10^6$

Table 2.1 Material properties of Al- and Ti-alloy as used for the fabrication of resonators.

The dimensions of a specific resonator at a certain design frequency, are determined by the propagation velocity of the longitudinal wave, c. Once a resonator has been fabricated of a certain material, the dimensions clearly are not valid anymore when another material will be chosen. As an example figure 2.3 shows the effect of the material choice on the overall dimensions of a 20 kHz resonator. This type of resonator will be discussed into more detail in chapter 10. The dimensions of both the cylindrical parts at the input and the output end are kept constant. The strong effect on length l is seen.

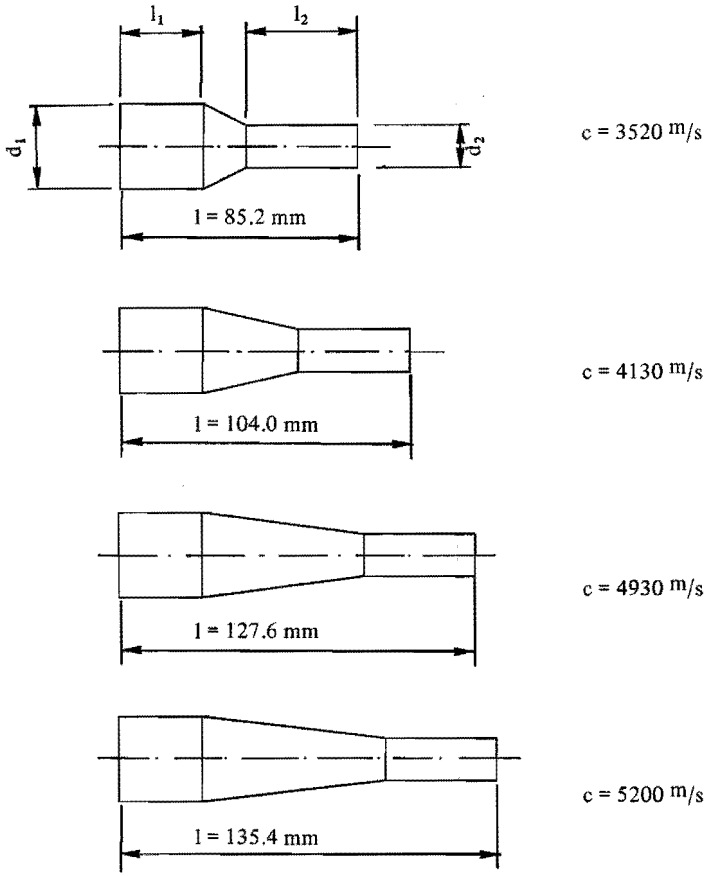

Fig. 2.3 The effect of the value of the propagation velocity c (various materials) on the resonator length l as calculated. (Design frequency 20 kHz, the lengths l_1 and l_2 as well as the diameters d_1 and d_2 of the cylindrical parts are kept constant).

To conclude this introduction into the analysis of a vibrating rod the energy transmission through the resonator will be discussed.
An ultrasonic system is operated at resonance and mechanical energy is stored into it (which is periodically converted from kinetic to potential energy and vice versa). The stored vibrational energy can be calculated from equation (2.16) and (2.18). Normally an ultrasonic system consists of three resonators. At 20 kHz typically 1000 W electrical energy is converted into mechanical energy in the resonator and transmitted to the load. From equation (2.18) one can calculate the stored power capacity in the resonator. In the case of three resonators (50 mm diameter, material aluminium, mean amplitude 30 μm) the stored power amounts 300 kW. As the loadpower is 1000 W, one can conclude that in an ultrasonic system the stored mechanical energy is very much larger than the energy transmission to the load.

It can be understood from this that the resonating system can be kept in resonance under load conditions. In applications for which the transmitted energy is no longer small as compared to the stored energy, one will see that the system no longer can be kept in resonance ("stalling"-effect).

2.3. Vibration analysis

The most important parameters to characterize ultrasonic resonators are the resonance frequencies and the corresponding vibrational modes. A quick impression of the resonating body can be obtained from the location of nodal patterns. The use of fine sand which moves towards the velocity minima on a vibrating surface, was used for this purpose.
A point-by-point analysis of the vibrations was found to be most practical when using a "Fotonic Sensor", a non-contact optical proximity detector (Documentation Ref. 67). Only motion perpendicular to the surface can be measured. Up to frequencies of 100 kHz, amplitudes down to 0.1 μm can be measured on spots as small as 0.5 mm^2. The Fotonic Sensor was found to be more accurate than Eddy-current displacement detectors or mechanical contacting elements. Overall measurement of the vibrational amplitudes of a resonator is possible with holographic analysis (Herrmann (1982) (ref. 65); Tuschak (1975)). However, for the purpose of this study it does not show many advantages over the point-by-point methods. For the measurements in the present work the amplitudes have an accuracy of $\pm$ 0.2 μm.

Two ways of frequency measurement were used. The resonance frequency of the resonator itself was measured using piezoelectric elements. A variable frequency oscillator is used to drive one element (at constant voltage) which, in contact with the resonator to be studied, transmits mechanical vibrations through the resonator, which again are detected by the second element (which acts as receiver in contact with the resonator). The output voltage of the receiver-element is proportional to the amplitude measured, which is maximum in case of resonance in the resonator.
A spectrum analyzer (0-300 kHz) was used to find the resonance frequencies.
The second method is to couple the resonator under study to a transducer as used in a conventional welding equipment. The transducer has a fixed resonance frequency for the longitudinal vibration, say 20 kHz.
The resonance frequencies of the assembly are found when at the electrical terminals of the transducer a minimum driving impedance is measured (again with the aid of a spectrum analyzer with oscillator). This is equivalent to the mechanical resonance frequency of the system (as measured mechanically by the first method) when the electrical terminals are short circuited.
When the resonance frequency of the system is measured with open electrical terminals, a slightly higher frequency will be measured, which is called the anti-resonance frequency. In the present work only the resonance frequency will be considered, because most of the commercial equipment operates in the resonance frequency. All frequency measurements have an accuracy of $\pm$ 10 Hz (in the range of 20 kHz).

3. OBSERVATIONS ON A RANGE OF RESONATORS

3.1. General design requirements

When using half-wavelength resonators of the slender rod-type, the maximum output area is limited (the lateral dimensions are small as compared to the wavelength). At 20 kHz the half-wavelength is between 110 and 135 mm so that the lateral dimensions may not exceed 70-80 mm, and the output area typically is restricted between 500-2000 mm^2. Many applications, however, do require a much larger output area (up to 50000 mm^2). For each application the lateral dimensions of a resonator will have to be adjusted to the product dimensions, e.g. in case of ultrasonic welding of thermo-plastics. A resonator was called wide when at least one of the lateral dimensions exceeds one third of the wavelength ($\lambda/3$) of the longitudinal wave at the design frequency ($\lambda = \frac{c}{f}$). The resonator with a wide output cross-section also has to be designed to vibrate in resonance and the desired vibrational mode is mostly described as "longitudinal" mode. The vibrational mode of the resonator is called "longitudinal" when the amplitude of motion at the input and output surface is uniform in magnitude along the surface and has a direction perpendicular to these surfaces. The amplitudes at the input and output surface are 180^o out of phase, and the amplitude is zero in the nodal plane, located about halfway the distance between the output and the input surface. Generally the actual mode will only approximate these characteristics of the "longitudinal" mode. The differences in the output amplitude will seldom be smaller than 10%, neither can the component of the output amplitude in the plane of the output surface be obtained smaller than 10% of that amplitude.

It will be clear that there is an enormous variety of shapes possible which do fulfil these requirements with respect to the longitudinal mode. The basic requirements are shown in figure 3.1 for an arbitrary shaped resonator. The output surface must be matched to the dimensions of the products to be welded. The input surface must be such that the resonator can be coupled to the vibrations generating part of a welding apparatus. The desired amplitudes of vibration at input and output surface are shown. The resonance frequency for the longitudinal mode must coincide with the operating frequency of the welding apparatus. It is the task of the ultrasonic engineer to choose the resonator shape so that it fulfils these requirements. Below some additional criteria for a good resonator design will be discussed.

3.2. Classification of resonator shapes

The general approach to make a resonator is very straight forward. Referring to figure 3.2 a brief description will be given now. The lateral dimensions are matched to the productparts to be welded. The resonator length is chosen somewhat longer than the length of the half-wave of the longitudinal vibration mode in that specific resonator material and at the design frequency.
All the resonators are in some way provided with slots, bores, holes or cutouts to satisfy the conditions for which they will be able to resonate in a "longitudinal" mode. (These will be discussed in chapter 4).

The locations of slots, bores etc. will be such that all lateral dimensions in the zone of maximum stress produced by the longitudinal wave (nodal plane) does not exceed $\lambda/4$ to compensate for cross-coupling, and to correct for distortion of the longitudinal

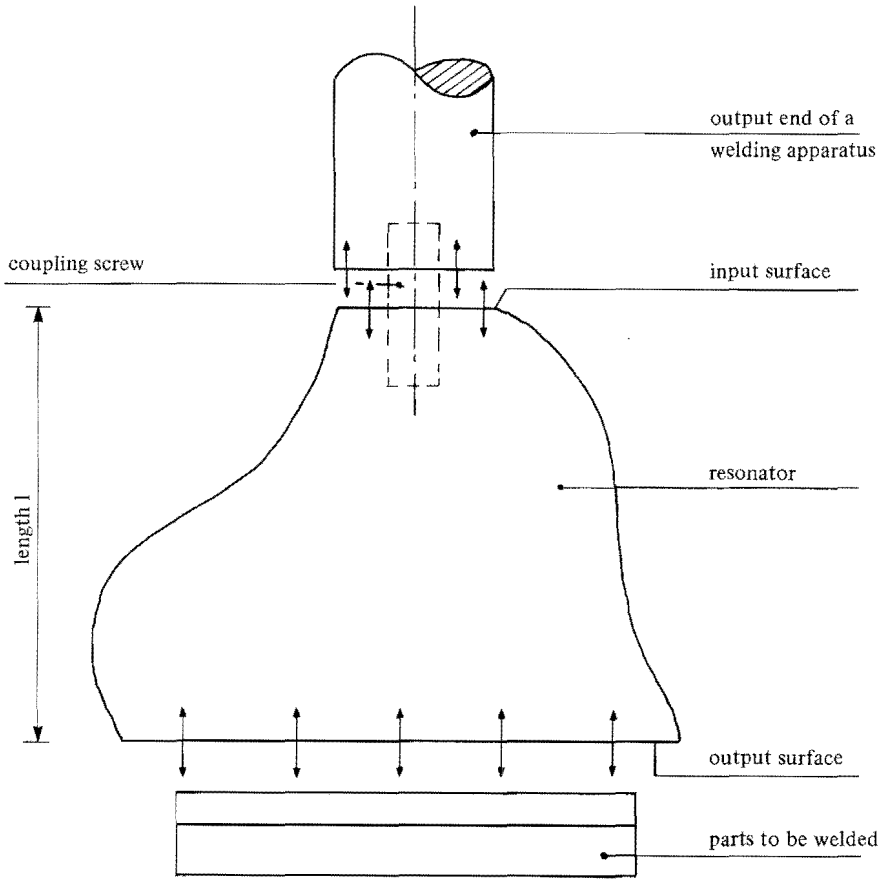

Figure 3.1 Basic design requirements for a resonator with a wide output cross-section (three -dimensional body, not necessarily a body of revolution); the arrows indicate the amplitude of vibration.

wave. (This wil be discussed in chapter 5 and 6). Secondly the resonator length will be shortened by small steps until the measured resonance frequency coincides with the design frequency.

A study of various resonator shapes as used in practice, reveals some generality in the geometry. On the basis of their geometrical shape, resonators with wide output cross-sections can be classified into three groups. These groups are shown in figure 3.3.
The resonator types are:

1. **cylindrical type**, diameter $> \lambda/3$;
2. **blade-like type**, only one dimension $> \lambda/3$;
3. **block-like type**, both dimensions $> \lambda/3$.

Capitals will be used for the overall dimensions of these resonator types only.

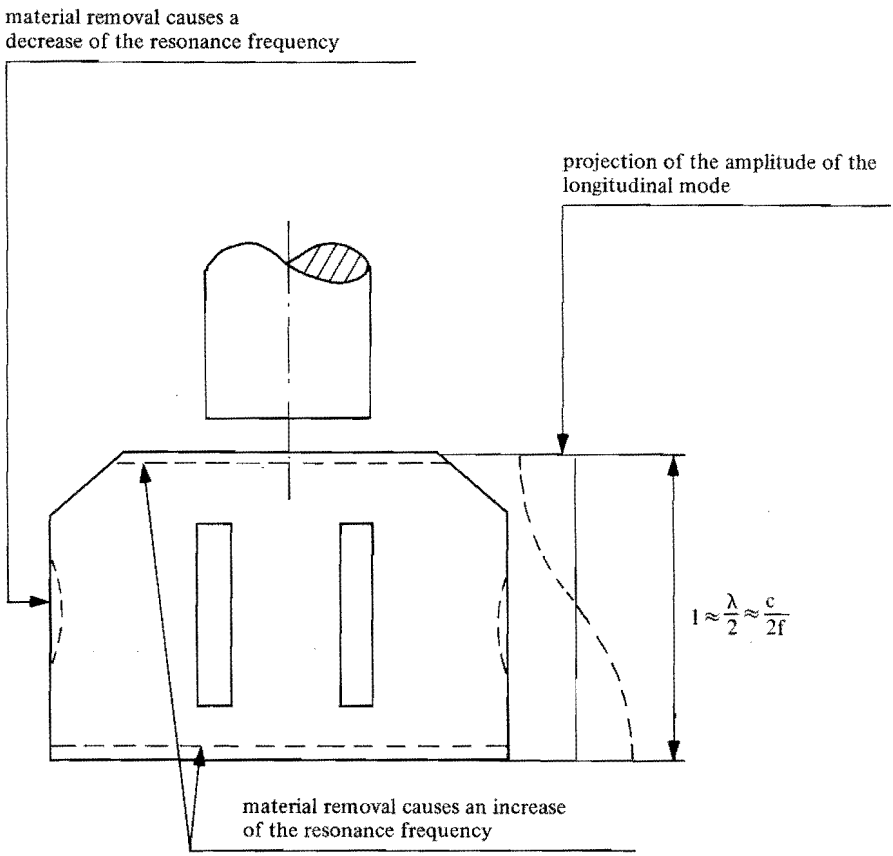

Fig. 3.2 General lay-out of a wide resonator and methods to alter the resonance frequency.

At 20 kHz the width of the blade-like resonators ranges from 80 to 400 mm; block-like resonators are between 100x100 and 200x200 mm^2; cylindrical resonators usually are between 100 and 200 mm diameter, occasionally up to 300 mm; the resonator length l is in the range of 110 to 135 mm (close to the half-wavelength in a slender rod $\lambda/2 = \frac{c}{2f} = 130$ mm for aluminium).
In resonators of the cylindrical or blade-like type an amplitude gain is often built in, created by a discontinuity of the cross-section in the zone of the nodal place, see fig. 3.3, nr. 2. Block-like resonators are never provided with an amplitude gain.

The wide output resonators are mostly used for direct energy transmission to the load. Sometimes they are used as a base resonator, where small half-wavelength resonators are attached to it (they serve as an energy distributor), see figure 3.3, nr. 4.

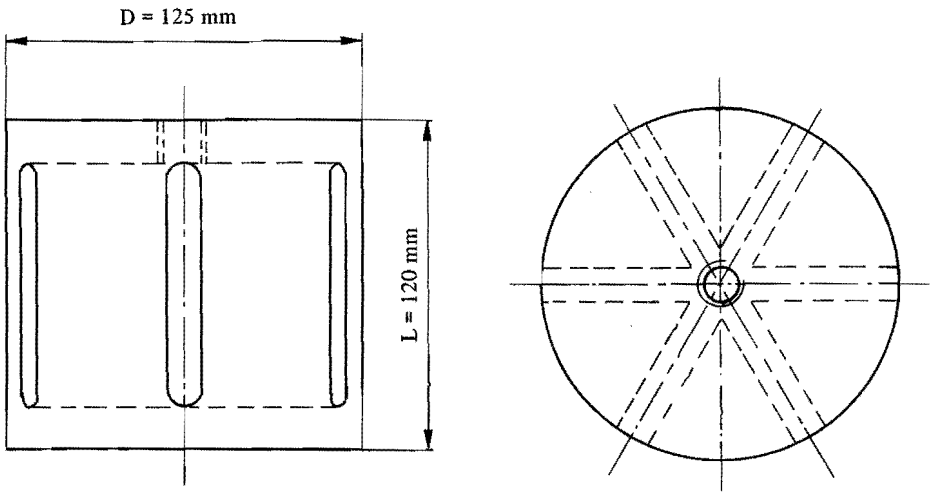

Fig. 3.3 nr. 1 Cylindrical type resonator (typical dimensions); diameter D and length L.

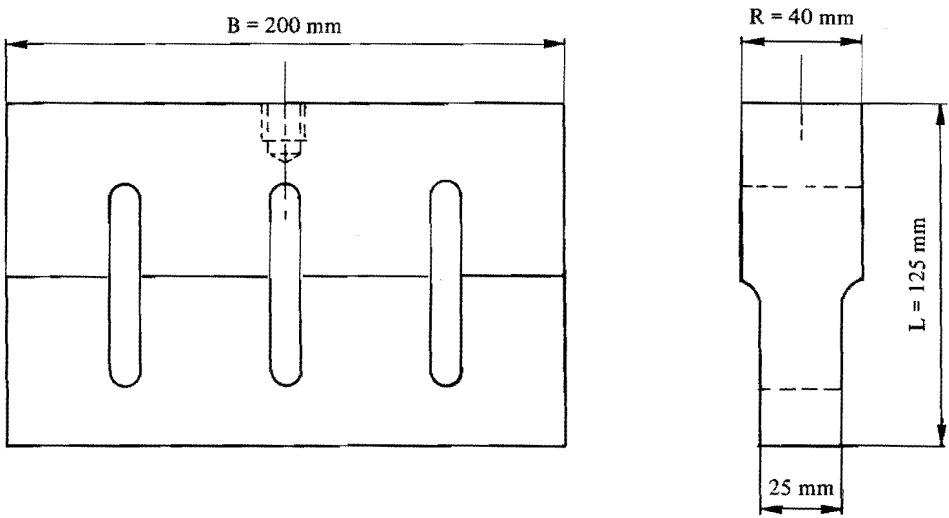

Fig. 3.3 nr. 2 Blade-like resonator (typical dimensions); width B, thickness R and length L.

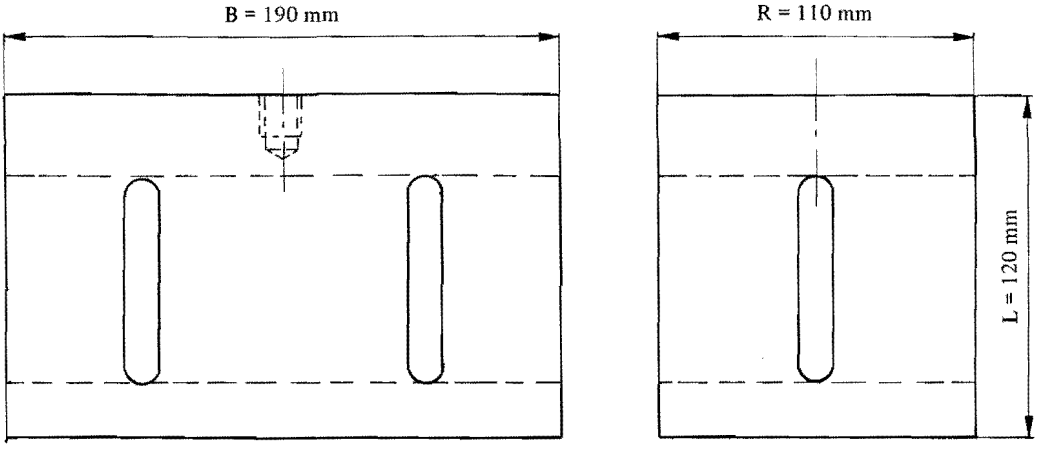

Fig. 3.3 nr. 3 Block-like resonator (typical dimensions); width B, thickness R and length L.

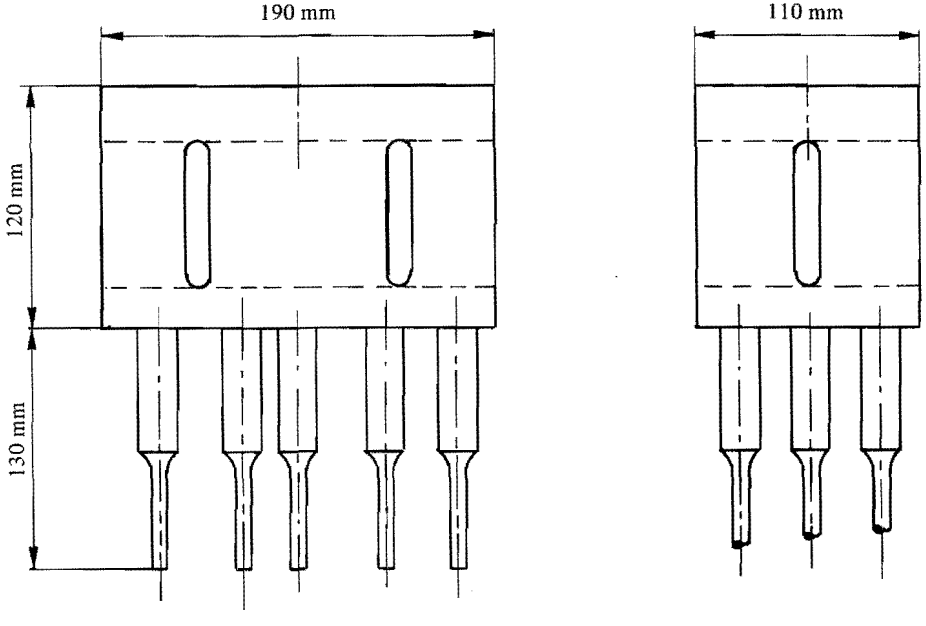

Fig. 3.3 nr. 4 Base resonator with small resonators attached to it (typical dimensions)

The output area will not always be a plane. Often it is profiled to match the product shape to assure optimum energy transmission. Generally the profiles are much less than $\lambda/4$ deep.

As the resonator dimensions are matched to each application individually, no "standard" dimensions, but rather a wide variety of resonator dimensions will be encountered. For high power applications the operating frequency of an ultrasonic apparatus is some fixed value between 20 and 22 kHz, depending on the choice of the manufacturer or supplier. This means that for each type of equipment other dimensions are required. Equipment operating at 30, 36 and 40 kHz has become of real interest of late. Therefore the variety of resonator dimensions has been enlarged enormously. Although the problems in designing are identical for all these frequencies, there are no scaling laws available to predict the resonance behaviour for all these frequencies from one reference value. In the present work resonators in the 20 kHz range will be studied.

As mentioned before, the resonator material usually is an aluminium alloy, only for relatively small resonators a titanium alloy is used (at 20 kHz for dimensions < 100 mm). Although superior to aluminium, the titanium alloy is unfavourable above these dimensions for reason of its bad machineability and the price of the raw material.

3.3. Analysis of some resonators

In order to quantify the problems encountered in devicing wide output resonators, an analysis of 37 existing resonators was set up. They cover the whole range of dimensions as commonly used in ultrasonic plastic welding applications at 20 kHz. The most important characteristics measured are: frequency spectrum and modes of vibration. Of interest are the resonance frequency of the "longitudinal" mode (if existing) and the shape of this mode. The presence of other resonances near the operating frequency indicates the risk that the resonator is used in another mode than the desired one, or that coupled vibrational modes are present. All resonators, in some way tuned as close to the optimum as possible, were coupled to a welding apparatus. The vibrational modes were measured optically in unloaded condition (the ultrasonic generator is activated but the welding head does not contact any load, it is freely vibrating). Only the amplitudes perpendicular to the surface are measured, along the contours of the resonator. In this way enough information can be obtained for interpretation of the vibrational mode.
Special attention is paid to the amplitudes along the output surface. The uniformity is indicated by the differences in amplitude as related to the maximum amplitude.

In tables 3.I, 3.II and 3.III the results of the study are summarized. No detailed information on vibrational modes and corresponding resonance frequencies are given here. The main dimensions of the resonatorshape are listed as well as the number of resonances within the range of 18 to 22 kHz.

The number slots provided in each resonator (see figure 3.3) is an important characteristic. The evaluation of the analysis is presented by four judgments. "Tuning problems" does not mean that it is difficult to let coincide the resonance frequency of the longitudinal mode with the design frequency. It also can mean that there are spurious resonance frequencies close to the frequency of the longitudinal

mode which could not be eliminated. If the longitudinal mode is coupled to some spurious mode it is classified as "coupled modes". The uniformity of the output amplitude is a very important parameter. In the tables the maximum difference of the output amplitudes (as measured) is given. Differences smaller than 10% are not listed.

As an example the vibrational modes and corresponding frequencies for one specific resonator are shown in more detail in figure 3.4, for some values of the resonator length. The length obviously has a great influence on the vibration mode that is excited when the resonator is coupled to an ultrasonic welding apparatus. At the output surface, the energy transmission will be far from optimum if the length is not chosen properly.

As a result of this study and from experiences with resonator designing for production apparatus in general, the observations can be summarized as follows:
- Within the range of 18 to 22 kHz the number of resonance frequencies detected is between 2 and 5, one of which is the desired frequency of the "longitudinal" mode.
- In most cases the "longitudinal" vibrational mode is not optimal; amplitude differences along the output surface from 10-80% are observed, resulting into unequal energy transmission during welding. Even nodes (no motion) and a phase shift in amplitude are observed, which does not resemble a longitudinal mode at all.
- The longitudinal mode is sometimes coupled to another ("spurious") mode; the effect is mostly a distortion of the longitudinal mode with a non-uniform amplitude along the output surface as a result.
- At the output surface of a resonator the vibrational mode very often has both an amplitude perpendicular to the surface and an amplitude in the plane of the surface. The latter causes small resonators attached to it (in the case of a base resonator (figure 3.4, nr. 4) to vibrate both in a longitudinal (where it was designed for) and a flexural mode. The flexural mode has very large amplitudes when its resonance frequency coincides with that of the longitudinal one. The flexural mode is not desired and often causes a failure of the clamping screw due to excessive mechanical stress.

With the aid of vibration mode analysis and the measurement of the frequency spectrum, in many cases an optimum operation of the resonator can be reached, on account of the interpretation of these modes and adequate variation of the dimensions.
During these optimization procedures (called "tuning") various striking effects were observed:
- Tuning is to reach a condition in which a specific resonator is vibrating in the desired mode at the design-frequency, by successive material removal on strategically chosen places; optimization of frequency and vibrational mode do not necessarily go in the same proportions or direction as a result of a change in dimensions.

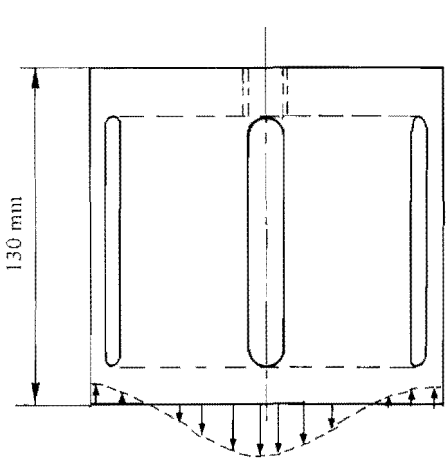

1: f = 19.14 kHz

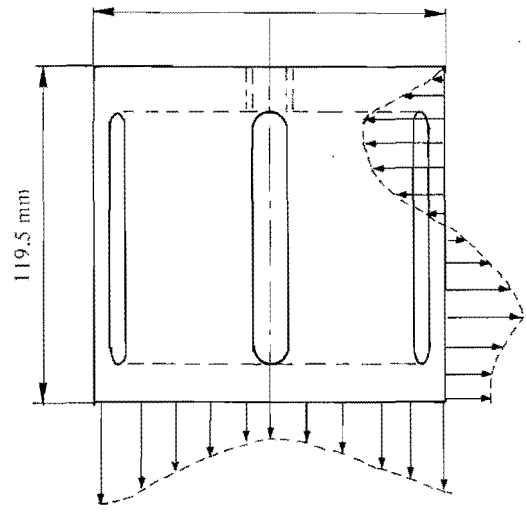

2: f = 19.44 kHz

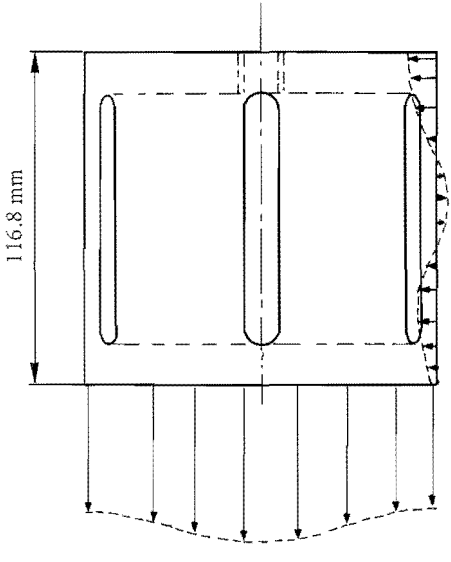

3: f = 19.78 kHz

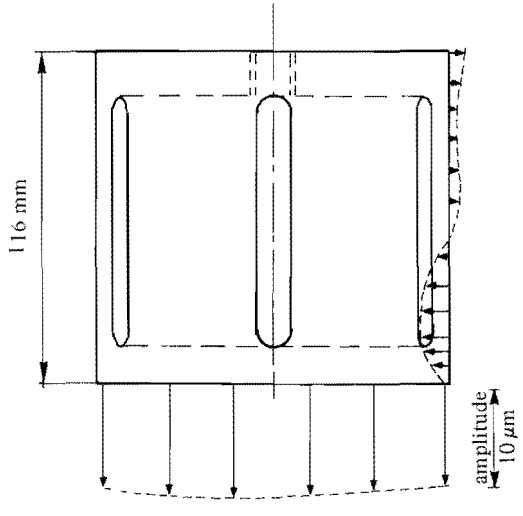

4: f = 19.93 kHz

Fig. 3.4 Vibrational modes and resonance frequencies of a cylindrical-type resonator of 125 mm diameter (material aluminium, design frequency 20 kHz). Shown here are those modes which could be excited on the ultrasonic welding apparatus used, for various values of the resonator length.

- Although an attempt will be made to reach the optimum in careful small steps, overshooting is not unrealistic; consequently a shift in the reverse direction may become extremely difficult.
- While changing the desired mode, also *all* other modes and their corresponding resonance frequencies will change; this can interfere with the attempts to optimize the desired mode.
- The amount of changes after material removal is not easy to predict.
- The optimum is reached, but the resonance frequency of some spurious mode is very close to the frequency of the desired mode (say within the operating range of the ultrasonic generator) so that it is not possible to discriminate between both; for 20 kHz equipment no spurious modes are allowed within a bandwidth of 600 to 1000 Hz on both sides of the operating frequency; the elimination of this spurious mode without changing the optimum, is extremely difficult, if not impossible.

The conclusion has to be that, only by systematical analysis of resonance frequencies and vibrational modes as a function of the resonator shape, perfectly operating resonators can be obtained. Devicing a resonator on a trial and error base is time consuming and results in material waste and unrealistically high costs for the resonator as compared to the total costs of a welding apparatus (sometimes up to 50% of the total amount).

Nr.	dimensions (mm) width, depth, length B R L	number of slots	number of resonances 18-22 kHz	no problems	tuning problems	coupled modes	output amplitude difference	
1	90 x 30 x 124	1	1			x	40%	
2	100 x 35 x 126	1	3	x				
3	100 x 69 x 123	2	1	x				
4	103 x 40 x 125	2	1		x			
5	124 x 40 x 136	2	–			x	80%	
6	130 x 35 x 130	2	3		x		80%	
7	130 x 55 x 129	2	2			x	70%	
8	131 x 35 x 122	2	2	x				
9	138 x 40 x 123	2	–			x	10%	
10	140 x 50 x 120	2	3				60%	
11	145 x 35 x 124	2	5	x				
12	150 x 40 x 132	2	–			x	20%	
13	150 x 40 x 123	2	2	x			25%	special cutouts
14	152 x 40 x 123	2	2				20%	
15	180 x 55 x 124	2	1				10%	
16	180 x 80 x 121	2	3			x	30%	special cutouts
17	184 x 73 x 125	2	–				10%	
18	200 x 80 x 120	2	1	x				
19	232 x 60 x 130	4	3		x			
20	240 x 38 x 124	4	3		x			special cutouts
21	264 x 39 x 124	4	4		x	x		
22	370 x 60 x 120	4	3		x			
23	299 x 35 x 123	5	4				20%	

Table 3.I: Resonators of blade-like type (all aluminium, only nr. 12 Titanium; (–) denotes not measured); see figure 3.3 nr. 2.

Nr.	dimensions (mm) width, depth, length B R L	number of slots (in 2 directions)	number of resonance 18-22 kHz	no problems	tuning problems	coupled modes	output amplitude difference
24	190 x 105 x 113	2 and 0	3			x	
25	185 x 112 x 113	2 and 2	4				10%
26	180 x 125 x 120	2 and 1	4			x	10%
27	179 x 100 x 119 (B)	2 and 1	3			x	30%
28	152 x 120 x 120 (B)	2 and 1	3			x	25%
29	185 x 120 x 121	2 and 1	2			x	
30	160 x 160 x 121	2 and 2	3		x	x	
31	190 x 180 x 120 (B)	2 and 2	2			x	50%

Table 3.II: Resonators of block-like type (aluminium, B = base resonator); see figure 3.3, nr. 3.

Nr.	dimensions (mm) diameter, length D L	number of slots	number of resonances 18-22 kHz	no problems	tuning problems	coupled modes	output amplitude difference	
32	152 x 126	none	2	x				no longitudinal mode
33	152 x 98	none	2				80%	distortion of longitudinal mode
34	152 x 123	6	3		x	x		bell-shaped (hollowed resonator)
35	160 x 119	6	3			x	60%	
36	125 x 116	6	3			x	10%	
37	190 x 119	6	3		x	x		bell-shaped (hollowed resonator)

Table 3.III: Resonators of cylindrical type (aluminium); see figure 3.3, nr. 1.

4. SURVEY OF PATENT LITERATURE (PATENTS AND PATENT APPLICATIONS) ON RESONATORS WITH WIDE OUTPUT CROSS-SECTIONS

4.1. Introduction

Most of the information on the design of ultrasonic resonators having large dimensions in planes perpendicular to the direction of the longitudinal vibrations to be transmitted, can be obtained from patent literature. After all, the design of well functioning resonators (horn) requires much skill and experience. Therefore most of the knowledge will be kept company confidential, resulting in a very limited number of publications on this item.
The available patents and applications can be categorized into three groups: the first group describes design principles, the second gives means by which the mode of vibration can be influenced, and the third group describes the coupling of resonators to a multiple resonator system. Without pretending to fully cover the patents and applications published until now, below the most significant features encountered will be discussed.

4.2. Design principles

In a resonator which is designed to resonate in the longitudinal mode, generally the maximum dimensions in the planes perpendicular to the direction of the vibrations may not exceed one quarter to one third of the wavelength of these vibrations, when a plane wave front is to be obtained. If these dimensional limits are not observed, the amplitude of the vibrations at the output surface is greater at the center than at the periphery (amplitude fall-off). Attempts to obtain a plane wave front at the output surface using a number of transducers at places on the input surface at distances smaller than the limiting dimensions mentioned above, failed. For reason of cross-coupling of waves (caused by Poisson's constant ν) to the generated vibrations at the nodal planes caused complex vibrations so that no in phase vibration and no uniform amplitude at the output could be obtained. (Kleesattel (1963)).
The invention of Kleesattel e.o. is to provide the resonator with *slots* extending therethrough at right angles to the input and output surfaces so that the slots break the cross-coupling between the sections of the resonator. The sections act as individual resonators with lateral dimensions not exceeding the design limits.
A resonator with one large output dimension (blade-like) is shown in figure 4.1a.
The sections are connected by narrow connecting bridges adjacent to the output and input surfaces. If the resonator is in the form of a rectangular block with large side dimensions, then the slots for breaking the cross-couplings can be in a grid arrangement (see figure 4.1b). (Kleesattel (1963)).

In Kleesattel's publication a transducer is connected to each of the sections to transmit vibrational energy. However in most industrial applications today, only one transducer is coupled at the center of the input surface (see for example figure 4.5).

The maximum width of a blade-like resonator is limited. For some applications a very wide working dimension may be needed. However, when increasing the effective working dimension of the resonator beyond a certain value, the costs of producing such a resonator increase disproportionally to become prohibitive (Long (1973)), Kleesattel's solution gives practical solutions from three inches to ten inches (75-250 mm).
More convenient is the use of a plurality of resonators of relatively small dimensions as shown in figure 4.2.

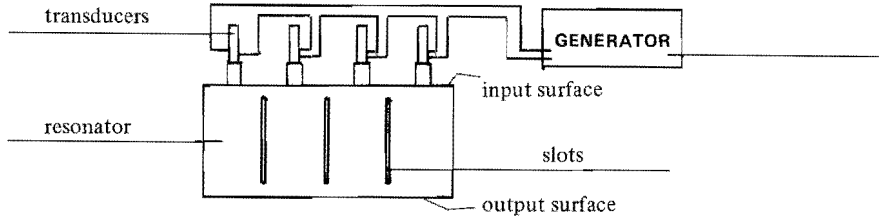

Fig. 4.1a: Resonator provided with slots to avoid cross-coupling (Kleesattel (1963)).

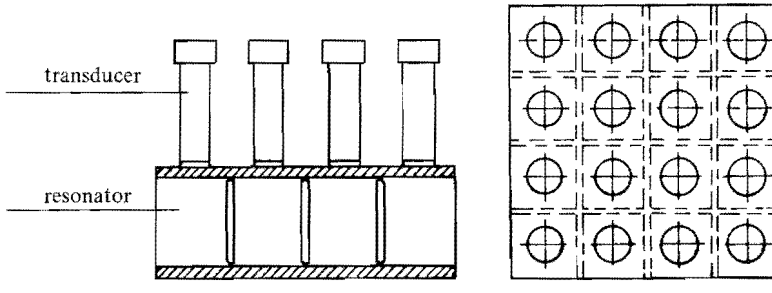

Fig. 4.1b: Resonator with large dimensions in two directions; slots in a grid arrangement (Kleesattel (1963)).

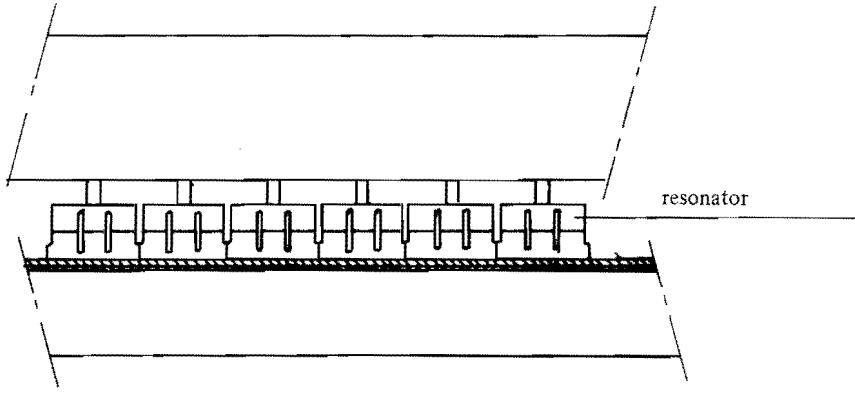

Fig. 4.2: Arrangement of six resonators to cover very wide working dimensions (Long (1973)).

The use of slots to interrupt cross-couplings will not always be a solution of practical value. In practice it is sometimes found, that it is not only difficult to machine slots of the type as suggested before, but when using certain materials such as titanium, the machining of slots is time consuming and expensive. It has been suggested to provide a less expensive means for breaking cross-couplings by internal holes or bores parallel to the direction of the longitudinal vibration and extending across the nodal plane of the resonator (see figures 4.3a and 4.3b). (Biro (1971)).

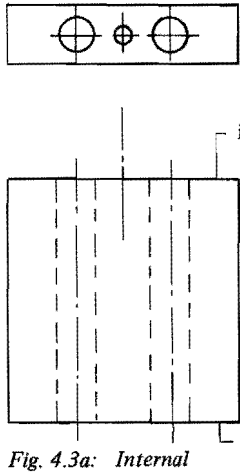

Fig. 4.3a: Internal bores to break cross-couplings (Biro (1971)).

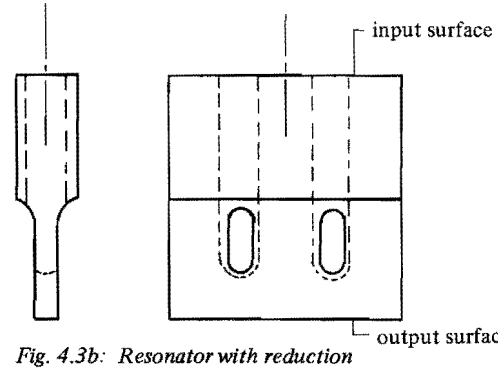

Fig. 4.3b: Resonator with reduction in the cross-section to increase the output amplitude (Biro (1971)).

The resonator is designed so that its dimensions from the input surface to the opposite output surface correspond to an integral number of half wavelengths of the vibration. However, no information is given with respect to the positioning of the bores. Instead of one large bore, a multiple set of small bores is said to be possible. Figure 4.3b gives an example of a resonator with an increased output amplitude; a bore results into a slot in the reduced cross sectional area.

In the same way as described hitherto cylindrical resonators can be made to resonate in a longitudinal mode. Above a certain diameter slots and/or holes are to be provided to avoid cross-couplings. An example of such a resonator is shown in figure 4.8b.

4.3. Influencing the output vibration amplitude

Up to now blade-like and rectangular block resonators have been discussed. Where for example plastic welding along a circular ring is needed with a resonator having a diameter larger than a quarter to a third of the wavelength of the vibration, such expedients as hollowing out the resonator to provide a bell-shaped structure having longitudinal slots through the bell wall and extending along the length of the bell are used (see figure 4.8b). Great difficulties are encountered in obtaining a uniform distribution of vibration amplitude over the output surface of the resonator.

It was suggested by Davis (1978) that a solid cylindrical resonator with large diameters can be used without the use of slotting or other expensive machining operations. Generally a solid resonator will show a smaller amplitude in the peripheral area compared to the center of the cylinder. By providing a groove in the outer surface of a large solid resonator extending about the body, preferably near the middle zone of the resonator length, the amplitude at the peripheral area can be increased.
The so-called "accordion-horn" is shown in figure 4.4a.
The width and depth of the groove is small in comparison with a quarter wavelength at the operating frequency. Figure 4.4b shows the influence of the location of the groove on the amplitude distribution at the output surface. As an example, at 20 kHz resonators with a diameter between 100 and 175 mm suffer a non-uniform amplitude distribution. The groove is said to compensate for this effect.

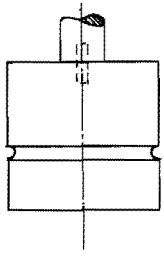

Fig. 4.4a: "Accordion horn" with a groove in the outer surface (Davis (1978)).

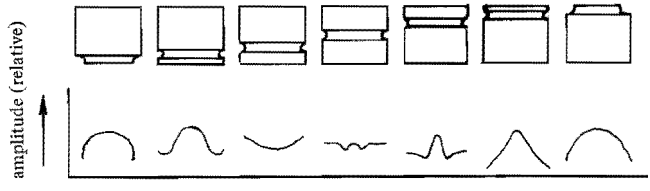

Fig. 4.4b: The influence of groove location on the amplitude at the output surface (Davis (1978)).

In general the designer of a resonator will aim at obtaining a uniform amplitude distribution at the output surface. The use of slots as taught in Kleesattel's patent (1963) is a main contribution to this purpose. However, sometimes it is desired to have smaller amplitudes at certain regions of the output surface. As an example, an apparatus for simultaneously welding and cutting textile material (Grgach (1976)), requires a small amplitude at the lateral edge regions of the resonator to reduce wear problems and to greatly reduce in magnitude audible chatter. Here the aim is a blade-like resonator which exhibits a non-uniform motional amplutide along its output surface (see figures 4.5a and 4.5b).
The reduction of amplitude as shown in figure 4.5b is achieved by providing two notches at the input surface of the resonator, one on each side. The significant reduced amplitude is 20 to 30 percent of the amplitude in the center portion.

In figure 4.5c an alternative way is shown where in the rear portion of the resonator is provided with a cutout section extending a quarter wavelength from the input surface. Additionally two slots are provided extending from the output surface, a quarter wavelength toward the input surface. A resonator, 216 mm long, showed an amplitude at the edges of about a quarter of the center region amplitude (Grgach (1976)). However, the results of the slots is that flexural vibrations are generated in the studs in a direction perpendicular to the direction of the longitudinal motion. There are means to damp these flexural vibrations by mechanical actions (Grgach (1976)).

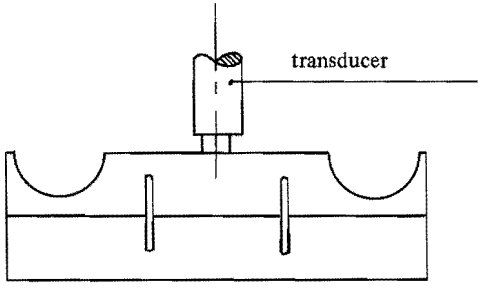

Fig. 4.5a: Notches at the input surface reduce the amplitude at the output surface (blade-like resonator) (Grgach (1976)).

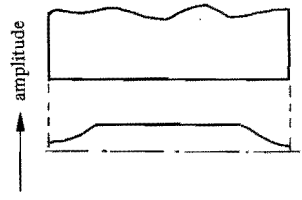

Fig. 4.5b: Reduction of the amplitude at the lateral edges (shown is the amplitude distribution along the width of the resonator of fig. 4.5a. (Grgach (1976)).

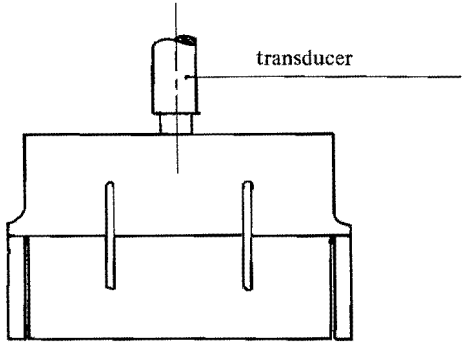

Fig. 4.5c: Narrow slots at the edges and cutout sections are provided to reduce the output amplitude near the edges (Grgach (1976)).

When using blade-like resonators, above a certain width, it is said to be impossible to obtain a uniform amplitude distribution along the output surface. As an example at 20 kHz a resonator of 500 mm width, shows a uniform amplitude along 200 mm symmetrical to the central axis, and a significant reduction at the outer regions (Scotto (1974)). During welding operations bad energy transmission is observed at the outer regions. By providing mechanical filters of half-wavelength onto the resonator the amplitude reduction can be eliminated (see figure 4.6a and 4.6b).
These filters are preferably positioned in the region of amplitude reduction, either by screwing, welding or glueing. The filters may be of any shape or material, provided that their resonance frequencies of the longitudinal mode do coincide with those of the wide resonator and the transducer.

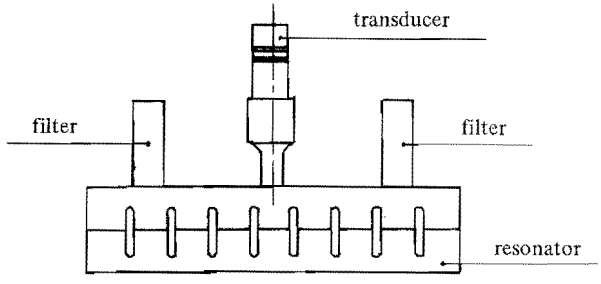

Fig. 4.6a: The use of mechanical filters or half wavelength resonators to eliminate amplitude reduction (Scotto (1974)).

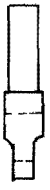

Fig. 4.6b; Cross section of fig. 4.6a.

Ultrasonic plastic sealing techniques use vibrational motion perpendicular to the surface of the materials to be joined; relatively little heat is produced by such motion in the joint and the seal is effected at low temperature and high pressure. In contrast in ultrasonic metal welding large heat build-up occurs due to a shear mode of vibration (in the same plane as the surface of the materials to be joined). For sealing thin sheets of plastic materials it is advantageous to combine both types of motion simultaneously (in shear and perpendicular to the surface).
A resonator providing the desired bi-directional ultrasonic vibration is described (Balamuth (1966)). Figure 4.7a shows a resonator with the well-known slots, but formed to provide a seal along a S-shaped configuration. The lower section is provided with a relatively thin lip portion extending along the entire width of the resonator and in such a way as to produce an asymmetry or mass unbalance with respect to the vertical plane through the centre of the resonator (figure 4.7b). The result of this unbalance is an elliptical vibration at the tip, the magnitude of the amplitudes depending on the mass. According to the same principle a cylindrical resonator is provided with a plurality of slots evenly spaced about the circumference (figure 4.7c).

Blade-like resonators which suffer an amplitude fall-off at the outer edges, are the subject of the invention presented by Holze (1982). A stepped resonator is designed to produce a large output amplitude, the amplitude gain being somehow proportional to the masses at both sides of the nodal plane of the longitudinal vibration in the resonator. It is suggested that the amplitude gain should be increased along the resonator width to compensate for the amplitude fall-off. The way to achieve this is shown in figure 4.10. The masses of the upper portion at the lateral sides are enlarged by addition of an extra mass at the input surface. This solution is said to reduce a fall-off from 15% to only 2% for resonators of 150 to 230 mm width. The studs can be up to 12 mm high. It is mentioned that the resonance frequency of the resonator will change, and a tuning procedure is necessary.

4.4. Coupling of resonators to a multiple resonator system

The lateral dimensions of blade-like, block-like and cylindrical resonators are limited. At 20 kHz ultrasonic frequency resonators with widths above 350 mm and diameters above 300 mm are difficult to produce.

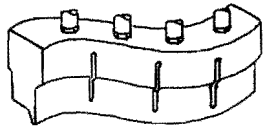

Fig. 4.7a: S-shaped resonator with lip portions at the output surface (Balamuth (1966)).

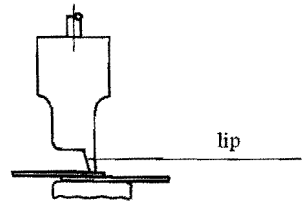

Fig. 4.7b: Mass unbalance causes elliptical motion near the welding area (amplitudes depend on the mass of the lip (Balamuth (1966)).

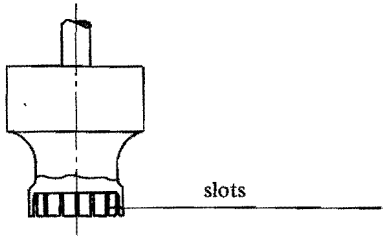

Fig. 4.7c: Cylindrical resonator with a plurality of slots to produce bidirectional motion (Balamuth (1966)).

Using more ultrasonic resonator systems, pieces with large dimensions can be welded. To overcome this problem partly it is suggested to use a multiple resonator system (Scotto (1974)). Characteristic is an extra resonator with wide output cross section to the output surface of which two or more large resonators are coupled. They are resonating in the longitudinal mode at the same frequency. Figure 4.8a shows a coupling of blade-like resonators. The resonator assembly in figure 4.8b is composed of a blade-like resonator with two cylindrical resonators coupled to it, covering an area of 500 x 225 mm^2 if e = 280 mm.

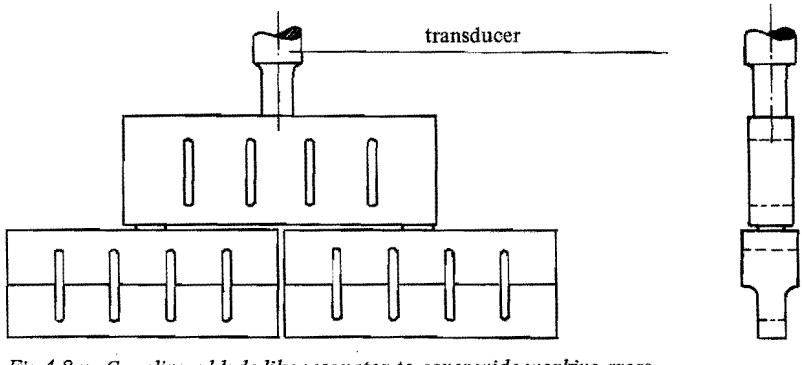

Fig.4.8a: Coupling a blade-like resonator to cover wide working areas (Scotto (1974)).

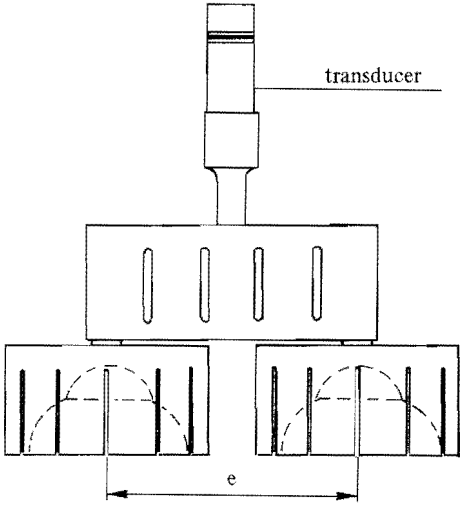

Fig. 4.8b: Arrangement of a blade-like resonator with two cylindrical resonators (bell-shaped) (Scotto (1974)).

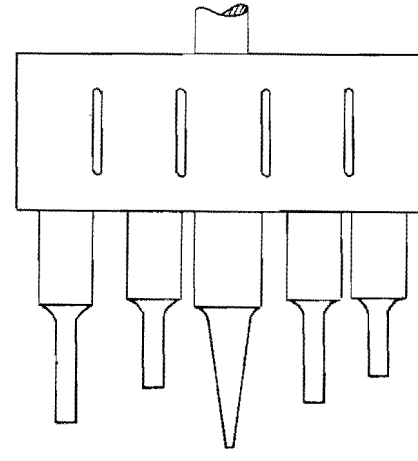

Fig. 4.8c: Coupling of many small resonators (of different length) to a wide blade-like resonator (Scotto (1974)).

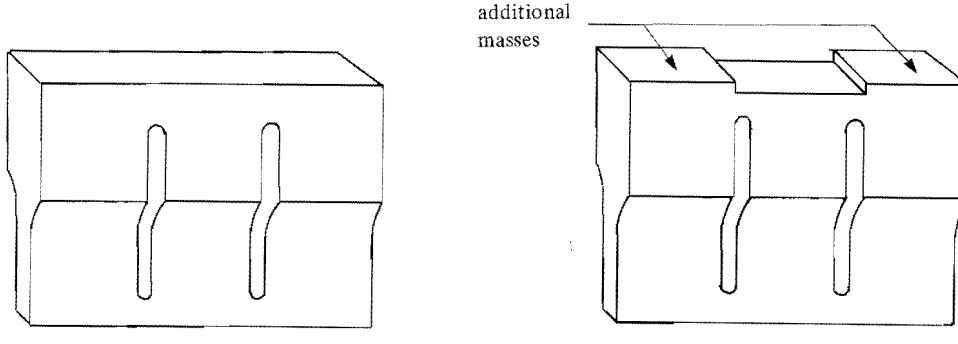

Fig. 4.9: Blade-like resonators with additional masses at the input surface to compensate for amplitude fall-off. (Holze (1982)).

The cylindrical resonators are provided with slots, slightly different from Kleesattel's proposals, and an internal bore. It is also possible to use a wide blade-like resonator to transmit ultrasonic energy to a multiple set of resonators with different length and lateral dimensions, but resonating at the same frequency (see figure 4.8c). Such an apparatus is adequate for welding at various heights in one single product.

4.5. Some remarks

The designer of resonators for ultrasonic high power applications may employ one of the principles mentioned above, to influence either vibrational modes or the energy transmission to the output surfaces. In practice many more, mostly unpublished techniques for providing slots, bores or cutt-offs into a resonator at arbitrary places, will be encountered. It is believed, however, that the survey given convers the basic principles most commonly to be dealt with.

5. SOLID CYLINDRICAL RESONATORS

5.1. Introduction

The use of slender rods as half-wavelength resonators has been discussed in chapter 2. When the lateral dimensions are no longer small as compared to the wavelength, the wave propagation is not uniform in a cross-section perpendicular to the direction of the wave propagation. This results in non-uniform output amplitudes when designing resonators. A second result is that the wave propagation velocity decreases due to this dispersion effect. In the next chapter the solid cylindrical resonator will be studied to evaluate its applicability in ultrasonic high power applications. Of practical interest are cylindrical resonators for which the diameter to length ratio is between zero and unity. It is the objective to find formula to calculate the resonance conditions for the longitudinal mode in the cylinder. The presence of other vibrational modes which could interfere with the longitudinal one is to be investigated.
Finally, a number of cylindrical resonators have been analyzed experimentally. The coupling of a resonator to a transducer of a welding apparatus will cause its resonance frequencies to shift. Some frequencies will even disappear. Amplitude measurements are carried out to measure the uniformity of the amplitude of the output surface, and from it conclusions are drawn up to what diameters the deviations are within the acceptable range ($< 10\%$).

5.2. Literature review

The studies of vibrations in solid cylinders of finite length are often related to practical problems. The application of solid cylinders in underwater transducers requires the understanding of the frequency characteristics in that range in which the cylinders themselves have natural modes of vibration and cannot be considered as lumped mass anymore (McMahon (1964)). A second example is the need for understanding the modes of vibration in cylinders for gravitational wave detectors (weighing several tons) (Rasband (1975)). In the present work the understanding of the modes is essential for designing efficient ultrasonic resonators.
In general we will have to solve the three dimensional equations of the linear theory of elasticity when we want to study small vibrations of elastic rods. This will not lead to difficulties when the rod is of infinite length. Equations giving a solution were first formulated by Pochhammer (1876) and Chree (1884) and an exploration of these equations was first undertaken by Bancroft (1941).
Bancroft presented the decrease of the wave propagation velocity c as function of the diameter to wavelength ratio in the infinite cylinder for some values of Poisson's ratio. The only experimental work that has been referred to in literature on the vibrations of solid cylinders of finite length has been worked out thoroughly by McMahon (1964). Until then no existing theoretical analysis was adequate to predict the natural frequencies of solid cylinder of finite length with diameter to length ratios up to unity. The introduction of a method for axisymmetric solutions was done by Hutchinson (1967) (1972). His procedure is based on choosing a series of functions with unknown coefficients which satisfy the governing equations and boundary conditions. Even for the simplest cases of a solid cylinder the method is cumbersome. A method for approximate solutions was presented by Rumerman (1971) to compute natural frequencies in both solid and hollow cylinders, based on the expansion of the displacements in series of functions which correspond to the modes to be be expected in the cylinder.

The first paper on non-axisymmetric vibrations of finite cylinders was presented by Rasband (1975). However, no numerical data are available here. Finally, the complete discription of vibrations in solid cylinders was published by Hutchinson (1980). The numerical results show complete agreement with the experimental results of McMahon (1964).

All theoretical analyses mentioned above are far from easy in analytic formulation and the generation of numerical results requires much computer time. For practical use these exact solutions are inaccessible. Fortunately, the finite element analysis packages available today are a good alternative.

For the design of ultrasonic resonators the longitudinal mode in the solid cylinder is of interest. In the next an approximate, simple formula will be derived to calculate the resonance frequency of this mode for a given cylinder. It is based on assumptions suggested by Mori (1977) that the actual longitudinal mode can be considered to be the result of a coupling of the longitudinal wave solutions in slender rods to those for the radial vibrations in thin discs.

5.3. Cylinder dimensions of interest

In chapter 3 it was discussed that the diameter d of cylindrical resonators is between 0 and 200 mm at an operating frequency of 20 kHz. Up to diameters of 60 à 80 mm the length l of the cylinder equals the half-wavelength $\lambda/2$. Depending on the material $l = 120$ à 130 mm. Above $d = 80$ mm the resonators very often are slotted and a resonance condition is found at length $l = 110$ à 130 mm. At other frequencies (40 or 60 kHz) similar limitations to the dimensions are found.

Using the wavenumber k (see equation 2.3) the cylinder dimensions of interest can be presented in a non-dimensional notation. At 20 kHz the diameter range of interest is: $60 < d < 200$ mm, and the length is in the order of $l = 130$ mm.
So the non-dimensional frequency parameter (which is referred to the diameter) kd is between: $1.5 < kd < 5$ and the length to diameter ratio l/d is between: $0.6 < l/d < 2$.

5.4. Experimental studies of the vibrations of solid cylinders by McMahon (1964)

The vibrations of twenty of the graver modes in solid aluminium and steel cylinders were studied experimentally by McMahon (1964), covering cylinders having length to diameter ratios between $0 < l/d < 1.7$ and for frequency parameters between $1.2 < kd < 6.2$. These values almost completely do cover the range of interest for the design of ultrasonic cylindrical resonators.

The cylinder characteristics are shown in figure 5.1. Referring to the cylindrical coordinates r, θ and z, the cylindrical surface is at $r = d/2$ and the plane surfaces are at $z = \pm l/2$. The radial, tangential and axial displacements are u, v and w respectively. The mode of the longitudinal vibration is shown in figure 5.2 (on an enlarged scale). The modes of the vibrations observed by McMahon are presented in figure 5.3. The modes are classified according to the circumferential and longitudinal symmetry of the vibrations. Radial displacements are proportional to $\cos(n\theta)$ and the circumferential order n indicates the symmetry with respect to rotation about the axis of the cylinder. Modes are longitudinally symmetric or anti-symmetric if the radial and tangential displacements are symmetrical $u(z) = u(-z)$ or anti-symmetrical $u(z) = -u(-z)$ about the median plane of the cylinder.

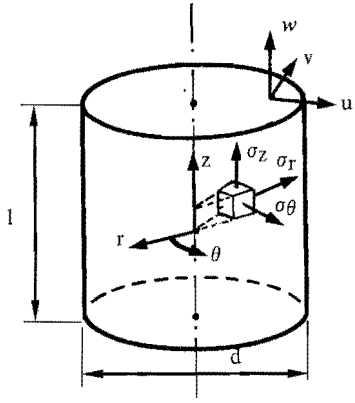

Fig. 5.1 Cylinder of length l and diameter d; definition of symbols

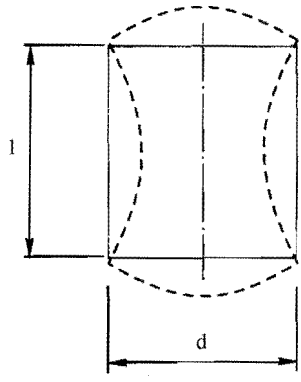

Fig. 5.2 Mode of the longitudinal vibration in the cylinder (axially symmetric)

McMahon denotes symmetric modes by even numbers and anti-symmetric modes by odd numbers.

Figure 5.3 shows the approximate form of the vibrations at a diametrical cross-section. Heavy lines represent nodes on the surface of the cylinder and arrows show the directions along which fine sand (sprinkled on the horizontally placed cylinder surface) moves toward the nodal lines. Where no arrows are shown it moves directly to the nodes.

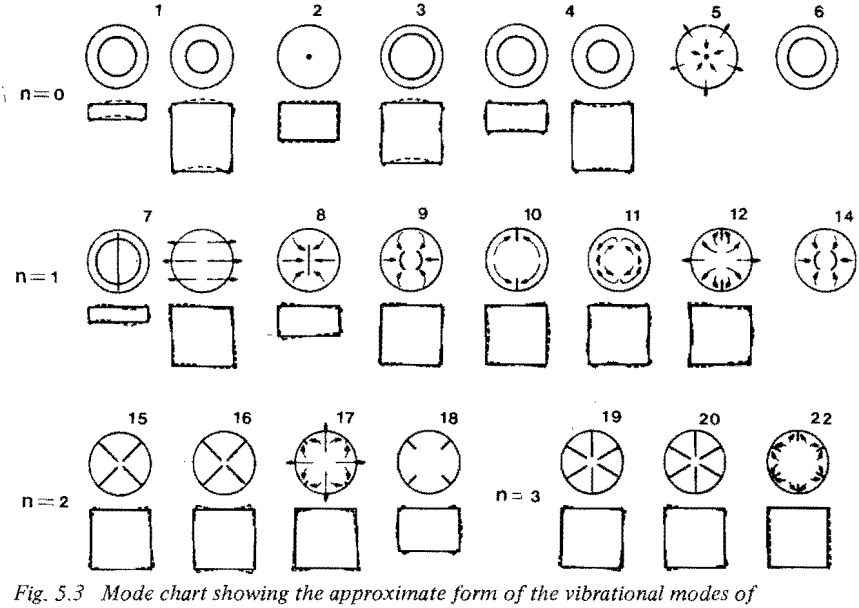

Fig. 5.3 Mode chart showing the approximate form of the vibrational modes of cylinders at a diametrical cross-section and the nodal lines on the surfaces. The circumferential order n indicates symmetry in radial direction. Even mode numbers are symmetric and odd mode numbers are anti-symmetric about the median plane of the cylinder (McMahon).

Figures 5.4, 5.5, 5.6 and 5.7 show the frequency spectra determined experimentally by McMahon. For all modes of vibrations according to the numbers in figure 5.3 the non-dimensional frequency parameter kd is presented versus the length to diameter ratio l/d. These frequency spectra are valid for aluminium cylinders, where $\nu = 0.344$ and $c = 5150$ m/s (McMahon).

We will now use these results to observe the problems that can be encountered when designing a solid cylindrical resonator for ultrasonic welding applications. All modes, except mode 2, show at least one nodal line at the output surface and therefore do not meet the requirement that for a well-designed resonator the output amplitude along the surface must be as uniform as possible. The longitudinal mode in the cylinder as shown in figure 5.2 is denoted in figure 5.3 as mode number 2. The frequency spectrum of figure 5.4 shows mode branch 2. For small values of the length to diameter ratio ($l/d < 0.2$) this mode corresponds to the radial mode of vibrations in thin discs ($kd \approx 4.4$). For large values of l/d ($l/d > 1.5$) this mode is the half-wavelength longitudinal mode in slender rods (see chapter 2). Here the mode branch converges in the spectrum to $kd\frac{l}{d} = \pi$ (following equation 2.6). As the range of interest ($0.6 < l/d < 2$) is almost completely covered by McMahons work, the resonance frequency for any cylinder dimension for the longitudinal mode can be determined from figure 5.4.

From the frequency spectra one can find those cylinder dimensions l/d for which mode branch 2 is crossing any other branch, and where interference of these modes will occur in the cylinder. From figure 5.4 it is clear that for $\frac{l}{d} \approx 0.77$ mode 2 will interfere with mode 1 (see figure 5.3).
Other crossings are found for modes 7 ($l/d \approx 1.25$), mode 16 ($l/d \approx 0.97$), mode 15 ($l/d \approx 1.18$), mode 20 ($l/d \approx 0.2$) and mode 19 ($l/d \approx 0.66$).
Figure 5.5 also reveals that modes 7 and 8 are closely coupled to mode 2 over a large range. This means that when designing a resonator at least three resonance frequencies will be measured very close to each other.
To conclude, there is no value of l/d for which the difference between the resonance frequency of the longitudinal mode and that of any other is larger than 10%. If in a specific resonator the resonance frequency of any of the unwanted (spurious) modes is too close to the longitudinal one (according to own experiences when the difference is less than 5%) the frequency spectra can be very helpfull to learn what dimensions have to be changed to improve the situation.

In the next formula will be presented to calculate the resonance frequency of the longitudinal mode for any length to diameter ratio.

5.5 Rayleigh's correction to the wave propagation velocity

The propagation velocity c of longitudinal waves in cylinders will decrease for increasing diameters. Lord Rayleigh presented a correction formula for the wave propagation velocity in cylinders that compensates for the finiteness of the diameter. The formula is accurate up to diameter to wavlength ratios of 0.4. It will be used here to calculate part of the mode branch 2 in figure 5.4. The corrected propagation velocity c' (see appendix 2 for the derivation) for a cylindrical resonator equals:

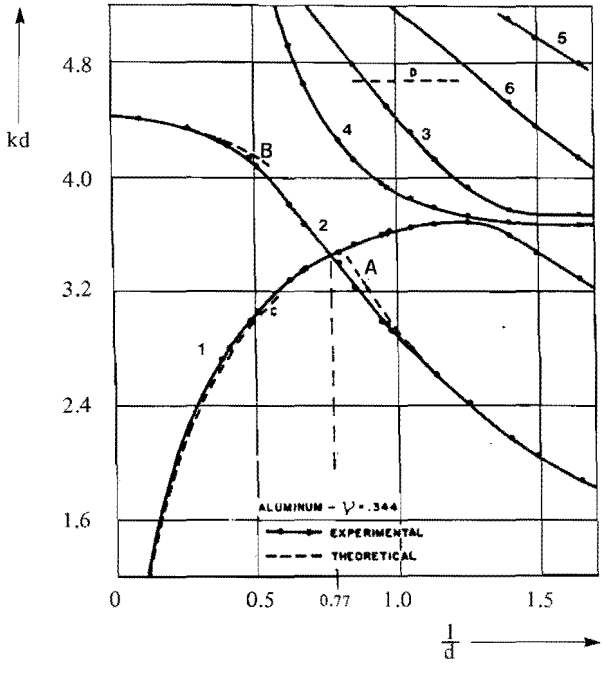

Fig. 5.4 Frequency spectra for modes of circumferential order n = 0, mode numbers according to figure 5.3 (McMahon).

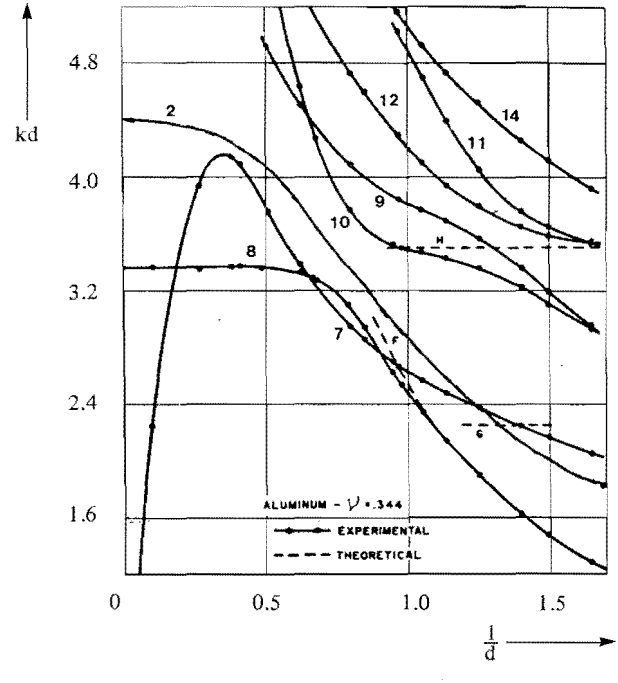

Fig. 5.5 Frequency spectra for modes of circumferential order n = 1, mode numbers according to figure 5.3 (McMahon)

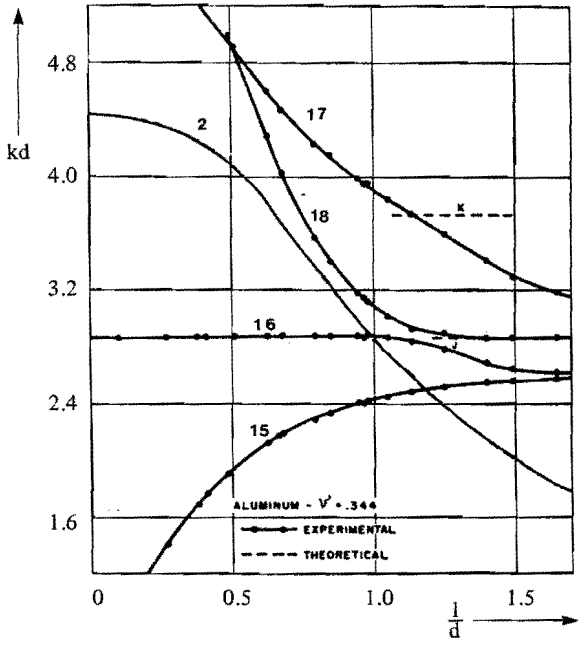

Fig. 5.6 Frequency spectra for modes of circumferential order n = 2, mode numbers according to figure 5.3 (McMahon)

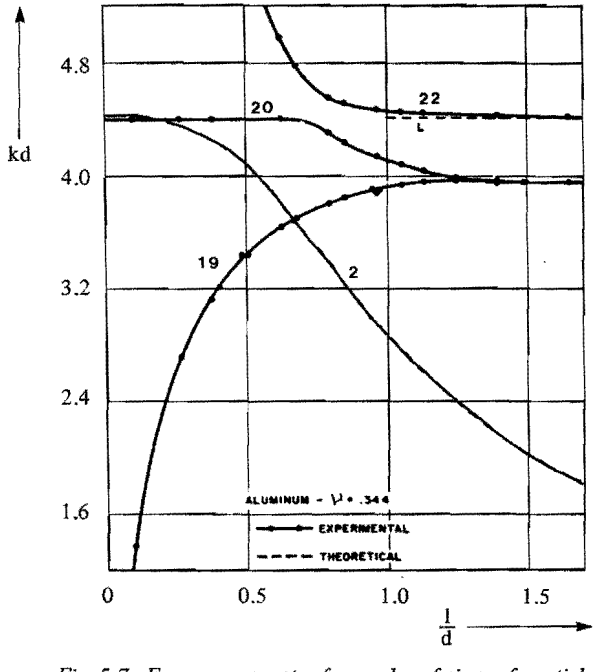

Fig. 5.7 Frequency spectra for modes of circumferential order n = 3, mode numbers according to figure 5.3 (McMahon)

$$c' = c\,(1 - (\frac{\nu \pi d f}{2c})^2) \qquad (5.1)$$

where: ν : Poisson's ratio (–)
d : diameter of cylinder (m)
f : frequency of the vibration (s^{-1})

In figure 5.4 (curve A, dotted line) the calculated resonance frequency with equation (5.1) is shown. A similar correction formula exists for the radial vibrations in discs (curve B in figure 5.4).
In order to compare this correction formula with the results which will be presented in the next, equation (5.1) is rewritten in non-dimensional form, relating the cylinder length l and the diameter d.
The cylinder length l for the longitudinal mode equals (using equations (2.6) and (5.1)):

$$l = \frac{c'}{2f} \qquad (5.2)$$

Using the wavenumber $k = \frac{\omega}{c}$ and equation (2.6), the non-dimensional length kl is related to the non-dimensional diameter kd as follows:

$$kl = \pi \frac{c'}{c} = \pi\,(1 - (\frac{\nu\, kd}{4})^2) \qquad (5.3)$$

Figure 5.8 shows this correction to the resonator length versus the diameter (Poisson's ratio $\nu = 0.344$ in order to compare it to McMahon's results).

5.6. Approximate theory for the calculation of the resonance frequency of the longitudinal mode

McMahon (1964) investigated the relation between the cylinder length and diameter experimentally whereas Hutchinson (1980) elaborated analytic solutions with large computer effort. An approximate theory to calculate the resonance conditions for the longitudinal mode in a cylinder for a wide range of the length to diameter ratios, resulting in simple formula would be of great value for practical use. Mori (1977) suggested a way to derive such a formula. Mori presented the results graphically and did only derive part of the approximate theory in his paper. We will now present the approximate theory and derive the formula.

Mori's theory is based on the assumption that the actual vibrational mode of the longitudinal wave in a cylinder for which the diameter to length ratio is near unity, can be considered as an interaction of two orthogonal waves. One being the longitudinal wave in slender rods, the other the radial extensional wave in thin discs.
The interaction of the two waves is realized by introducing a wave coupling factor m, which is based on certain assumptions to the stresses in the cylinder, which are explained below.

The resonant length of the cylinder for small diameters was derived in chapter 2 (equation 2.6):

$$kl = \pi \qquad (5.4)$$

where $k = \omega\sqrt{\frac{\rho}{E}}$, the wavenumber.

The wave equation for harmonic vibrations in thin discs, according to the definitions in figure 5.1 equals (Gladwell (1967)) (where u is the radial amplitude).

$$\frac{d^2u}{dr^2} + \frac{1}{r}\frac{du}{dr} - (k_r^2 + \frac{1}{r^2})\,u = o \tag{5.5}$$

Where the wavenumber k_r for radial vibrations is defined by $k_r = \omega \sqrt{\frac{\rho(1-\nu^2)}{E}}$
Solutions for the axisymmetric radial vibrations in thin discs, for the fundamental radial extensional mode, yield the following equation:

$$\frac{k_r d}{2} J_0 (\frac{k_r d}{2}) = (1 - \nu) J_1 (\frac{k_r d}{2}) \tag{5.6}$$

Where J_0 and J_1 are the zero and 1-st order Bessel functions of the first kind. The first root of equation (5.6) is (Kleesattel (1968)):

$$\frac{k_r d}{2} = a \tag{5.7}$$

The solutions for a depend on Poisson's ratio. In Kleesattels paper a is presented graphically. It can be approximated by:

$$a = 1.84 + 0.68\nu \tag{5.8}$$

Now we have to find a theory to couple the solutions of equations (5.4) and (5.7). For the derivation of equation (5.4) it was assumed that in the slender rod both radial and tangential stresses are zero ($\sigma_r = 0$ and $\sigma\theta = 0$). It is proposed by Mori that with increasing diameters, σ_r and $\sigma\theta$ will increase and can be approximated by:

$$\begin{aligned} \sigma_r &= \frac{1}{m}\sigma_z \\ \sigma\theta &= \frac{1}{m}\sigma_z \end{aligned} \tag{5.9}$$

Using Hooke's law, the axial strain ϵ_z then follows:

$$\begin{aligned} \epsilon_z &= \frac{1}{E}(\sigma_z - \nu(\sigma_r + \sigma\theta)) \text{ or} \\ \epsilon_z &= \frac{1}{E}\sigma_z (1 - \frac{2\nu}{m}) \end{aligned} \tag{5.10}$$

According to Mori an apparent elasticity for the vibrations in axial direction is defined by:

$$E' = E (1 - \frac{2\nu}{m})^{-1} \tag{5.11}$$

In fact, this is identical to a decrease of the wave propagation velocity. The corrected resonator length due to this apparent elasticity follows from equation (5.4):

$$kl = \pi (1 - \frac{2\nu}{m})^{-1/2} \tag{5.12}$$

For the radial vibrations in thin discs it was assumed that the axial stress $\sigma_z = 0$. Again, Mori suggests to approximate the axial stress σ_z (with increasing thickness of the disc) using the same wave coupling factor m by:

$$\sigma_z = m\,\sigma_r \tag{5.13}$$

Using Hooke's law the radial and tangential strain ϵ_r and $\epsilon\theta$ follow:

$$\epsilon_r = \frac{1}{E}\,(\sigma_r\,(1 - m\nu) - \nu\sigma\theta)$$

$$\epsilon\theta = \frac{1}{E}\,(\sigma_\theta - \nu\sigma_r\,(1 + m)) \tag{5.14}$$

The radial stress σ_r is related to ϵ_r and $\epsilon\theta$ by:

$$\sigma_r = E(\epsilon_r + \nu\,\epsilon\theta)\;((1 - \nu^2) - m\nu\;(1 + \nu)) \tag{5.15}$$

The apparent elasticity for the radial vibrations is defined by comparing this stress relation to that for the case where $\sigma_z = 0$.
For the thin disc ($\sigma_z = 0$ and m = 0) the radial stress would produce:

$$\sigma_r = E\;(\epsilon_r + \nu\,\epsilon\theta)\;(1 - \nu^2) \tag{3.16}$$

So combining equations (5.15) and (5.16), the apparent elasticity for radial vibrations becomes:

$$E' = E\;(1 - \nu^2)\;((1 - \nu^2) - m\nu\;(1 + \nu))^{-1} \tag{5.17}$$

The corrected diameter would follow from equation (5.7) by introducing (5.17). For convenience the non-dimensional cylinder diameter is defined using the wave number k (instead of k_r). From equations (5.7), (5.16) and (5.17) it follows:

$$\frac{k\,d}{2} = a\;((1 - \nu^2) - m\nu\;(1 + \nu))^{-1/2} \tag{5.18}$$

Elimination of the wave coupling factor m from equations (5.12) and (5.18) results in a relation between cylinder length l and diameter d:

$$\left(\frac{kl}{\pi}\right)^2 = \frac{1 - (1 - \nu^2)\left(\frac{kd}{2a}\right)^2}{1 - \left(\frac{kd}{2a}\right)^2\;(1 - 3\,\nu^2 - 2\,\nu^3)} \tag{5.19}$$

In order to compare this approximate theory with McMahon's experimental results, the solution of equation (5.19) is plotted in figure 5.8 for Poisson's ratio $\nu = 0.344$. McMahon's results as shown in figure 5.4 (mode branch 2) are translated into figure 5.8 as well. Clearly, the apparent elasticity method deviates from McMahon's results, the mean difference is 3 à 6%.

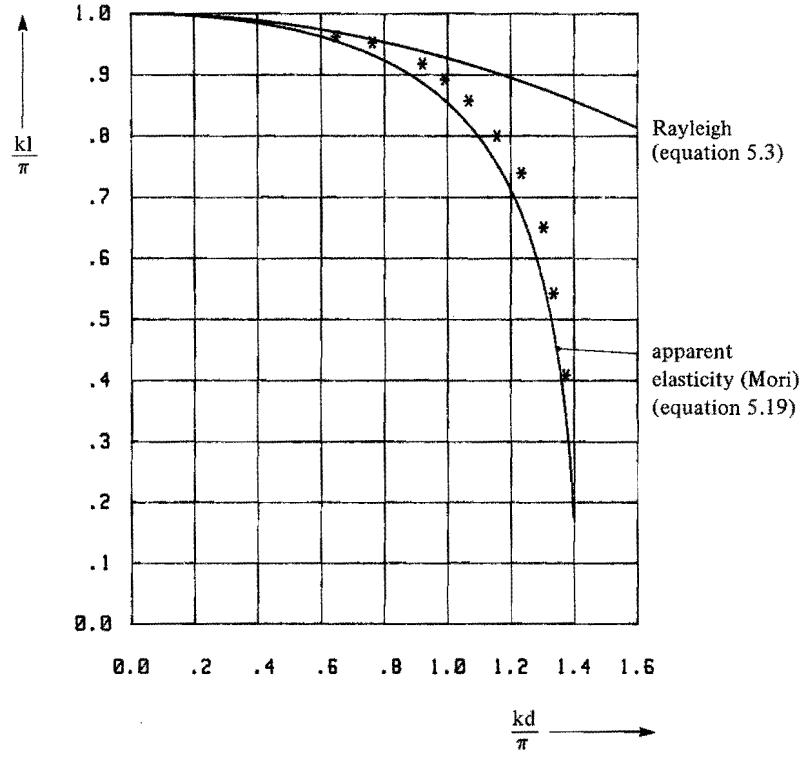

*Fig. 5.8 Non-dimensional representation of the cylinder length l versus the diameter d (Poisson's ratio ν = 0.344, * are points from McMahon).*

The solution of equation (5.19) has two asymtotic values which were already discussed ($\frac{kd}{\pi} \to 0$ gives the slender rod vibration and $\frac{kd}{\pi} \to 1.41$ gives the radial disc vibration). Mori's theory gives a too short cylinder when designing an ultrasonic resonator, which would result into too high resonance frequencies. However, the formula fairly well approximates the experiments and is easy to handle for practical applications.

The influence of Poisson's ratio on the cylinder dimensions are shown in figure 5.9. The nature of wave coupling is present by favour of Poisson's ratio; it is obvious that it strongly influences the solutions of equation (5.19).

According to Mori's approximate theory the length of aluminium cylindrical resonators has been calculated as function of the diameter for the longitudinal mode of vibration at frequencies of 20, 36, 40 and 60 kHz (these are frequently encountered in ultrasonic high power applications such as welding). The properties of the aluminium can be found in table 2.I.

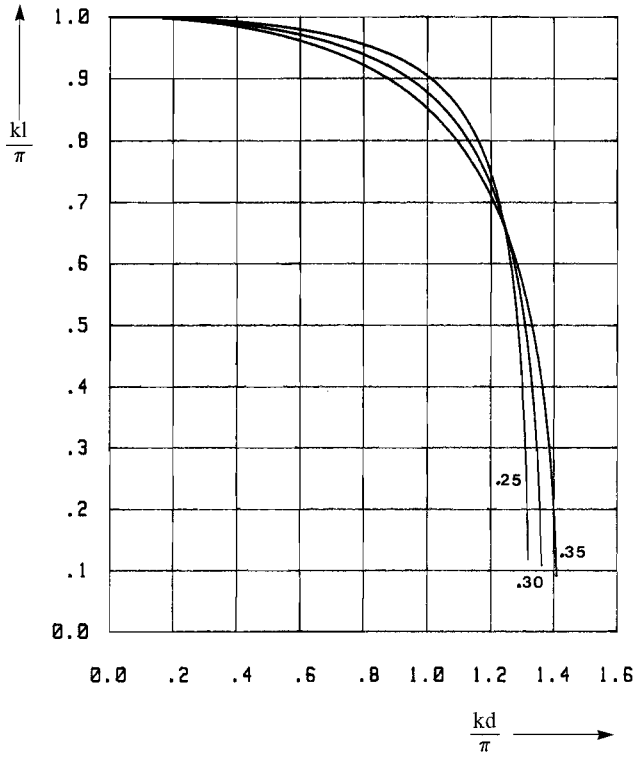

Fig. 5.9 Influence of Poisson's ratio ν on the cylinder length l and diameter d for the longitudinal vibrational mode (according to Mori's theory, equation (5.19)) (ν = 0.25, 0.30, 0.35).

Figure 5.10 shows the length to diameter relation for various resonance frequencies. The effect of variations in the wave propagation velocity c is shown in figure 5.4 at a frequency of 20 kHz.

5.7 Resonance frequency measurement of five cylinders

Five aluminium resonators have been designed in order to study the resonances in the solid cylinder. Table 5.I summarizes the dimensions of the cylinders which are designed to be in resonance in the longitudinal mode at 20 kHz. From the actual cylinder dimensions the resonance frequency was calculated from Mori's approximate theory, using equation (5.19). The deviation of the measured frequencies to the calculated ones is listed in table 5.I. Clearly the approximate theory gives frequencies of 1-2% below the measured ones (this is in accordance with the analysis above). The experimental values of McMahon are used to predict the frequencies of the cylinders with aid of figure 5.4. Although McMahon's results are based on $\nu = 0.344$, they still may be used for comparison. According the equation (5.19) the frequencies with $\nu = 0.344$ will be ± 0.3% lower with respect to those calculated with $\nu = 0.355$. The deviation of the measured frequencies to the results of McMahon are listed in table 5.I. If the differences of Poisson's ratio are considered, one can conclude that the approximate theory, McMahon's results and the own measurements are in good agreement.

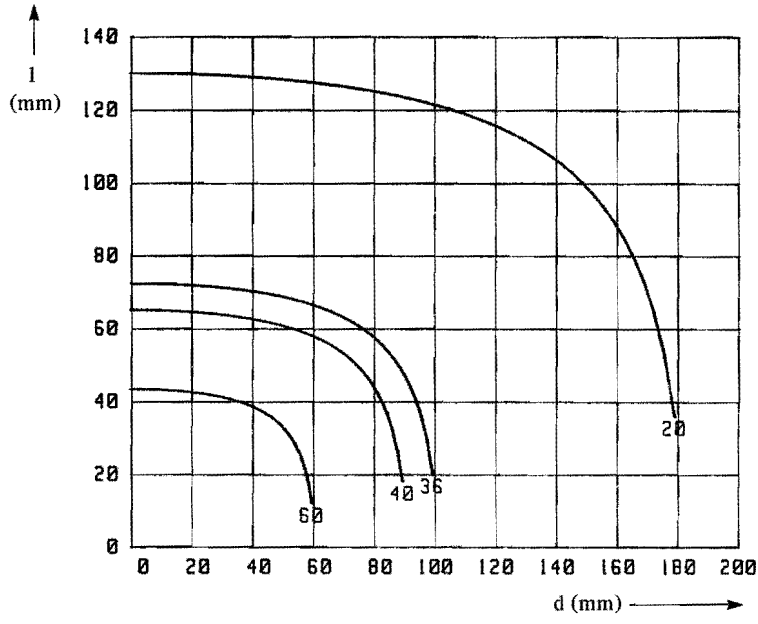

Fig. 5.10 Resonator length l versus the diameter d for various frequencies f (kHz). The material is aluminium c = 5200 m/s, ν = 0.335 (equation (5.19))

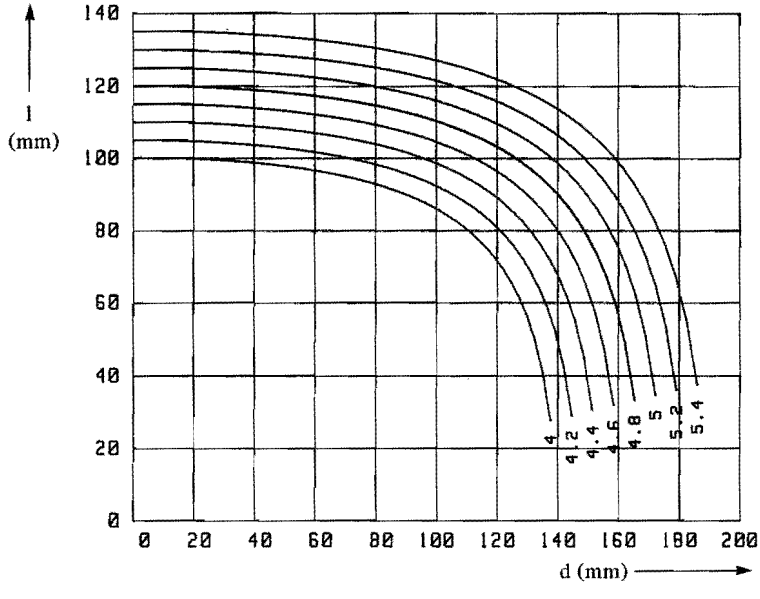

Fig. 5.11 Resonator length l versus the diameter d for various values of the wave propagation velocity c (10^3 m/s). The frequency f = 20 kHz, ν = 0.335. *(equation (5.19))*

Nr.	d (mm)	l (mm)	l/d (–)	f (kHz) measured	f (kHz) theory	deviation	f (kHz) McMahon	deviation
1	80	126	1.57	20.20	19.86	+ 1.7%	20.00	+ 1 %
2	100	122	1.22	20.26	19.92	+ 1.7%	20.09	+ 0.8%
3	130	116	0.89	19.80	19.50	+ 1.5%	19.72	+ 0.4%
4	160	91	0.57	20.05	19.82	+ 1.2%	20.11	0.3%
5	165	74.3	0.45	20.34	20.48	+ 0.7%	20.63	– 0.7%

Table 5.I Resonance frequencies for the longitudinal mode in 5 cylinders; comparison of own measurements to Mori's theory and McMahon's experiments: material aluminium c = 5200 m/s, ν = 0.335. (McMahon's results are for ν = 0.344).

5.8 The effect of coupling to a transducer and spurious modes

In the solid cylinder various modes of vibration can occur. For certain cylinder diameter to length ratio's modes are coupled to the longitudinal mode. Spurious modes are all modes which occur in the cylinder and that are not the longitudinal design mode. For the 5 cylinders studied before (table 5.I) the resonance frequencies of all spurious modes which are close to the design frequency of 20 kHz, are determined from McMahon's results (figures 5.4 to 5.7), see table 5.II. McMahon's results were obtained experimentally. The vibrational mode shapes are classified according to the definitions in figure 5.3, and are given between parenthesis.

cylinder	1	2	3	4	5
diameter (mm)	80	100	130	160	165
frequency (kHz)	**20.00 (2)** 21.43 (7)	19.60 (7) **20.09 (2)** 20.14 (15) 22.90 (16)	17.80 (7) 17.80 (8) 18.30 (16) **19.72 (2)** 22.6 (1)	16.33 (1) 17.04 (7) 18.06 (8) 18.27 (19) **20.11 (2)** 22.45 (20) 23.17 (18) 23.78 (9)	16.64 (19) 16.75 (8) 19.73 (7) **20.63 (2)** 21.92 (20)

Table 5.II Resonance frequencies of spurious modes determined from McMahon's experiments as listed in figures 5.4 to 5.7. The numbers between parenthesis are the mode numbers.

The spurious modes were also determined by own experiments. The results are listed in table 5.III. Again the cylinder dimensions are those in table 5.I. It can be concluded that these measurements are in agreement with McMahon's results from table 5.II (again one has to remember that McMahon's data are for $\nu = 0.344$). Identification of the vibrational modes was difficult and not always unambiguous. Some modes could not even be detected. The number of modes near the 20 kHz is largest of the larger diameters. For diameters $d < 80$ mm no spurious modes are present when designing solid cylindrical resonators.

cylinder	1	2	3	4	5
diameter (mm)	80	100	130	160	165
frequency (kHz)				17.14	
			17.26	17.84	16.75
		19.47	17.70	19.48	19.37
	20.20	**20.26**	**19.80**	**20.05**	**20.48**
	21.56	22.26	22.00	23.73	21.83
			22.38		

Table 5.III Measurement of spurious modes in the aluminium resonators as defined in table 5.I.

When a resonator is coupled to the transducer and booster of a welding apparatus (see figure 5.12), some of the vibrational modes in the resonator will not be possible. The resonator-booster-transducer system will show resonances at frequencies corresponding to vibrational modes that are possible in the complete system only. When the resonator is coupled its boundary conditions differ from those of the free resonator. Only those modes in the resonator for which the mechanical impedance does match to that of the transducer-booster assembly, will also appear in the coupled resonator.

In table 5.IV the resonance frequencies of three coupled cylinders are given. The cylinders were coupled to a transducer-booster assembly which vibrates in the longitudinal mode at 20.30 kHz. Vibrational modes (1) and (2) according to McMahon's definition could be identified by sprinkling sand on the vibrating surfaces which moved to the nodal lines. From table 5.IV we can learn that all solid cylinders have been designed as good resonators in which the unwanted spurious modes are not close to the operating frequency of 20 kHz (it was discussed in chapter 1 and 3 that for optimum operation no spurious modes are allowed in a 1 kHz range about 20 kHz). However this result would not have been predicted from table 5.II. Obviously many modes disappear when the cylinders are coupled.

Comparing table 5.II and 5.IV one may conclude that only modes of order $n = 0$, which have no nodal lines crossing the contact area of coupled cylinder to the booster, preferably will be excited. However, one can imagine the transducer and booster vibrating in a flexural mode rather than the longitudinal mode. In that case modes of order $n = 1$ with one nodal line in the contact area will be possible in the complete system.

cylinder	3	4	5
diameter (mm)	130	160	165
frequency (kHz)	13.76 **19.73 (2)** 22.15 (1) 23.95	16.52 (1) **20.05 (2)** 23.52	15.31 **20.46 (2)** 23.75

Table 5.IV Resonance frequencies in the resonator-booster-transducer system; the vibrational mode number between parenthesis (booster-transducer have a resonance frequency at 20.3 kHz).

5.9 Amplitude measurements

Resonators are used to transmit vibrational energy. It is important to know how uniform the vibrational amplitudes are over their output surfaces. The five cylinders as presented in table 5.I were coupled to the transducer of a welding apparatus. The amplitudes along the cylinder surfaces were measured (with an optical detector, see chapter 2, with accuracy of ± 0.2 μm) while it was activated in its resonance frequency at an input amplitude w_o = 10 μm.
Figure 5.13 shows the typical shape of the longitudinal mode. A maximum amplitude is reached at the centre of the cylinder at the input and output surface (w_o) and at the midplane of the cylindrical surfaces (u_o). These maxima decrease towards the edges ($w_o \rightarrow w_e$ and $u_o \rightarrow u_e$, see figure 5.13). The dotted lines indicate the vibrational maxima at the positive and negative phase (half a period phase shift).

Both radial amplitudes u and axial amplitudes w are shown in figure 5.14 and 5.15 respectively. The amplitudes are normalised to the maxima u_o and w_o respectively.

With increasing diameter the output amplitude strongly decays from the centre towards the outer diameter. The available amplitude at $r = \frac{d}{2}$ as compared to the input amplitude is summarized in table 5.V (w_e/w_o).
If an amplitude decay of maximum 10% is acceptable, the maximum diameter for solid cylindrical resonators would be ± 60-70 mm at 20 kHz (extrapolation of the results in table 5.V).
In figure 5.14 it can be seen that for the largest diameters the amplitude shows an extremely sharp fall-off towards the outer diameter, resulting into a relatively small area of the output surface that can be used effectively. It certainly would be of no use to design cylindrical resonators of larger diameters to reach the largest effective area that is possible. For instance at d = 130 mm only 12% (up to d = 45 mm) of the area has an amplitude higher than 90% of the input amplitude, whereas at d = 80 mm this amounts to 65% (up to d = 65 mm).

The degree of coupling of the radial to the axial vibrations is expressed by $\frac{u_o}{w_o}$ in table 5.V. Strong radial amplitudes are measured for the largest diameters.
This is in agreement with the observation in the frequency spectra for the longitudinal

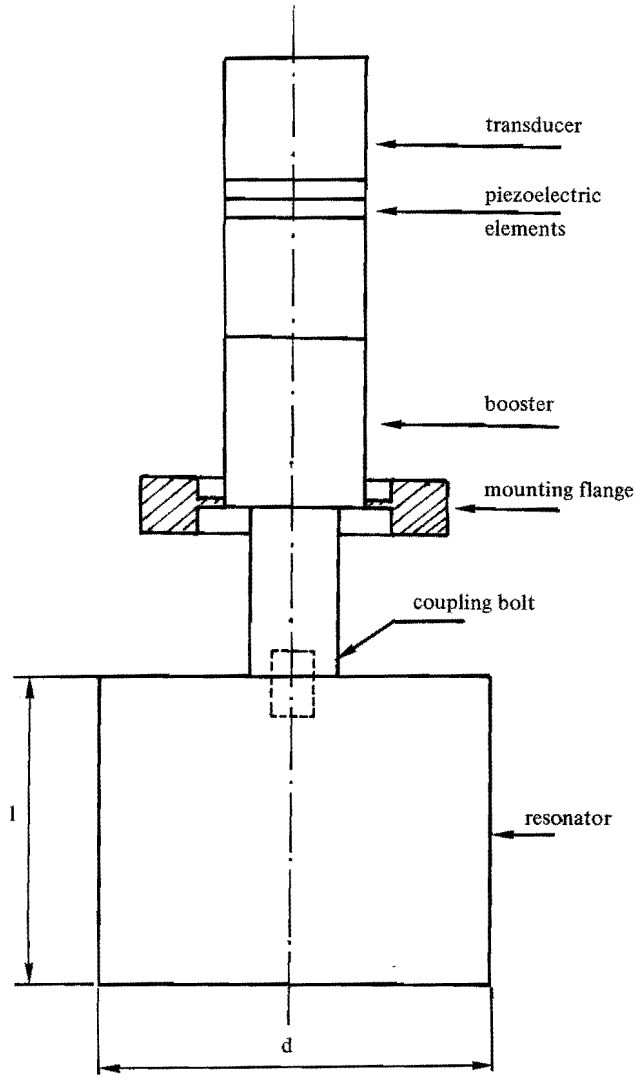

Fig. 5.12 Coupling of a resonator (solid cylinder) to a booster and transducer.

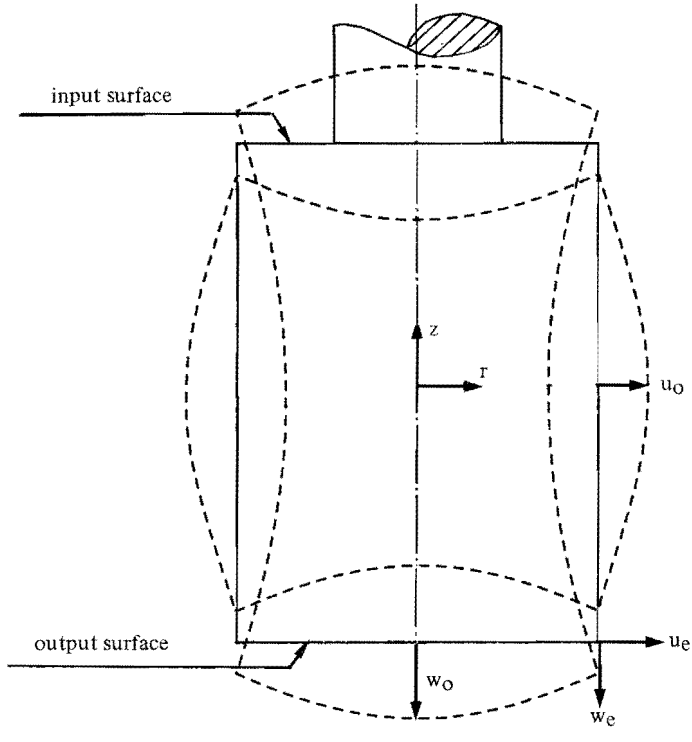

*Fig. 5.13 Typical shape of the longitudinal mode in a solid cylinder. (mode 2); amplification of the amplitudes shown 1000 *).*

cylinder	1	2	3	4	5
diameter (mm)	80	100	130	160	165
$\frac{w_e}{w_o}$	0.83	0.76	0.40	0.25	0.18
$\frac{u_o}{w_o}$	0.36	0.44	0.54	0.65	0.90
$\frac{u_e}{u_o}$	0	0.1	0.20	0.61	0.66

Table 5.V Typical amplitude ratios as measured for the longitudinal mode in cylindrical resonators.

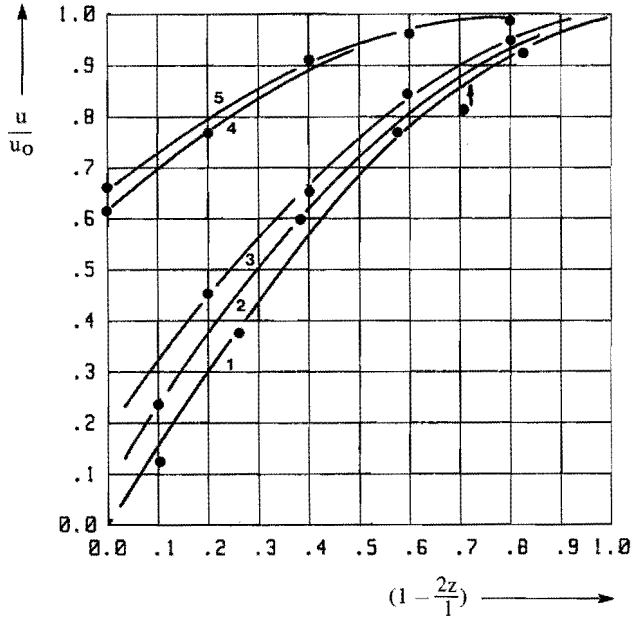

Fig. 5.14 Measured normalised radial amplitudes at the cylindrical surface, $r = \frac{d}{2}$, for the cylinders of table 5.I.

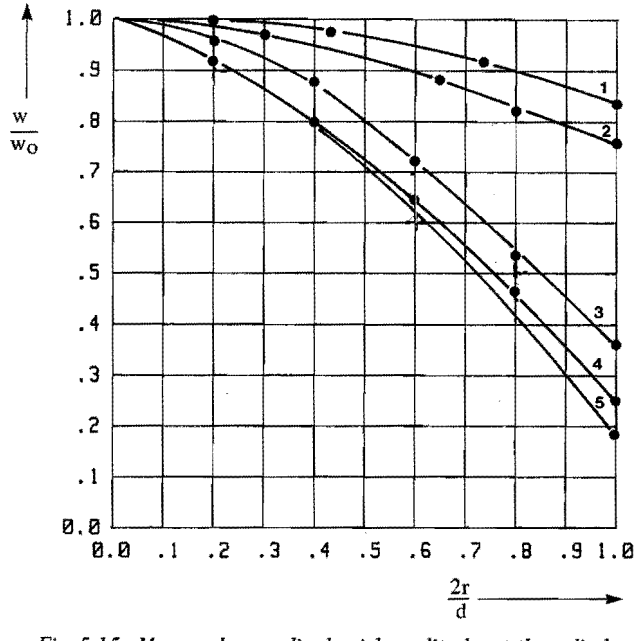

Fig. 5.15 Measured normalised axial amplitudes at the cylinder output surface, $z = -l/2$, for the cylinders of table 5.I.

mode as derived by McMahon and theoretically. For large diameters the spectrum approaches asymptotically the solutions for radial vibrations in thin discs. At 20 kHz the thin disc of aluminium is in radial resonance at d = 180 mm (see figure 5.8), or equation (5.19).

5.10 Other modes of vibrations

Finally, it was concluded that the longitudinal mode in the solid cylindrical resonator only is possible up to diameters of ± 165 mm. Above this diameter other vibrational modes would be needed when devicing resonators. However, in this case nodal circles at the output surface will always be observed, according to McMahon's frequency spectra. Two resonators were designed with aid of figures 5.4 to 5.7 at d = 220 mm and d = 300 mm, showing one and two nodal circles respectively when coupled to a welding apparatus. The vibrational modes are axisymmetrical (the dimensions and frequencies were: d = 300 mm, l = 145 mm, f = 20.65 kHz and d = 220 mm, l = 130 mm, f = 20.20 kHz).
In both cases the modes showed an amplitude ratio at the output surface of $\frac{w_e}{w_o} = -1$ (d = 220) and $\frac{w_e}{w_o} = 1$ (d = 300). Although it was possible to make welds at a restricted area near the outer diameter, problems did arise in order to keep the complete system in resonance (the ultrasonic generator would not lock to the resonance frequency). It is not the objective of the present work to explore other vibrational modes than the longitudinal one.

5.11 Conclusions

Solid cylindrical resonators can be used effectively up to diameters of 60-70 mm at 20 kHz, provided that an amplitude fall-off at the output surface of maximum 10% is acceptable. However, when only restricted areas of the output surface are to be used (for example a small part near the outer diameter) diameters up to 165 mm are possible, however with only 20% of the input amplitude available.

The approximate theory to calculate the resonance conditions in the cylinders for the longitudinal mode is very useful and of reasonable accuracy. McMahon's frequency spectra are of importance to determine the presence of spurious modes and the coupling of them to the longitudinal one. When designing solid cylindrical resonators never spurious modes will be present for diameters d $<$ 80 mm (at 20 kHz). The coupling of these resonators to a welding apparatus results into disappearance of many spurious modes, but for the larger diameter still modes are present near 20 kHz.

6. SOLID RECTANGULAR RESONATORS

6.1 Introduction

For ultrasonic high power applications the resonator with a rectangular cross-section perpendicular to the propagation direction of the longitudinal wave into it is very often used (see figure 6.1). At 20 kHz the output surface has typically dimensions in the range of 50 x 50 mm^2 to 50 x 150 mm^2, mostly one dimension not exceeding 50 mm. As discussed in the previous chapters these dimensions are typical for wide output resonators (dimensions $> \lambda/3$). Their dimensions are also of the order of $\lambda/2$, the half-wavelength of the longitudinal wave, so that the determination of the resonance frequency of the resonator is more complicated than as would be predicted by the fundamental theory for longitudinal waves in slender rods. As discussed in chapter 3, very wide output resonators of the blade-like and block-like type are separated through slotting in half-wavelength resonators of rectangular cross-sections. Therefore it is important to know the characteristics of the rectangular resonators for determination of the number of slots needed and their location and dimensions. It is to be studied in this chapter up to what dimensions solid rectangular resonators can be used effectively, regarding the uniformity of the output amplitude.
Available literature on the subject will be reviewed. From it correction formulae for the wave propagation velocity in the rectangular resonator are presented. In a very similar way as Mori (1977) used the apparent elasticity method for solid cylinders, in this chapter the resonance conditions of the longitudinal mode will be derived. Using the Rayleigh method, the resonance conditions will also be derived while certain assumptions on the shape of the longitudinal mode are made. The calculated mode shape and the resonance frequency will be compared with own experiments. Other modes (spurious modes) will not be discussed as extensively as was done for the cylindrical resonator. Some information on it can be derived from very recent papers of Hutchinson and Zillmer (1983) and Leissa and Zhang (1983), but not on an even elucidative way.

6.2 Literature review

For small resonator dimensions (lateral dimensions $< \lambda/4$) approximate theories for the decrease of the wave propagation velocity of the longitudinal wave have been derived (the basical work of Love, and in publications of Morse (1959), Kynch (1957) and Redwood (1960)). Very recently Hutchinson and Zillmer (1983) and simultaneously Leissa and Zhang (1983) published papers on the vibrations in rectangular parallelepipeds. In both, complex numerical manipulations are needed to derive the resonance frequencies. Hutchinson derives the lowest order modes for some dimensions and his results are converging to the elementary solutions exactly. Leissa uses the Ritz method to derive the frequencies for the 5 lowest modes, based on assumptions for the displacement functions. Some mode shapes are presented. However, Leissa's idealisation regarding the zeros for the displacements at one face of the parallelelepiped makes his results not useful for the design of resonator. Hutchinson's paper, however, deals with free parallelepipeds. His results do not contain mode charts or descriptions of the actual mode shapes, in relation to frequency spectra, to enable the study of the presence of spurious modes of vibration in the rectangular resonator which could be coupled to the longitudinal one.

When the thickness and width of the resonator comes in the order of the half-wavelength of the longitudinal wave, strong lateral resonances will be observed, coupled to the longitudinal mode. Itoh and Mori (1971) studied experimentally this effect and showed that it is possible to design directional converters, in which ultrasonic vibratory energy can be transmitted in perpendicular directions. However, to use them effectively, the output area is limited to those of slender rod resonators.

Stepamenko (1979) developed an approximate theory to calculate the resonance frequencies of rectangular resonators for which only one of the lateral dimensions is small, while the other is of the same magnitude as the wavelength of the longitudinal mode. Stepamenko created very wide output resonators by coupling several rectangular resonators by favour of the presence of lateral resonances (see appendix 3). The validity of his model will be compared to those of others. From measurements by Stepanenko, it followed that these resonators did not show a uniform output amplitude (differences up to 30% are observed).

6.3 Corrections to the wave-propagation velocity

There exist two propagation modes for the longitudinal waves in resonators of rectangular cross-sections. The extensional character of this wave causes a cross-section perpendicular to the propagation direction to expand or contract in the width direction (width-mode) or in the thickness direction (thickness-mode). These are shown in figure 6.1 on an enlarged scale (cross-section through the midplane of the resonator, z = 0). Morse (1950) studied both modes. In the range of practical interest for ultrasonic applications the thickness-mode has much higher a propagation velocity than the width mode. The width mode will normally be observed when designing resonators.

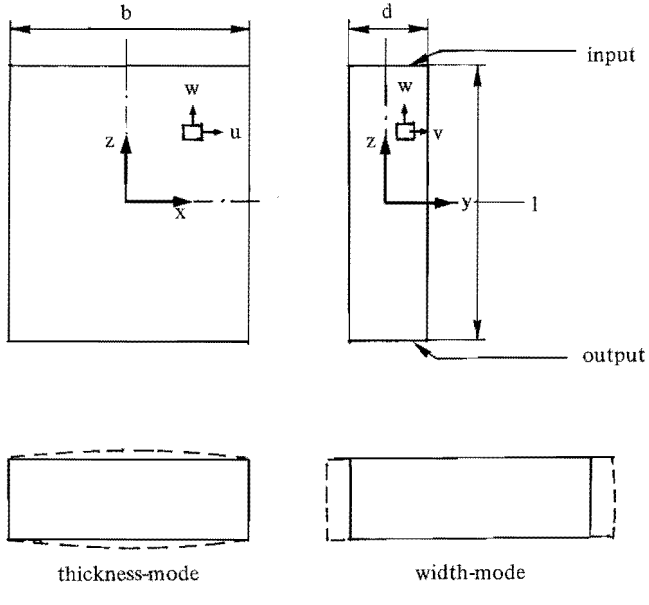

Fig. 6.1 Solid rectangular resonator of length l, width b and thickness d; two propagation modes for the longitudinal wave are shown; the thickness-mode has much higher a propagation velocity than the width-mode (the modes shown are a cross-section through the midplane z = 0).

The resonance frequency for the longitudinal mode of the half-wavelength ($\lambda/2$) resonator of length l for small lateral dimensions ($b < \lambda/4$ and $d < \lambda/4$) (see figure 6.1) follows from:

$$l = \frac{c}{2f} \text{ or } kl = \pi \tag{6.1}$$

With increasing width and thickness the longitudinal wave propagation is to be corrected for the effect of lateral inertia, caused by Poisson effects. Love derived a theory to calculate a correction for resonators of rectangular cross-section (see also Kynch (1957) and Leissa (1983)):

$$c' = c\ (1 + \nu^2\ k^2\ K^2)^{-1/2} \tag{6.2}$$

where k = wave number, K = polar radius of gyration of the cross-section. After linearisation of equation (6.2), it follows for the rectangular resonator:

$$c' = c\ (1 - \frac{1}{24}\ \nu^2\ k^2\ (b^2 + d^2)) \tag{6.3}$$

Again, for comparison with the results below, the actual resonator length l is calculated as function of the width b. Using equations (6.1) and (6.3), in non-dimensional form, it follows:

$$\frac{kl}{\pi} = 1 - \frac{1}{24}\ \pi^2\ \nu^2\ (\frac{kb}{\pi})^2\ (1 + (\frac{d}{b})^2) \tag{6.4}$$

Often the decrease of the propagation velocity is calculated from a modified Rayleigh approximation taking into account Poisson's ratio and the cross-sectional area rather than its actual shape and dimensions by use of the radius of gyration. This modification is basically not correct. The deviation to equation (6.4) is compared in figure 6.2, amongst the other theories (where d/b = 0.3).
The corrected velocity equals (see also equation 5.1):

$$c' = c\ (1 - \nu^2\ k^2\ \frac{bd}{4\pi}) \tag{6.5}$$

Within the range of validity, ($d < \lambda/4$ and $b < \lambda/4$ or $\frac{kb}{\pi} < 0.5$), the difference is less than 0.5%. The deviations from the elementary value of the wave propagation velocity is small (for which $\frac{kl}{\pi} = 1$). From figure 6.2 it follows that up to width to length ratios $b/l \sim 0.7$ the deviations of the corrected velocity is less than 1% ($b/l \approx \frac{kb}{kl}$).

The effect of the thickness to width ratio d/b on the propagation velocity following equation (6.4) is shown in figure 6.3, by comparing the resonance length l versus the resonator width b. Within the range of validity, the difference between $\frac{d}{b} = 0{,}2$ and $\frac{d}{b} = 1$ amounts about 1%.

6.4 Apparent elasticity method

In a very similar way as was shown for the cylindrical resonator, the apparent elasticity method can be used to determine the resonant length of a resonator with a rectangular cross-section. In the following only one dimension will be small as compared to the others ($d < l$ and $d < b$) (fig. 6.1). We will assume the plain stress case. The resonator is supposed to resonate in the z-direction in the longitudinal mode. Due to Poisson's contraction the largest lateral motions are to be expected in the x-direction.

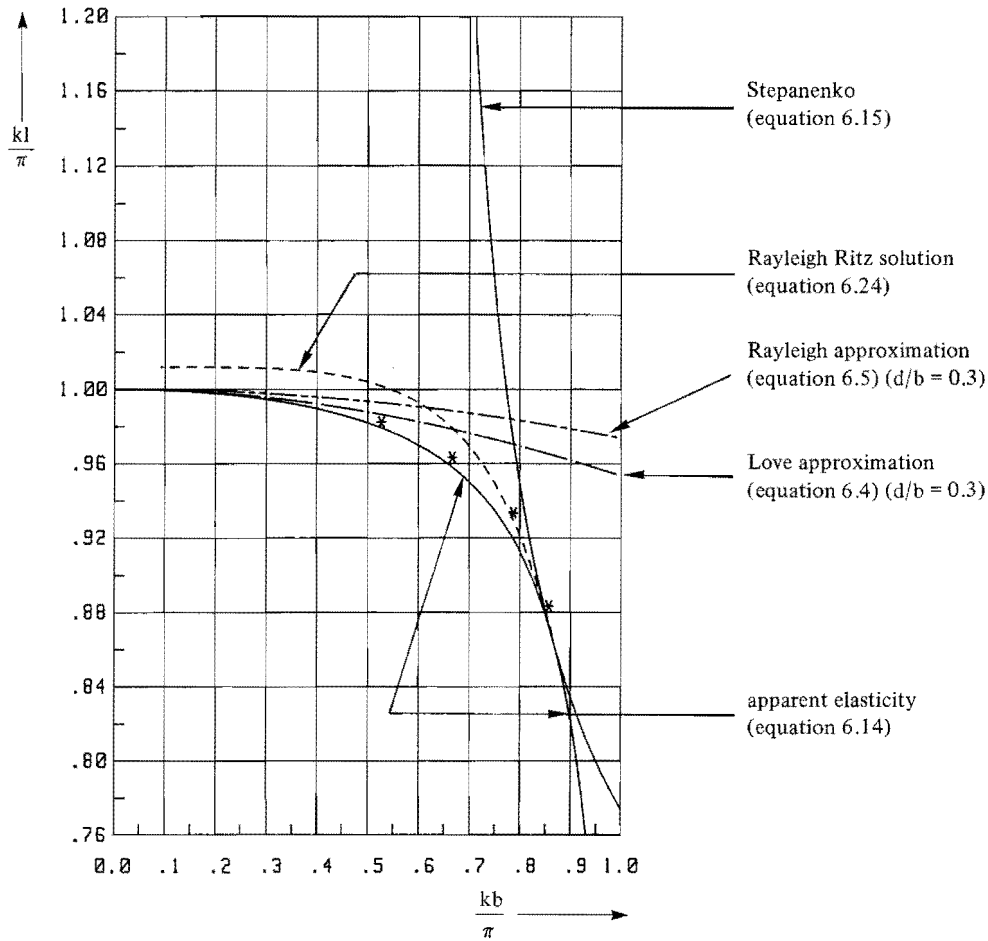

Fig. 6.2 Non-dimensional representation of the length l of a rectangular resonator versus its width b; comparison of various theories (ν = 0.335); own experiments are marked with asterics (*).

We will now derive the resonance conditions in the resonator in a very similar way as Mori did for the cylindrical resonator. The equations of motion fo both x- and z-direction are coupled by introducing the wave coupling factor m. Consider two extreme situations, first the slender rod resonator in z-direction ($l \gg b$ and $l \gg d$), secondly the slender rod resonator in x-direction ($b \gg l$ and $b \gg d$).
The resonance conditions for the half-wavelength mode are respectively:

$$kl = \pi \quad (l \gg b, l \gg d) \tag{6.6}$$

$$kb = \pi \quad (b \gg l, b \gg d) \tag{6.7}$$

The governing equation was discussed in chapter 2 (equation 2.1).

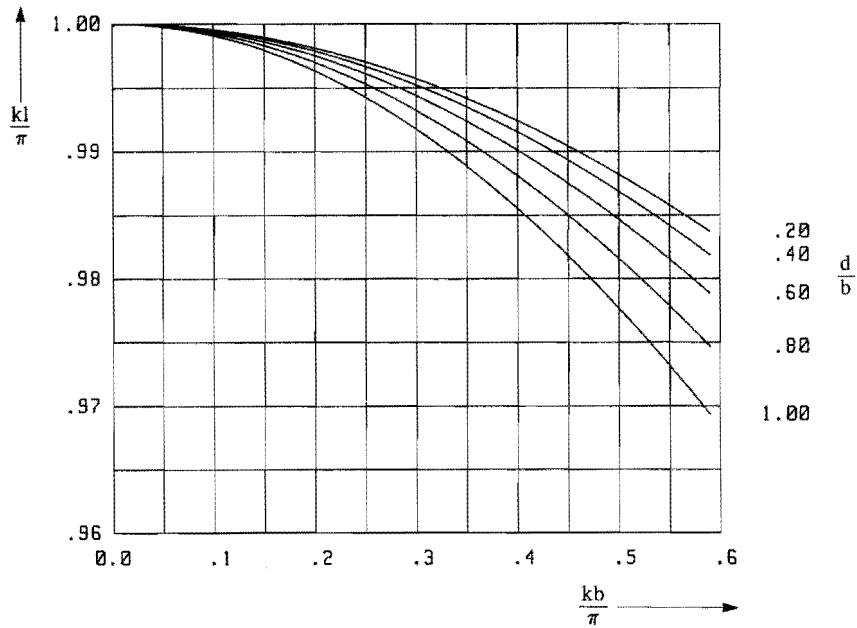

Fig. 6.3 The effect of the thickness to width ratio d/b on the resonant length l versus the width b for a rectangular resonator (correction on the wave propagation velocity according equation (6.4)) (ν = 0.335).

For the first situation ($kl = \pi$) both stresses σ_x and σ_y are zero. For increasing width b the stress in x-direction will increase. For reason of $d < b$ and $d < l$ σ_y will be zero. It is assumed that σ_x is related to σ_z by:

$$\sigma_x = \frac{1}{m}\sigma_z \tag{6.8}$$

In z-direction, Hooke's law gives the stress-strain relation:

$$\epsilon_z = \frac{1}{E}(\sigma_z - \nu\sigma_x) \text{ or} \tag{6.9}$$

$$\epsilon_z = \frac{1}{E}(\sigma_z (1 - \frac{\nu}{m})) \tag{6.10}$$

The apparent elasticity in z-direction is defined by E':

$$E' = E(1 - \frac{\nu}{m})^{-1} \tag{6.11}$$

The second situation ($kb = \pi$), yields to exactly the same apparent elasticity in the x-direction (where $\sigma_y = 0$). The resonant length l and width b (equations (6.6) and (6.7)) are calculated by introducing E' instead of E.

$$kl = \pi (1 - \frac{\nu}{m})^{-1/2} \tag{6.12}$$

and

$$kb = \pi (1 - \frac{\nu}{m})^{-1/2} \tag{6.13}$$

Elimination of the wave coupling factor m from these equations, results in the frequency equation relating the elastic properties and the dimensions of the rectangular resonator:

$$\frac{kl}{\pi} = (1 - \frac{\nu^2}{1 - (\frac{\pi}{kb})^2})^{-1/2} \tag{6.14}$$

Clearly this solution is independent on the resonator thickness d. The solution of equation (6.14) is shown in figure 6.2. In the case of l = b, the resonance frequency relation becomes $\frac{kl}{\pi} = 0.865$ for $\nu = 0.335$. From figure 6.2 it is clear that this theory gives much lower resonance-frequencies than those obtained from the corrections to the wave propagation velocity. The agreement with own experiments (which are explained below) is excellent. For small width the theory converges to the slender rod solution, as expected. So, it can be concluded that the theory is adequate for larger widths whereas the corrections to the wave propagation velocity are not.

6.5 Resonance conditions according to Stepanenko

Stepanenko*) (1979) derived a theory to calculate the resonance condition in a resonator of rectangular cross-section where one dimension was small compared to the others. In his model both length l and width b are of the same magnitude, resulting in a strong coupling of the lateral vibrations to the longitudinal mode. A complete derivation of the theory can be found in Stepanenko's paper. The theory holds only for a small range of the width b. Using the non-dimensional notation mentioned above, the resonance condition becomes for the half-wavelength longitudinal mode:

$$\frac{kl}{\pi} = (2(1+\nu) - \frac{1}{(\frac{kb}{\pi})^2})^{-1/2} \tag{6.15}$$

Width b has to fulfill the following limitations:

$$\sqrt{\frac{1-\nu}{1+\nu}} < \frac{kb}{\pi} < \sqrt{\frac{1-\nu}{1+\nu}\,\frac{1}{1-2\nu}} \tag{6.16}$$

For $\nu = 0.335$, these limitations are $0.71 < \frac{kb}{\pi} < 1.23$. The solution of equation (6.15) is shown in figure 6.2. Clearly, this theory strongly deviates from the apparent elasticity method, or from the experiments. There is only a small range where this solution coincides with the apparent elasticity solution, namely for those values of l and b for which $\frac{l}{b}$ is near unity ($\frac{kl}{\pi} = 0.865$). It is in this range that Stepanenko designed his ultrasonic resonators.

*) (see appendix 3).

6.6 Rayleigh-Ritz method to determine the resonance frequency and mode of vibration

In order to calculate the resonance frequency of the longitudinal mode in the rectangular resonator, we will derive the resonance conditions while an assumption is made for the displacement function, which best fits the actual vibrational mode. By equating the maximum kinetic energy and the maximum potential energy during a cycle of vibration in the resonator, the resonance condition is found, yielding the frequency equation. The displacement function, which will be described below, contains one unknown variable. The unknown variable is found from the requirement that it must minimize the calculated resonance frequency. This method is known as the Rayleigh-Ritz method. The results obtained will give a frequency higher than the exact value.

Figure 6.4 shows the rectangular resonator and the relevant definitions of coordinates and displacements. The mode shape is plotted in the same figure. We will assume the resonator thickness d to be small as compared to the other dimensions. The stress in y-directions is zero: $\sigma_y = 0$ (see also figure 6.1). The resonator width to length ratio will be varied between $0 < \frac{b}{l} < 1$, for reason of symmetry. The displacement functions u (x,z) and w (x,z) related to the mode of vibration that is expected are chosen as follows: (again time-independent solutions are discussed, the vibrations are harmonic):

$$u(x,z) = u_o \sin\left(\frac{\pi}{b}x\right) \cos\left(\frac{\pi}{l}z\right) \tag{6.17}$$

$$w(x,z) = w_o \cos\left(\frac{\pi}{l}x\right) \sin\left(\frac{\pi}{l}z\right) \tag{6.18}$$

The displacements are independent of the thickness d. The unknown variable in equations (6.17) and (6.18) is $\eta = \frac{u_o}{w_o}$, which equals the ratio of the maximum lateral amplitude u_o to the maximum axial amplitude w_o. As a result of the analysis the frequency and η will be found.

When body forces are absent, the maximum potential energy $\hat{U}_p$, and the maximum kinetic energy $\hat{U}_k$, for the two-dimensional problem are:

$$\hat{U}_p = \frac{1}{2}\int_{vol} (\sigma_x \epsilon_x + \sigma_z \epsilon_z + \tau_{xz} \gamma_{xz})\, dV \tag{6.19}$$

$$\hat{U}_k = \frac{1}{2}\int_{vol} \omega^2 \rho\, (u^2(x,z) + w^2(x,z))\, dV \tag{6.20}$$

The stress-strain relations are related to the displacements by (for convenience displacements are denoted by u and w):

$$\epsilon_z = \frac{\partial w}{\partial z}$$

$$\epsilon_x = \frac{\partial u}{\partial x} \tag{6.21}$$

$$\gamma_{xz} = \frac{\partial w}{\partial x} + \frac{\partial u}{\partial z}$$

The contribution of the displacement v in the y-direction would contribute to the kinetic energy equation (6.20). By neglecting the displacements v, the calculated frequency will be somewhat higher; the effect of the displacement v is identical to the results of the correction formula which were derived for the wave propagation velocity (equation 6.3)).

Combination of equations (6.19), (6.20) and (6.21) and Hooke's law, the maximum potential energy and kinetic energies become:

$$\hat{U}_p = \frac{1}{2}\int_{vol}\left\{\frac{E}{1-\nu^2}\left[\left(\frac{\partial u}{\partial x}\right)^2 + 2\nu\frac{\partial u}{\partial x}\frac{\partial w}{\partial z} + \left(\frac{\partial w}{\partial x}\right)^2\right] + \frac{E}{2(1+\nu)}\left[\frac{\partial w}{\partial x} + \frac{\partial u}{\partial z}\right]^2\right\} dV \qquad (6.22)$$

$$\hat{U}_k = \frac{1}{2}\rho\omega^2\int_{vol}(u^2 + w^2)\, dV \qquad (6.23)$$

The frequency equation resulting in ω follows from the equation of equations (6.22) and (6.23). After some mathematical operations, it follows:

$$\frac{1}{2}\rho\omega^2\left(\frac{1}{\pi}\right)^2(\eta^2 + a_3) = \frac{E}{2(1-\nu^2)}(\eta^2 a^2 + a_3) + \frac{E}{4(1+\nu)}(\eta^2 + 2 - a_3 - 2\eta a_5)$$

$$+ \frac{\nu E}{(1-\nu^2)}(\eta a a_4) \qquad (6.24)$$

Where the constants a and a_1 to a_5 are defined by:

$$a = \frac{1}{b}$$

$$a_1 = \frac{1}{1 + 1/a}\sin\left(\frac{\pi}{2}(1 + 1/a)\right)$$

$$a_2 = \frac{1}{1 - 1/a}\sin\left(\frac{\pi}{2}(1 - 1/a)\right)$$

$$a_3 = 1 + \frac{a}{\pi}\sin\left(\frac{\pi}{a}\right)$$

$$a_4 = \frac{2}{\pi}(a_1 + a_2)$$

$$a_5 = \frac{2}{\pi}(a_1 - a_2)$$

In the frequency equation (6.24) ω must be minimised with respect to η.
So it follows:

$$\rho\omega^2\left(\frac{1}{\pi}\right)^2\eta = \frac{E}{(1-\nu^2)}(\eta a^2 + \nu a a_4) + \frac{E}{2(1+\nu)}(\eta - a_5) \qquad (6.25)$$

By elimination of ω from equations (6.24) and (6.25) a relation for η is obtained:

$$\eta^2 + \frac{a_3\,(a^2-1) + (1-\nu)\,(a_3-1)}{\frac{1}{2}a_5\,(1-\nu) - \nu\,a\,a_4} - a_3 = 0 \qquad (6.26)$$

A special solution of equation (6.26) is found for l = b or $a = 1$. In that case $\eta = -1$. The resonance frequency follows from equation (6.24):
$\frac{kl}{\pi} = \sqrt{\frac{1}{1+\nu}}$, or $\frac{kl}{\pi} = 0.865$ for $\nu = 0.335$ (see section 6.5 of this chapter; it is identical to the solution of Stepanenko's theory).
For small values of the width b the solutions will converge to the half-wavelength solution for the slender rod. For $\eta \approx 0$ equation (6.24) results in $\frac{kl}{\pi} \approx 1.05$. So, the theory presented here will result in ± 5% too high frequencies.

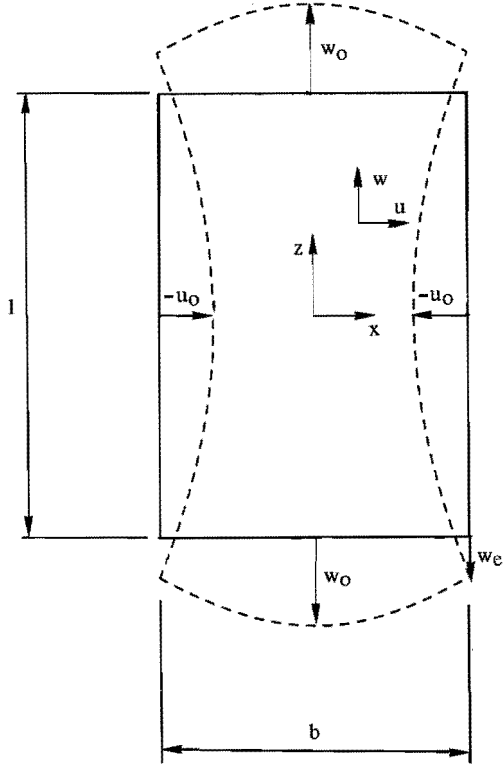

Fig. 6.4 The longitudinal mode in a rectangular resonator of small thickness; definition of the displacement functions; the maximum axial amplitude is w_o and the maximum lateral amplitude is u_o.

Equation (6.26) has two solutions for η, with a negative and positive number. As discussed before, the actual mode shape corresponds to the mode shown in figure 6.4, so the negative solution for η is to be evaluated.

The results of this theory are shown in figure 6.2 giving the resonator length l and the width b in non-dimensional notation. In figure 6.5 the solutions for the amplitude ratio $\eta = \frac{u_o}{w_o}$ as well as the amplitude ratio $\frac{w_e}{w_o}$ are shown, versus the resonator width b. ($\nu = 0.335$). The degree of uniformity of the output amplitude is expressed here by the amplitude at the edges w_e. If only 10% amplitude fall off is tolerated, the maximum resonator width is $\frac{kb}{\pi} = \pm 0.3$. The maximum lateral amplitude u_o can also be derived from figure 6.5.

The influence of Poisson's ratio ν on the solutions of the theory presented here is shown in figure 6.6. For small width b the influence on the resonant length l is small, whereas, it is great for large values of the width b. The influence on the amplitude ratio η is great for the whole width range.

6.7 Dimensioning of rectangular resonators

Using the apparent elasticity method (equation (6.14), the dimensions of rectangular resonators for the longitudinal mode were calculated for some resonance frequencies. Figure 6.7 gives the length l of the resonator versus its width b for the most commonly used frequencies between 20 and 60 kHz (material aluminium, see chapter 2).
Figure 6.8 gives the resonant length l versus the width b for various values of the wave propagation velocity c (4.0 to 5.2 10^3 m/s) at a design frequency f = 20 kHz.

6.8 Comparison with measurements

Four resonators of rectangular cross-section were made for a resonance frequency of ± 20 kHz to investigate the results as obtained from the various theories. The thickness of the resonators are small compared to the other dimensions: d = 30 mm. The material was aluminium, c = 5200 m/s, $\nu = 0.335$. The actual dimensions of the resonators are presented in table 6.I.
Resonators 1, 2 and 3 were provided with a threaded hole at the input surface to enable a coupling to an ultrasonic transducer of a welding apparatus for amplitude measurements. The resonance frequency of the longitudinal mode was measured while the resonator was suspended into thin wires (see also chapter 2), they are listed in table 6.I, column A. Due to the presence of a threaded hole at the input surface, the resonance frequency is higher than for the same resonator without a hole.
A correction for the resonance frequency can be approximated from the mass difference due to the hole. The volume of the hole is translated into a resonator volume along the input surface of width b and thickness d. The result is a small increase in the resonator length. The frequency correction is proportional to the change in length ($\frac{\Delta f}{f} = -\frac{\Delta l}{l} = \frac{-V}{bdl}$, where V = volume of the hole, V = 3000 mm^3).
The corrected frequencies are listed in table 6.I, column B. From the apparent elasticity theory (equation (6.14)), the resonance frequency was calculated for the actual resonator dimensions. The results are listed in table 6.I, column C. The measured frequencies are compared to the calculated ones in column D (the corrected frequency was used for resonators 1, 2 and 3). The deviations are small, from 0,5 to 1%. As expected the measured frequencies are higher than the calculated ones.
Finally, the non-dimensional length and width are calculated from the measurements to compare them with the theories (see table 6.I, column E and F). The measurements are shown in figure 6.2.

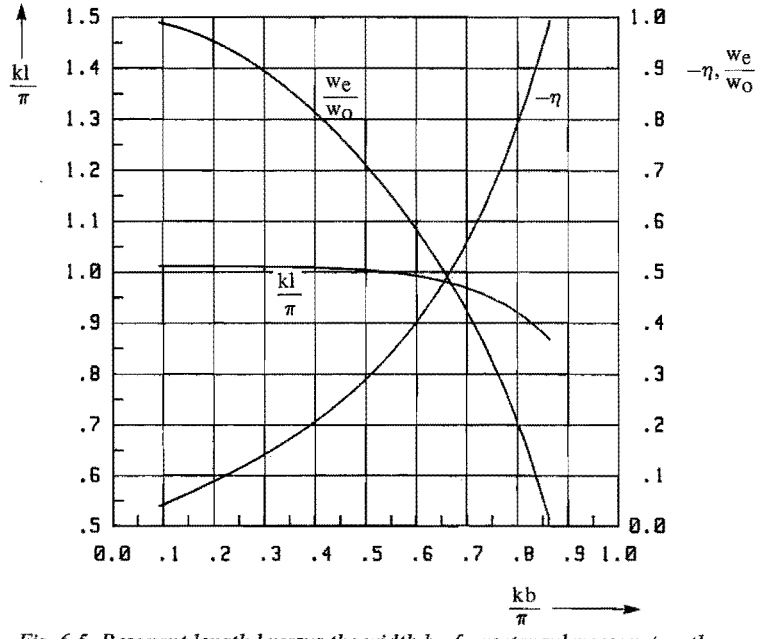

Fig. 6.5 Resonant length l versus the width b of a rectangular resonator; the amplitude ratio $\frac{w_e}{w_o}$ *and* $\eta = \frac{u_o}{w_o}$ *(according to equations (6.24) and (6.26) Rayleigh-Ritz) (*$\nu = 0.335$*)*

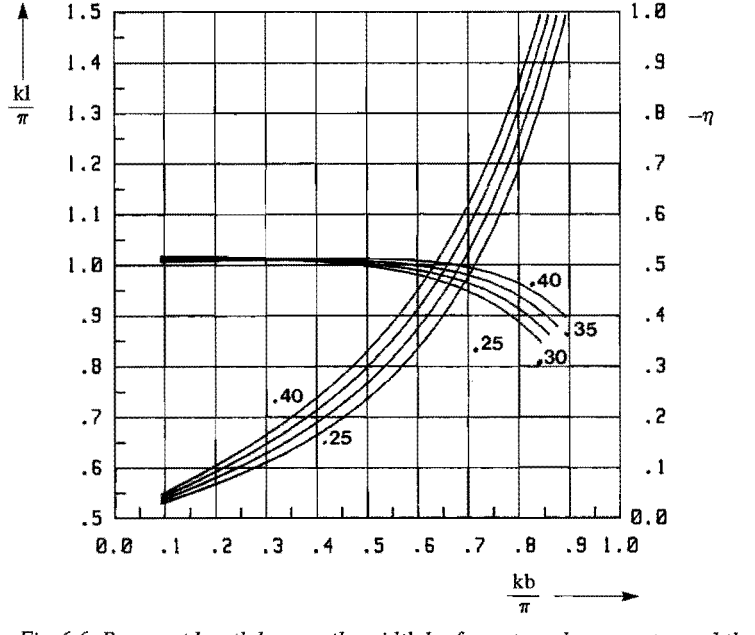

Fig. 6.6 Resonant length l versus the width b of a rectangular resonator and the amplitude ratio η *for various values of Poisson's ratio* ν *(equations (6.24) and (6.25) Rayleigh-Ritz)*

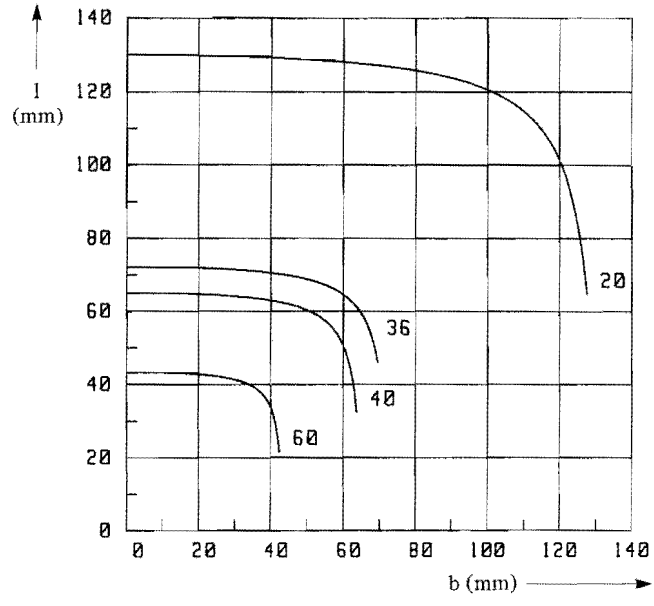

Fig. 6.7 Length l of the rectangular resonator versus the width b for some frequencies (kHz). (Material aluminium c = 5200 m/s and ν = 0.335) (equation (6.14)).

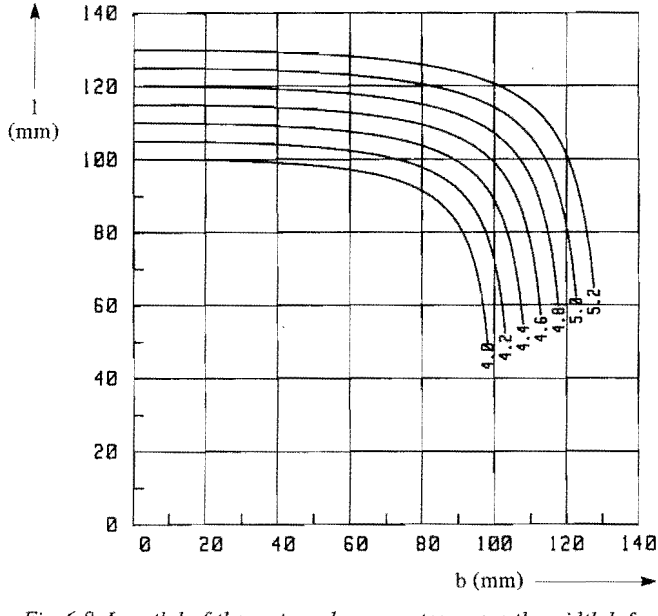

Fig. 6.8 Length l of the rectangular resonator versus the width b for some values of the wave propagation velocity c (10^3 m/s). (ν = 0.335, frequency f = 20 kHz) (equation (6.14)).

		A	B	C	D	E	F
Nr.	b (mm) * l (mm)	measured f (kHz)	correction f (kHz)	calculated f (kHz)	deviation	$\frac{kl}{\pi}$	$\frac{kb}{\pi}$
1	70 * 130	19.94	19.64	19.53	+ 0.6%	0.982	0.529
2	95 * 137	18.47	18.27	18.19	+ 0.5%	0.963	0.668
3	109 * 112	20.71	20.50	20.36	+ 0.7%	0.883	0.859
4	110 * 130	18.66	–	18.45	+ 1.0%	0.933	0.789

Table 6.I Measured resonance frequencies of 4 solid rectangular resonators (material aluminium c = 5200 m/s, ν = 0.335, d = 30 mm). Comparison to the calculated frequencies (equation (6.14)). Column B is a corrected frequency for the threaded hole in the resonator.

The actual vibration mode of resonators 1, 2 and 3 were measured after that the resonator was coupled to an ultrasonic transducer.
Fig. 6.8 shows the measured amplitudes and those as calculated from the Rayleigh-Ritz method. There is a good agreement with the theory. The amplitudes plotted here are strongly enlarged values, the actual maximum amplitude was 15 μm. The resonance frequency of the resonator-transducer assembly differs from the measured frequencies in table 6.I. The transducer itself had a resonance frequency of the longitudinal mode at 20.10 kHz. So, when coupling a resonator with another frequency, some intermediate value will be measured.
It is observed that the amplitude measurements for the wide resonator fits best to the calculated ones. The vibration modes of the smaller resonators are influenced by the coupling to the transducer with a diameter of 40 mm. This causes some stiffening and therefore a smaller amplitude fall-off at the input surface (see fig. 6.8).
The uniformity of the output amplitude is denoted by the ratio w_e/w_o (which was defined in figure 6.4). Resonator 1 (70 mm wide) already has 15% amplitude fall-off.

6.9 Conclusions

The longitudinal vibrational mode in solid rectangular resonator was studied. For small width and thickness the resonator length at a given frequency can be approximated by the correction formula for the wave propagation velocity (figure 6.3). The validity holds up to width to length ratios of 0.3 to 0.4 (see figure 6.2), or at 20 kHz to width $b \approx 0{,}4 * 130 \approx 50$ mm.
For the range $50 < b < 100$ mm, a longitudinal mode is possible in the resonator, and the resonance conditions are very well predictable by equation (6.14), following the apparent elasticity method. The deviations from the measurements are < 1%. The method presented by Stepanenko (1979), is only valid for resonators of width to length ratios near unit. The equations derived with the Rayleigh-Ritz method show similar results as the apparent elasticity, however the calculated frequencies are higher (± 5%). The mode shape, which is calculated with this method, fairly well approaches the measured mode shape. At 20 kHz the uniformity of the output amplitude is better than 90% for width $b < 70$ mm. Above it, the amplitude at the edges strongly falls, to become zero at $b = \pm 100$ mm, and the rectangular resonator is not suited when a constant energy transmission along the output surface is wanted.

The design of resonators at other operating frequencies than 20 kHz was not discussed. However with aid of the non-dimensional representation in the figures shown, the resonance conditions of a resonator at any operating frequency can be determined easily.

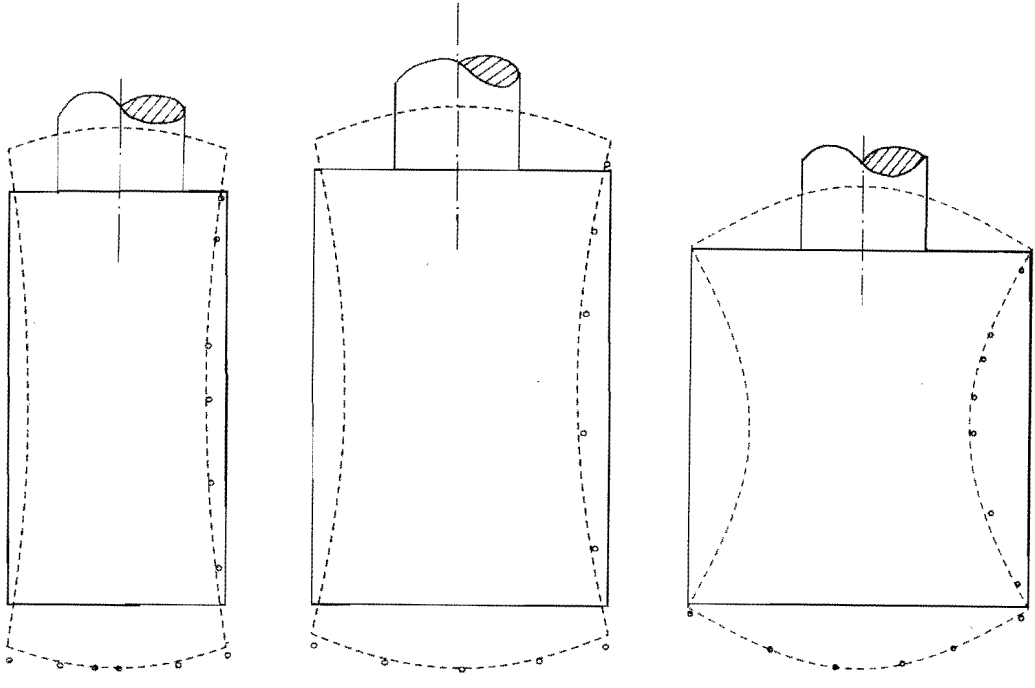

1: f = 19.78 kHz
$w_e/w_o = 0.85$
$u_o/w_o = 0.33$

2: f = 18.83 kHz
$w_e/w_o = 0.70$
$u_o/w_o = 0.52$

3: f = 20.11 kHz
$w_e/w_o = 0.18$
$u_o/w_o = 0.99$

Fig. 6.9 Vibrational modes of resonators 1, 2 and 3 when coupled to a welding transducer of 40 mm diameter. The input amplitude was 15 μm. Measured amplitudes are denoted by "0". The calculated mode shape from the Rayleigh-Ritz method (equation (6.24)) is presented by dotted lines. The resonance frequencies as measured, the uniformity of the output amplitude (w_e/w_o) and the wave coupling (u_o/w_o) are listed (see also figure 6.4).

7. OPTIMIZATION OF A RESONATOR: EXPERIMENTALLY AND WITH FINITE ELEMENT ANALYSIS

7.1 Introduction

In the previous chapters solid cylindrical and rectangular resonators were discussed. The resonance conditions for the longitudinal mode in these resonators could be determined analytically, with results in non-dimensional form. The objective of the present work is to study wide output resonators, with dimensions exceeding the limits for the cylindrical and rectangular resonators. In order to have wide resonators vibrating in a mode with a uniform output amplitude, commonly slots are provided in a way as was described in chapter 4 (patent literature). Clearly, analytical solutions for the vibrations in such resonators of complex shape will not be possible.
In this chapter the design of one specific wide output resonator of the blade-like type will be studied. First, it will be optimized to meet the design-requirements, on an experimental approach on account of the interpretation of the measurements of resonance frequencies and vibrational modes. Secondly, a finite element analysis method is used to study the characteristics of the resonator, and it will be shown that it yields a more successful optimization procedure.

Gladwell (1975) reports very briefly a finite element analysis of two practical resonator shapes as used in ultrasonic welding (axisymmetric cylindrical and a bell-shaped resonator), using a finite element method which was published earlier for the analysis of thin disc and ring-type ultrasonic resonators (Gladwell (1967)). Only the mode shape of the resonator vibrating at 20 kHz is described and it is observed that locally there are strong radial amplitudes (not desired). Gladwell concluded to state that the major design problem remains to find a resonator shape which shows only small radial vibrations as compared to the longitudinal ones. Generally, the problem is to find basical design rules which result in a resonator shape very close to the final optimum shape. These are not given by finite element analysis. The presence of other resonance frequencies near the operating frequency (spurious modes) is not mentioned in Gladwell's paper, so that no information on the reliability of the resonator under operating conditions can be obtained.

7.2 Description of the resonator shape

From experiences of suppliers of ultrasonic equipment it is known that designing blade-like resonators of about 130 to 150 mm width at 20 kHz can be troublesome. Below, a 131 mm wide and 35 mm thick resonator will be studied. Generally, a resonator having at least one lateral dimension exceeding a quarter of the wavelength ($\lambda/4$) will be provided with slots or cut-outs to compensate for Poisson coupling (see chapter 4). It is attempted in this way to have the resonator vibrating in a "longitudinal" mode. The description "longitudinal" mode very often is used to denote that the mode must show a uniform amplitude along the output surface. By providing slots the wide resonator is separated in slender rod-like resonators in which a pure longitudinal mode is generated, which shows indeed a uniform output amplitude. From it originates the description "longitudinal" mode when the wide resonator is meant.

Figure 7.1 shows the resonator and its dimensions, provided with two slots, thus representing three slender-rod resonators which are coupled at the ends. This coupling is effectuated in a zone where the lateral strain in the resonator is minimum (see chapter 2, vibration analysis). The mutual disturbance of the longitudinal wave in each part will be minimized as a result. The choice of the width of the slots is not critical, but will be kept as small as possible. For reason of machineability these slots usually are 8 to 12 mm wide for 20 kHz resonators. The length of the slots is a compromise between two arguments. To have a good decoupling of the parts, the length will be maximized. However through the remaining bridging elements mechanical power has to be transmitted. So mechanical stresses and the overall stiffness of the resonator would demand larger dimensions of these coupling elements. Usually, the slot length is such that the remaining bridging elements are 10 to 25 mm high. There are no strict criteria for the location and number of slots to be provided. Usually, the width of the elements is between $\lambda/8$ and $\lambda/4$, so that the number of slots depends on the resonator width. The location almost always is such that the width of the elements is nearly identical for all elements. In the next chapter this subject will be discussed more extensively.

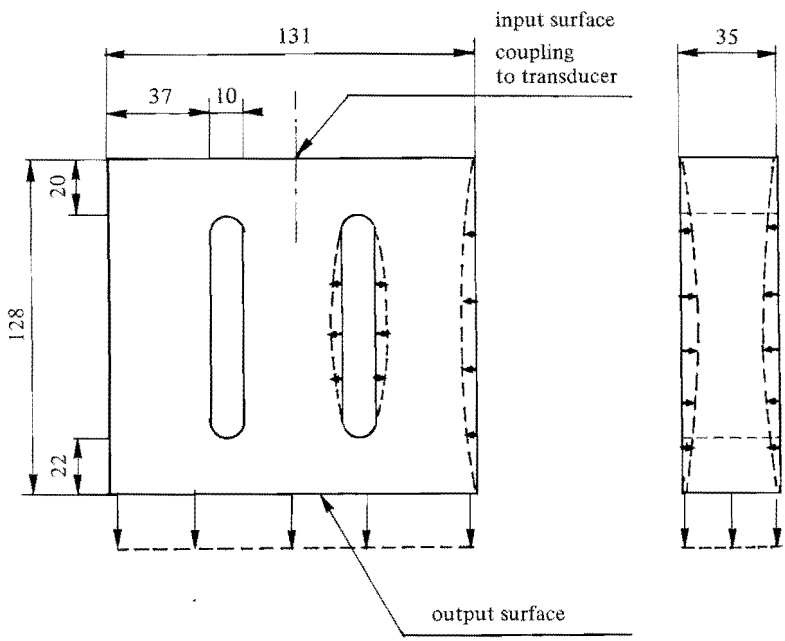

Fig. 7.1 A blade-like resonator of 131 mm width and 35 mm thickness designed to resonate in a longitudinal mode at 20 kHz (dimensions in mm). Part of the vibrational mode that is to be expected is shown. Amplitudes are presented on a strongly enlarged scale.

The resonator material is alumium (see chapter 2 for the properties), so the half-wavelength at 20 kHz for the longitudinal mode in a rod-type resonator equals:

$$\lambda/2 = \frac{c}{2f} = 130 \text{ mm}$$

As the wide resonator is composed of slender-rod resonators, it should be resonant at a length l, which is about $l \approx 130$ mm.
The actual resonator length is chosen l = 128 mm. The amplitudes of vibration, as desired, at the output surface, are illustrated in figure 7.1 too. The overall vibrational mode which can be expected because of the Poisson contraction in each element is shown (only part of mode is shown).

7.3 Optimization on an experimental approach

A resonator was deviced as shown in figure 7.1. In the range of 20 kHz, four resonance frequencies could be detected (the measuring method is described in chapter 2): $f_1 = 18.50$ kHz, $f_2 = 19.42$ kHz, $f_3 = 20.63$ kHz, $f_4 = 21.57$ kHz. The resonator was coupled to a transducer of a welding apparatus, of which the resonance frequency of the longitudinal mode was measured to be 20.30 kHz. After coupling, in the same frequency range only two resonances could be detected: $f'_1 = 19.30$ kHz and $f'_2 = 19.52$ kHz. The coupling causes two frequencies to disappear.

When the transducer-resonator system is mounted in the apparatus so that the output surface faces upwards, the vibrational mode of this output surface can be studied using fine dry sand. When the transducer is connected to a low power frequency oscillator, the sand moves towards nodal lines (if present) in case of excitation in a resonance frequency. In this way f'_1 and f'_2 were excited, and no difference in sand patterns was observed. At the output surface no nodal lines were detected, and therefore no discrimination between these modes was possible.
On the welding apparatus only f'_2 could be tuned to (the frequency range of the generator is always very limited, in this case from 19.50 to 20.30 kHz).
The overall vibrational mode of the resonator was measured while it was activated at an output amplitude of 10 μm at a frequency $f'_2 = 19.52$ kHz (this corresponds to about 100 W output power of the generator). The amplitudes were measured optically (see chapter 2, Fotonic Sensor measurements). The mode is shown in figure 7.2.

The amplitude at the output surface is far from constant. At the edges only 23% of the centre amplitude is available. This resonator showed poor welding results, especially near the edges (for good welding the difference must be less than 10%).
The amplitudes at the side surfaces, along the length are not those to be expected from the longitudinal mode (compare with 7.1). There seems to be a coupling of a lateral resonance to the longitudinal mode, resulting in a distortion of the latter. As the width is 131 mm, it is not unrealistic to expect a lateral resonance in the input- and output portion of the resonator, because the width is very close to the half-wavelength at 20 kHz. The mode shown in figure 7.2 is not acceptable, and measures have to be taken to improve the mode shape.

By providing various cut-outs (2 mm wide and 11 mm deep) in the upper and lower resonator portions, it was attempted to break the lateral resonance mode (all other dimensions are kept constant, see figure 7.1). The elimination of this (spurious) mode was studied in three steps, as shown in figures 7.3, 7.4 and 7.5.
The resonance frequency of the resulting modes is hardly influenced (this sounds reasonable because of the small amount of mass that is removed). However, a strong change in vibrational mode can be observed, resulting in a difference of less than 3% in amplitude at the output surface ($\frac{w_e}{w_o}$) when three cut-outs are provided, two at the input surface, one at the output surface, see figure 7.5.

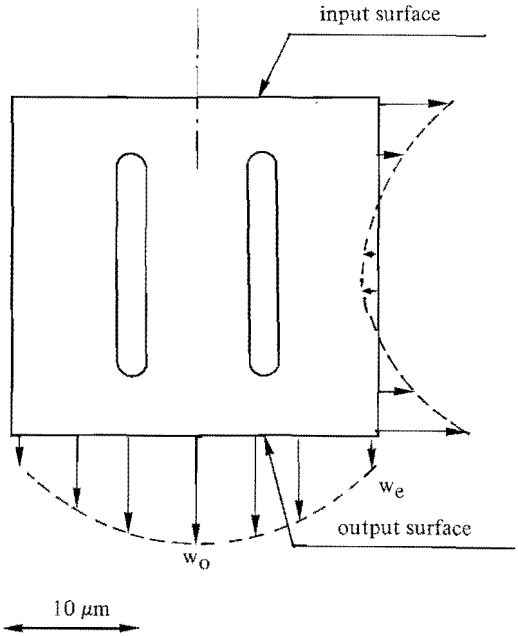

Fig. 7.2 Vibrational amplitude at f = 19.52 kHz

$$\frac{w_e}{w_o} = 0.23$$

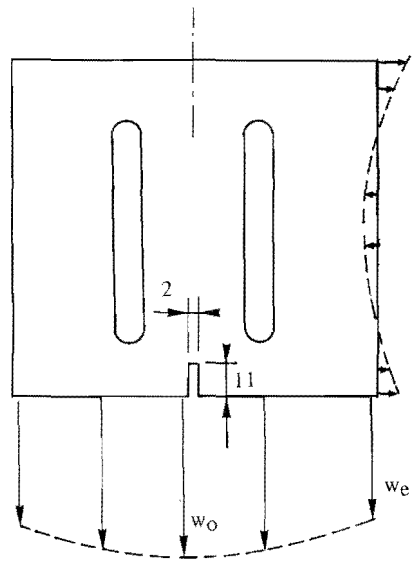

Fig. 7.3 f = 19.51 kHz, one cut-out at the output surface

$$\frac{w_e}{w_o} = 0.78$$

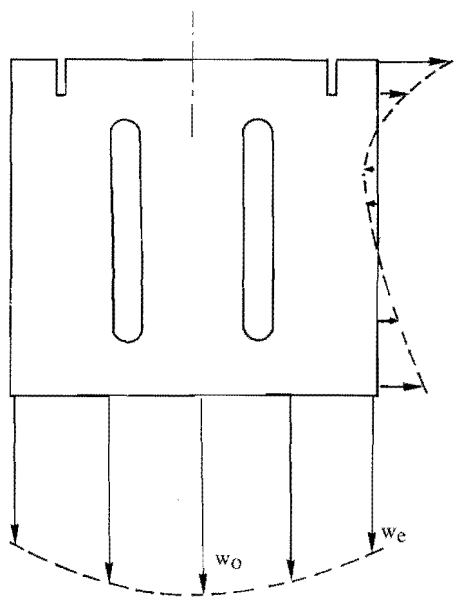

Fig. 7.4 f = 19.51 kHz, two cut-outs at the input surface

$$\frac{w_e}{w_o} = 0.80$$

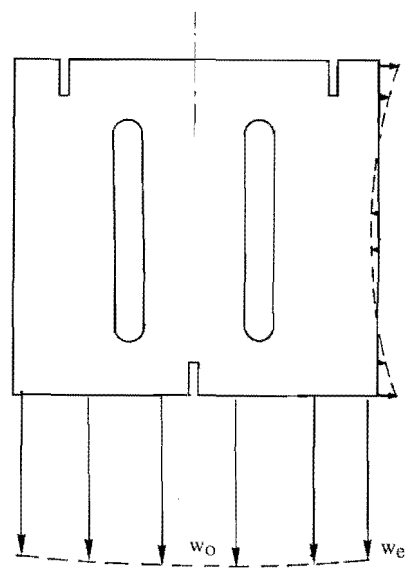

Fig. 7.5 f = 19.51 kHz, three cut-outs provided

$$\frac{w_e}{w_o} = 0.97$$

The side surface still shows some spurious mode, but of a relatively low amplitude as compared to the longitudinal one.
As for good welding a uniform output amplitude is required, this resonator should be adequate for welding applications. Experiments revealed that the welding results with this resonator were strongly improved.

So, on account of the interpretation of the frequency spectrum and the vibrational modes in four steps the resonator was optimized to an optimum vibrational mode. For a better frequency match to the transducer of the welding apparatus, finally a little increase of the resonance frequency may be realized.

7.4. Finite element analysis

The experimental approach gave a reasonable solution. Still, it can be considered whether there are resonator dimensions for which the "longitudinal" mode can be obtained without additional cut-outs, at a resonance frequency of about 20 kHz. Using computer programs based on a finite element method, the resonance frequencies and the corresponding vibrational modes in an arbitrarily shaped resonator can be calculated. The resonator is a three-dimensional body, in which vibrational modes can exist having amplitudes into three directions. The resonator under study, however, can be regarded as a two-dimensional body for the vibration analysis (plain stress problem). The thickness of 35 mm dictates that all resonance frequencies in this direction are at least 4 times higher as compared to the height and width direction.

Shear modes or plate vibrations with motions perpendicular to the plane of the resonator have relatively low resonance frequencies. Therefore only the in-plane vibration will be studied.
Figure 7.6 shows the resonator of which only a quarter has been divided into elements, for reasons of symmetry (no cut-outs are analyzed). All vibrational modes are symmetrical or anti-symmetrical with respect to the axes of symmetry. In this way the amount of computer time can be reduced. By adequate choice of the boundary conditions regarding the displacements on the axes of symmetry all modes can be calculated.
The resonator is not supported, so all rigid body motions have to be included in the analysis. The material is isotropic and the elastic properties are defined by Young's modulus E, Poisson's ratio ν and the density ρ (see table 2.I). The accurary of the computer calculations is determined by the number of elements and the mesh density, the number of frequencies to be calculated and the number of iterations. Five iterations were sufficient to obtain an acceptable convergence using the ASKA-package and QUAM-9 elements (Ref. 66).
Table 7.I gives the resonance frequencies of the 12 lowest vibrational modes (the three rigid body motions excluded). Within a 4 kHz range around 20 kHz, four frequencies are calculated (modes 7, 8, 9 and 10). Figure 7.7 shows the vibrational modes (a quarter of the resonator).
To obtain the mode of the complete resonator, the modes shown have to be transformed according to the symmetry or antisymmetry. For reason of symmetry, the output and input surface do vibrate in an identical way.

From figure 7.7 one can conclude that several modes will not be suited because of the presence of nodal lines, resulting into zero amplitudes, and a non-uniform amplitude of the output surface. Vibrational mode no. 8 is very similar to the mode measured in

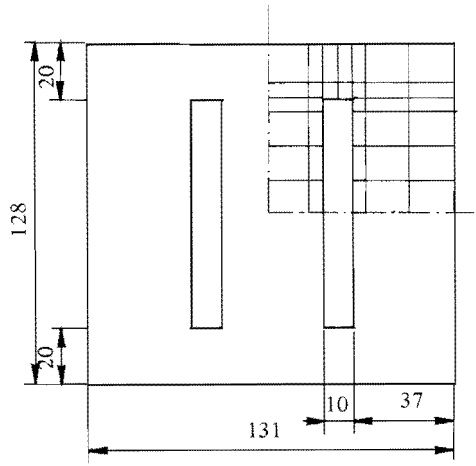

Fig. 7.6 A quarter of the resonator divided into QUAM-9 elements. (All dimensions in mm). $E = 0.73.10^{11}$ N/m², $\nu = 0.335$, $\rho = 2710$ kg/m³, thickness = 35 mm.

Mode no.	Resonance frequencies calculated (kHz) (finite elements)	Resonance frequencies measured (kHz)	Deviation (%)
1	6.58	6.80	3
2	7.32	7.50	2.3
3	8.04	8.30	3
4	9.88	10.38	5
5	14.32	14.45	0.9
6	14.97	15.18	1
7	19.16	19.15	0.07
8	19.38	19.38	0.03
9	19.86	19.98	0.6
10	21.31	21.32	0.07
11	24.56	24.67	0.43
12	26.98	26.95	0.1

Table 7.I Resonance frequencies calculated by finite element analysis and measured and the deviations; resonator dimension following figure 7.6.

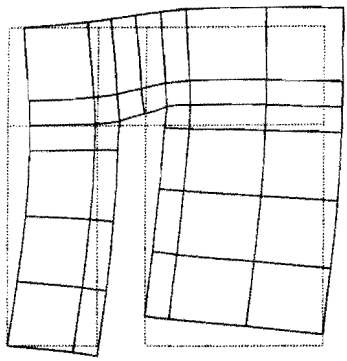

No. 1: 6.58 kHz

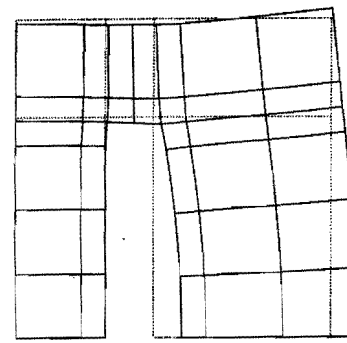

No. 2: 7.32 kHz

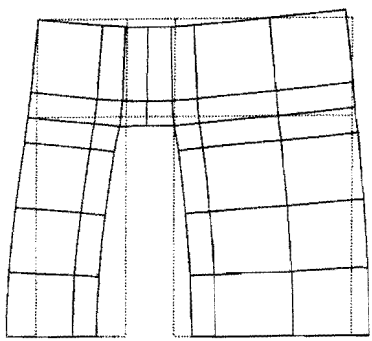

No. 3: 8.04 kHz

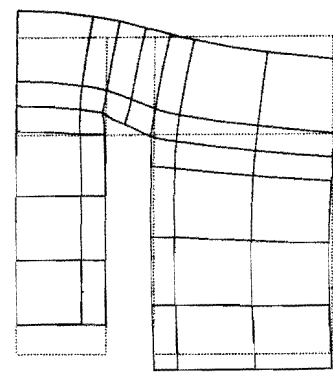

No. 4: 9.88 kHz

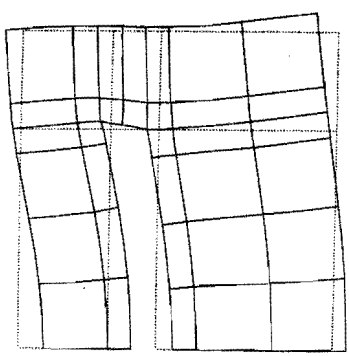

No. 5: 14.32 kHz

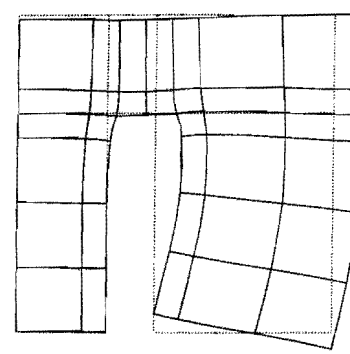

No. 6: 14.97 kHz

Fig. 7.7(1) Vibrational modes and corresponding frequencies as calculated from the finite element analysis. Only one quarter of the resonator is shown (modes are symmetric or antisymmetric with respect to the axis of symmetry of the resonator as shown in figure 7.6).

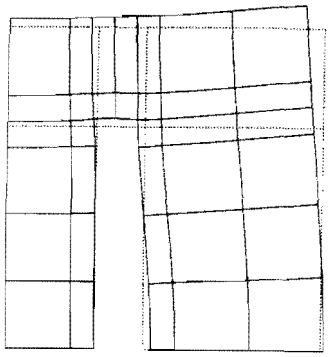

No. 7: 19.16 kHz

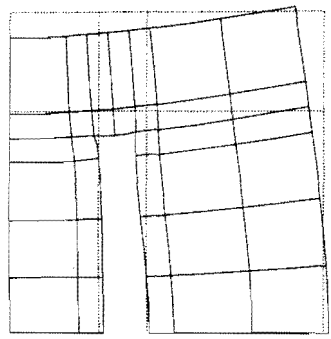

No. 8: 19.38 kHz

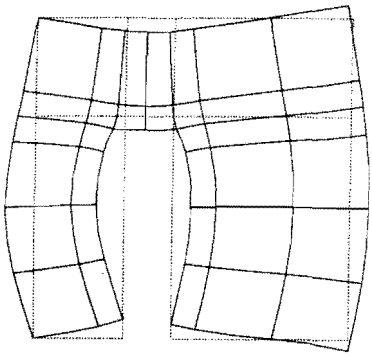

No. 9: 19.86 kHz

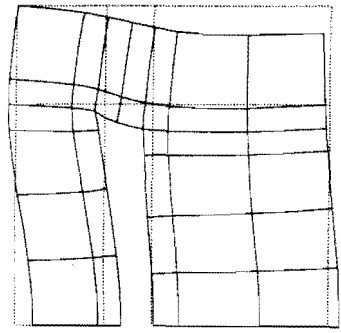

No. 10: 21.31 kHz

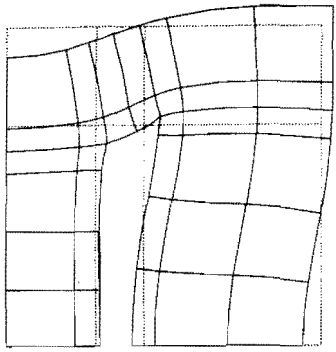

No. 11: 24.56 kHz

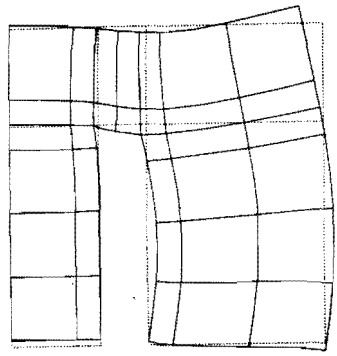

No. 12: 26.98 kHz

Fig. 7.7(2)

figure 7.2, showing a large amplitude near the centre and no motions at the edges. However, vibrational mode no. 7 has an amplitude distribution, which is very familiar to the desired "longitudinal" mode. It has even higher amplitudes near the edges.

From these calculations it can be concluded that it should be possible to have this 131 mm wide resonator vibrate in a "longitudinal" mode at 20 kHz without additional cut-outs etc.
Below measurements are presented to support these findings.

7.5 Experimental verification of the computer calculations

In order to investigate the accuracy of the frequencies as predicted by the calculations, a resonator was deviced having the same dimensions as used in the finite elment analysis. Two piezo-electrical vibration detectors and a spectrum analyzer were used to measure the frequencies (see chapter 2).
Figure 7.8 shows two frequency-spectra of the resonator. One of the detectors is used as transmitter and is connected to a variable frequency oscillator with constant output voltage. The second detector acts as a receiver and converts mechanical vibrations into an electrical signal. This signal is shown in fig. 7.8 on a linear scale. Each peak corresponds to a resonance condition. The transmission of mechanical energy and therefore the strength of the detected signal depends on the location of the transmitting elements. Clearly, when placed on a nodal line, no signal will be transmitted.
Fig. 7.8 shows the spectra for two locations of the detectors which are indicated by arrows. Obviously, some frequencies do disappear, or do result in a low signal transmission. Using this principle all vibrational modes could be identified and compared to those calculated. The frequencies detected in this way are summarized in table 7.I. (the accuracy of measurement is ± 10 Hz, see chapter 2).
A qualitative picture of the vibrational mode can be drawn using this method (vibration maxima, zeros etc. can be measured easily). It is not possible to obtain a phase relation for the various locations on the resonator.
Figure 7.9 shows the amplitudes of modes nr. 7, 8 and 9 as measured. For convenience these modes are shown in the same resonator, each representing a quarter of the complete mode.
The measurements are in good agreement with the calculations. For the lowest frequencies the deviation is 2-3%, but for the highest frequencies less than 0.5%. The computer calculations are therefore of sufficient accuracy.

7.6 Final optimization of the resonator

From the finite element analysis it was concluded that mode 7 has to be identified as the desired "longitudinal" mode. The resonance frequency of 19.16 kHz, however, is too low to assure a good coupling and high efficiency when coupled to the transducer of a welding apparatus. The resonator can be tuned to 20 kHz by shortening the length in the same proportion as the desired frequency change. The length at 20 kHz should therefore be:

$$l = \frac{19.16}{20.00} \; 128 = 122.6 \text{ mm}$$

The resonator of figure 7.4 was shortened to 122 mm in such a way as to guarantee a symmetric location of the slots. Figure 7.11a shows the frequency spectrum of the

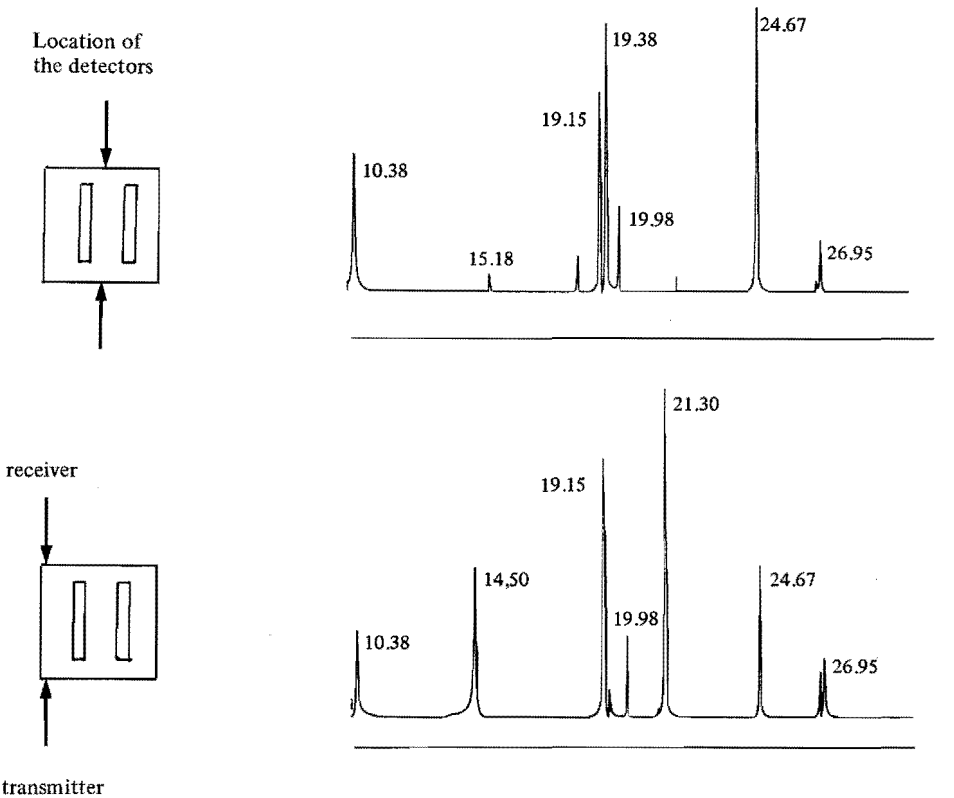

Fig. 7.8 Frequency spectrum for two locations of the detectors (vertically the detected signal is plotted on a linear scale, horizontally the frequency (kHz)), resonator dimensions according to figure 7.6.

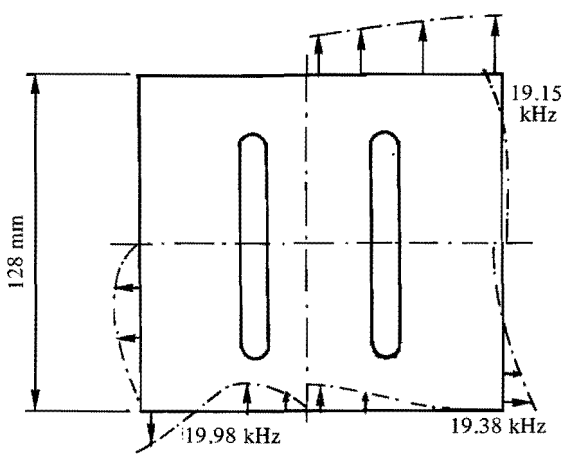

Fig. 7.9 Vibrational modes of three resonances as measured (only qualitatively)

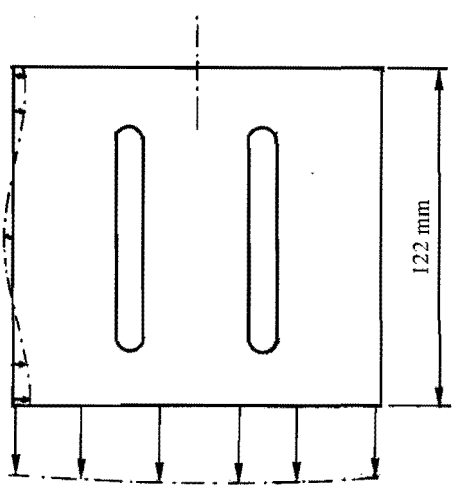

Fig. 7.10 Vibrational mode of the finally optimized resonator measured at 10 μm amplitude level, f = 20.06 kHz (resonator coupled to the transducer of a welding apparatus).

the resonator. The longitudinal mode is now in resonance at f = 20.57 kHz. This frequency is higher than 20 kHz because of the shorter length (influence ~ 250 Hz). The presence of the threaded hole at the input surface causes a higher resonance frequency (see chapter 5 and 6 where the influence was discussed briefly), the shift is about 150 Hz (hole 20 mm deep, 16 mm diameter).

The resonator was coupled to a transducer which has a resonance frequency of the longitudinal mode at 20.14 kHz (see figure 7.11b). The frequency-spectrum shows the admittance of the transducer when connected to a constant voltage source of variable frequency (see chapter 2); the admittance is proportional to the transducer current. There are no spurious modes detected in a 1 kHz range around this frequency. Figure 7.11c shows the spectrum of the resonator-transducer assembly. The "longitudinal" mode is found at 20.06 kHz. Comparison of figures 7.11a and 7.11c reveals that many resonances do disappear. Secondly it is found that coupling of two resonator systems results in a resonator assembly having a resonance-frequency which is lower than those of the components. The mass which is added by the coupling bolt causes a decrease of the resonance frequency. The only spurious mode detected at 19.59 kHz is of very low efficiency and could not be excited on the welding apparatus. It therefore does not influence the resonance behaviour of the longitudinal mode.
Figure 7.10 shows the amplitudes on the resonator surfaces measured, while the transducer was activated at high power level, comparable to that during welding. A very constant amplitude at the output surface is obtained indeed. This resonator showed good welding results.

7.7 Conclusion

It was shown that the design of resonators on an experimental approach not always results in the optimum solution. The success of it strongly depends on how good is the first "shot" to determine the overall dimensions of the resonator.
With finite element analysis the optimum was found in a much more effective way. However, there are still precautions to be regarded in the interpretation of the finite element calculations, because the coupling to a transducer causes frequencies to disappear and other to shift. The design of a 131 mm wide resonator presents no difficulty, in contradiction to the information from the suppliers of equipment. The resonator could be tuned to 20 kHz, without any disturbances due to coupling of some spurious modes.

In the following chapter an analysis will be presented to determine approximately the overall dimensions of the resonator for the "longitudinal" mode at a given design frequency.

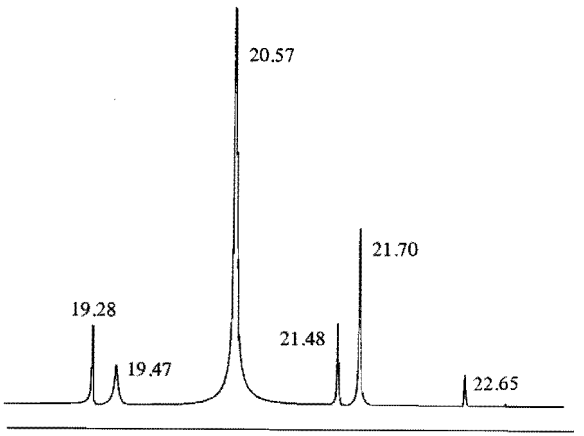

Fig. 7.11a Frequency spectrum of the final resonator of 122 mm length; horizontally frequency (kHz); vertically the detector signal (linear scale).

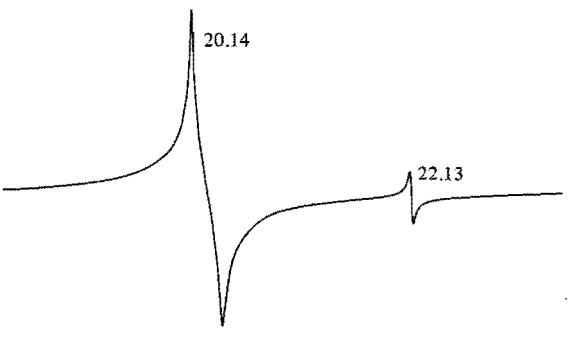

Fig. 7.11b Frequency spectrum of the transducer; horizontally the frequency (kHz); vertically the admittance of the transducer (logarithmic scale).

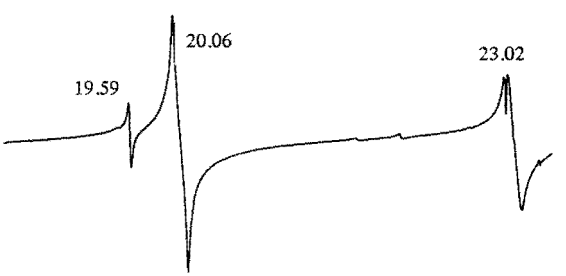

Fig. 7.11c Frequency spectrum of the transducer-resonator assembly; horizontally the frequency (kHz); vertically the admittance of the transducer (logarithmic scale).

8. A SIMPLIFIED MODEL TO CALCULATE THE RESONANCE CONDITIONS FOR THE LONGITIDUNAL VIBRATIONAL MODE IN WIDE RESONATORS

8.1 Introduction

In the previous chapter, the resonant length of a wide-output resonator was shown to be considerably smaller than the half-wavelength in a slender rod. To enable an efficient optimization, it was necessary to start with a resonator geometry close to the optimum geometry that will meet the design requirements. Some design rules will now be derived to approximate the optimum geometry. Although the wide resonator is separated into small resonators by slotting, there is the mass of the bridging elements that has to be taken into account. Below a simplified model will be presented to calculate the effect of this mass on the resonance frequency. The three resonator types as discussed in chapter 3 (blade-like, block-like and cylindrical-type) will be studied. The resonator is characterized by its overall dimensions, the length L, the width B, the thickness R or de diameter D, the number of slots, their location, length and width. Capitals are used here exclusively for the overall dimension.

Figure 8.1 shows a blade-like resonator of width B and length L, provided with three slots equally distributed over the width. The resonator thickness R is small as compared to the length ($R < \lambda/3$). The analysis will be restricted to slots of the shape as shown in fig. 8.1. The slot length (number of slots n, width t) is such that the bridging elements are s_1 and s_2 high respectively. A resonator can be divided hypothetically into a number of elements, each of which has exactly the same resonance frequency for the longitudinal mode. Figure 8.2 shows these elements, each to be considered as a slender rod with an additional mass at both ends for a blade-like resonator with two slots. The additional mass is identical for all elements. The number of slots usually will be chosen such that the width of these elements b is small as compared to the wavelength, but sufficiently wide to guarantee an acceptable overall stiffness of the resonator ($\lambda/8 < b < \lambda/4$). The separation into elements is such that each resonator has the same resonance frequency. After coupling, the complete resonator will have exactly the same resonance frequency as one of these separate elements.

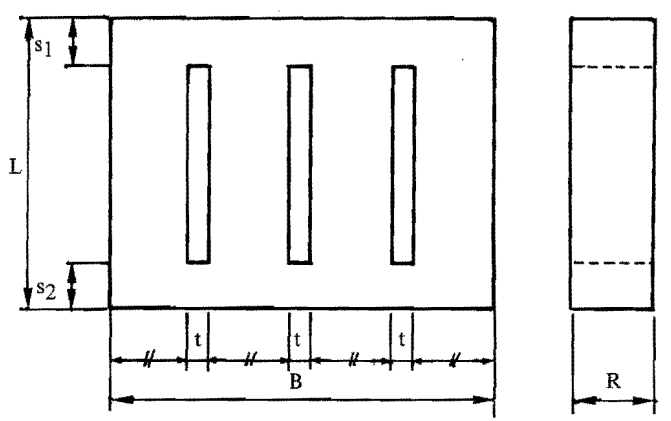

Fig. 8.1 Blade-like resonator with three slots of width t and length (L-s_1-s_2).

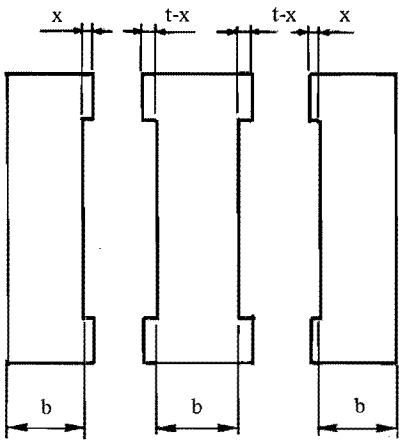

Fig. 8.2 Separation of a resonator into three equivalent elements, which can be considered as a slender-rod resonator

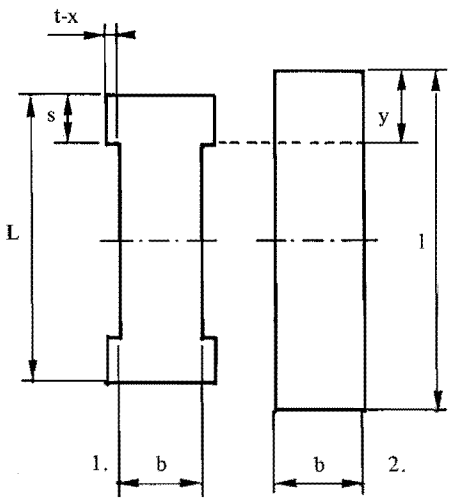

Fiig. 8.3 Comparison of the slender rod (2) to an element with additional masses (1).

In this model it is assumed that the vibrational mode of the resonator is not influenced by the coupling, so that at the output surface the vibration amplitude will be uniform as a result. (In chapter 6 it was demonstrated up to what width b the amplitude over the output surface remains constant).

8.2 The blade-like resonator

For the blade-like resonator of total width B, the width of the elements b follow from the number of slots n and their width t (see figure 8.2):

$$b = \frac{B-nt}{n+1} \tag{8.1}$$

The separation into elements is such that the total mass of each of the bridging elements is identical, no matter how it is distributed over the cross-section. We will assume for now that $s_1 = s_2 = s$.
From geometry the bridge section x follows: (see figure 8.2):

$$x = \frac{nt}{n+1} \tag{8.2}$$

At the design frequency f, the resonant length l of a slender rod with constant cross-section follows from (see figure 8.3.2.):

$$l = \frac{c}{2f} \tag{8.3}$$

At the same resonance frequency f, the resonant length L of one resonator element is smaller than l, for reasons of the added mass at the ends (see figure 8.3.1.). By equating the mechanical impedance (see chapter 2) of the longitudinal wave in the resonator element at distance s from the free end to the impedance in the slender rod resonator at distance y from the free end, a relation between y and s can be obtained.
From this the length L can be calculated. At distance y and s the modules of the mechanical impedance Z(y) and Z(s) are (see equation 2.13):

$$Z(y) = b\,R\,\rho c\,\tan(ky) \tag{8.4}$$

$$Z(s) = (b+x)\,R\,\rho c\,\tan(ks) \tag{8.5}$$

Both resonators are of identical materials so (8.4) and (8.5) give:

$$\tan(ky) = \frac{b+x}{b}\,\tan(ks) \tag{8.6}$$

From figure 8.3 it follows:

$$L = l - 2\,(y-s) \tag{8.7}$$

Combining equations (8.2), (8.3), (8.6) and (8.7) gives the resonant length L of the wide resonator:

$$L = \frac{c}{2f} + 2s - \frac{2}{k}\arctan\left[\left(1+\frac{nt}{B-nt}\right)\tan(ks)\right] \tag{8.8}$$

In chapter 6 the resonator of rectangular cross-section was discussed. The wave propagation velocity c depends on the ratio of the width and thickness to the half-wavelength, due to dispersion effects. It was shown that up to width to length ratios of 0.5 the resonant length can be calculated with sufficient accuracy with aid of the corrected value of the wave propagation velocity (equation 6.3).

By slotting the width of the elements will always be kept small ($< \lambda/4$) to keep the dispersion effect to a minimum. Using equation (6.3) the correction to the wave propagation velocity c' follows (using equation 8.1)):

$$\frac{c'}{c} = 1 - \frac{1}{6}\left(\frac{\nu \pi f}{c}\right)^2 \left(R^2 + \left(\frac{B-nt}{n+1}\right)^2\right) \qquad (8.9)$$

The wave number k and the velocity c, as used in equation (8.8) have to be corrected for the velocity c' ($k' = \frac{2\pi f}{c'}$).

For reasons of geometry it can be shown that for the case $s_1 \neq s_2$ equation (8.8) becomes:

$$L = \frac{c'}{2f} + s_1 + s_2 - \frac{1}{k'}\left[\arctan\left\{\left(1 + \frac{nt}{B-nt}\right)\tan(k' s_1)\right\} + \arctan\left\{\left(1 + \frac{nt}{B-nt}\right)\tan(k' s_2)\right\}\right] \qquad (8.10)$$

As an example figure 8.5 shows the resonant length L of a blade-like resonator versus its width B, with the number of slots as a parameter. The resonance frequency is 20 kHz, the resonator thickness is 35 mm, the slotwidth is 10 mm and the height of the bridging elements is equal for both ends s = 20 mm. Clearly the length L differs considerably from the half-wavelength $\lambda/2$ (130 mm). At B = 90 mm the difference between a resonator with no slots (n = 0) and two slots (n = 2) is about 6 mm or 5%.

In figure 8.4 the width b of the elements of the resonator is shown versus the number of slots. Generally, this width is chosen maximum $b \sim \lambda/4$ and minimum $b \sim \lambda/8$. For 20 kHz in aluminium or titanium resonators the choice is $30 < d < 60$ mm. When no slots are made, the maximum width is ± 70 à 80 mm (chapter 6). Using figures 8.4 and 8.5 one can easily determine how many slots are needed and what resonant length will be needed to have the resonator vibrating in a "longitudinal" mode at 20 kHz.

The maximum resonator width B in practice is about 300 mm at 20 kHz. Suppliers of ultrasonic equipment maintain that there are forbidden zones for the resonator width B. The range of $130 < B < 150$ mm and $190 < B < 220$ mm are such for bidden zones (Ref. 64), either because no mode could be found with a uniform output amplitude or because the resonators would always fail due to cracking. Others only apply an even number of slots. For odd numbers, the resonator will be coupled to the transducer right above such a slot. Strong arguments for these principles are not given.

Figure 8.5 reveals that in the case of only even slot numbers, the $80 < B < 110$ mm range cannot be used. At $B \sim 190$ mm there is a transition range, with only the two extremes for b. For wider resonators, the choice for the number of slots is less critical. The influence of the height of the bridging elements s and the slot width t on the resonant length L can be calculated from equation (8.10). For various resonators width B, the length L was calculated for a blade-like resonator of thickness R = 35 mm, slot width t = 10 mm and the number of slots being n = 3. See figure 8.6. The effect of this height s is little for wide resonators, but strong for the small ones. One can calculate from these how much the resonance frequency of an existing resonator can be raised when the height s is decreased. Conversely the frequency can be lowered by widening of the slot with t. The influence of t is shown in figure 8.7. As an example when t is widened from 8 to 10 mm, while all other dimensions are kept the same, the resonance frequency falls about 300 Hz (1,5%) (B = 140 mm, n = 3).

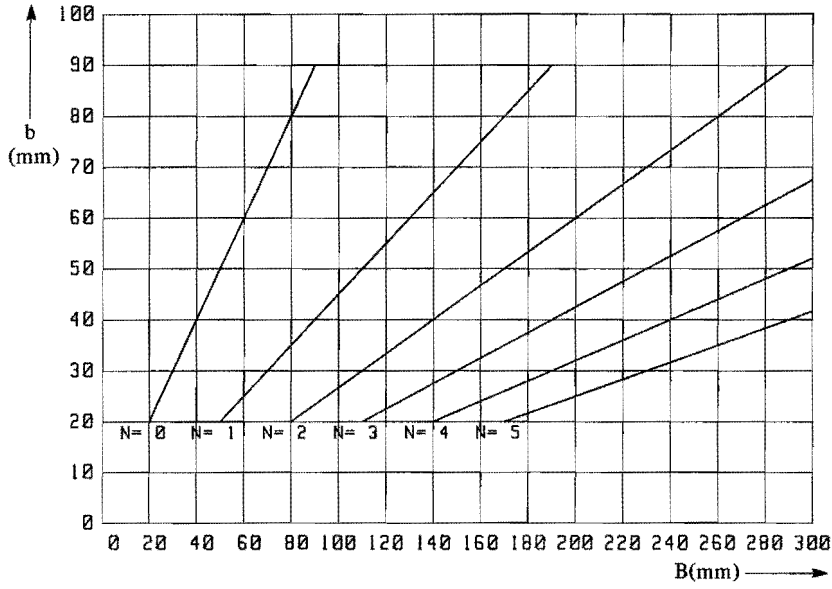

Fig. 8.4 The width b of the elements in a blade-like resonator versus the resonator width B as a function of the number of slots n. (f = 20 kHz, c = 5200 m/s, ν = 0.335, s = 20 mm, t = 10 mm, r = 35 mm). (equation 8.10)).

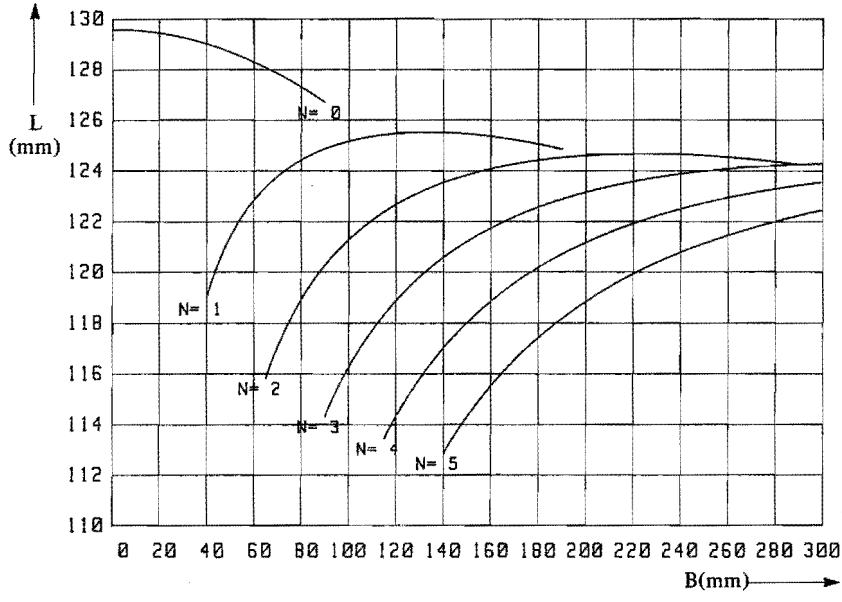

Fi.g 8.5 The resonance length of a blade-like resonator of width B as a function of the number of slots n (same conditions as in fig. 8.4). (equation (8.10)).

Figure 8.8 shows the effect of changing the resonator thickness R. This effect is small as compared to that of t or s.

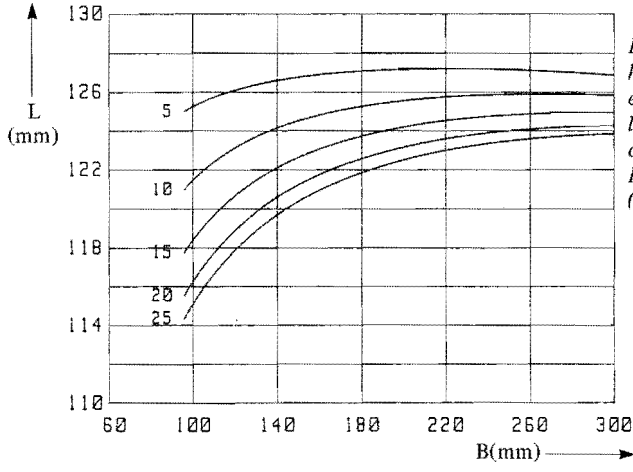

Fig. 8.6 The effect of the height s of the bridging elements on the resonant length (n = 3, f = 20 kHz, c = 5200 m/s, ν = 0.335, R = 35 mm, t = 10 mm). (blade-like resonator)

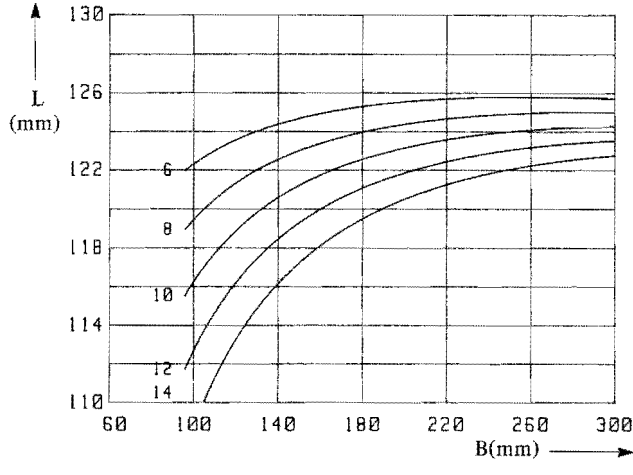

Fig. 8.7 The effect of the width t of the slots on the resonant length (n = 3, f = 20 kHz, c = 5200 m/s, ν = 0.335, R = 35 mm, s = 20 mm). (blade-like resonator)

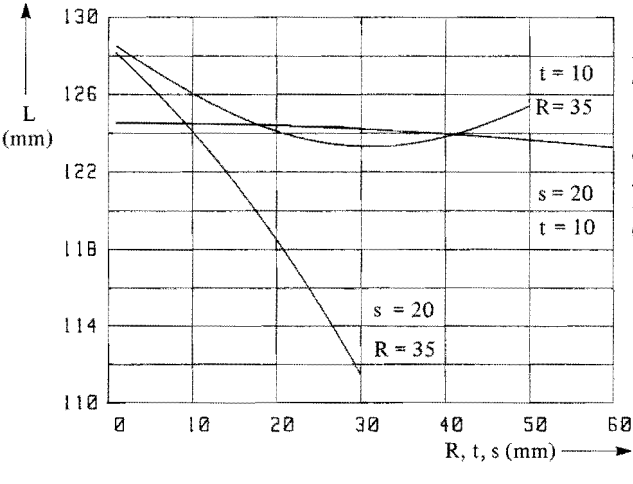

Fig. 8.8 The effect of the slot width t, the height of the bridging elements s and the resonator thickness R on the resonant length (n = 3, B = 160 mm, f = 20 kHz, c = 5200 m/s, ν = 0.335). (blade-like resonator)

Eight existing blade-like resonators were analysed.
Table 8.I summarizes the results. The resonance frequency of the longitudinal mode was measured. In order to check the validity of equation (8.10), the resonator length L' was calculated from (8.10) using the measured resonance frequency f_{res} as design parameter. This length L' is compared to the actual length L. The ratio L'/L is given in table 8.I. In almost all cases the deviation is less than 0.5%. Bearing in mind that a tolerance on the fabrication of the resonator of ± 0.5 mm already results in a frequency deviation of $\frac{0.5}{130} * 100 = 0{,}38\%$, one can conclude that equation (8.10) is accurate enough to calculate the resonant length of blade-like resonators.

	n	R * B * L	t	s1, s2	f_{res}	L'/L
	(–)	(mm^3)	(mm)	(mm)	(kHz)	(–)
Nr. 1	1	35 * 100 * 125	10	20	20.00	1.002
Nr. 2	2	35 * 145 * 124	10	20	20.02	0.997
Nr. 3	2	27 * 105 * 125	8	20	19.98	0.990
Nr. 4	2	63 * 100 * 121	9	16 20	20.10	1.004
Nr. 5	2	72 * 189 * 125	8	18 20	19.78	1.005
Nr. 6	2	49 * 184 * 125	8	19 20	19.92	1.004
Nr. 7	2	35 * 130 * 127	10	20	19.30	1.004
Nr. 8	5	35 * 229 * 123	10	20	19.85	1.004

Table 8.1 Analysis of 8 blade-like resonators of thickness R, width B and length L and slot number n; the measured resonance frequency f_{res}, is compared to the calculated one by equation (8.10) through L'/L. (Material Aluminium c = 5200 m/s, ν = 0.335).

8.3 The block-like resonator

The analysis of the block-like resonator is identical with that of the blade-like one. Figure 8.9 shows such a resonator. The difference is the large dimension in the thickness direction. The lateral dimensions B and R are provided with n_1 and n_2 slots respectively. For completeness the resonant length of this resonator type will be determined for different height of the bridging elements (s_1 and s_2). Using equation (8.9) and (8.10) it follows:

$$\frac{c'}{c} = 1 - \frac{1}{6}\left(\frac{\nu \pi f}{c}\right)^2 \left[\left\{\frac{B-n_1 t}{n_1+1}\right\}^2 + \left\{\frac{R-n_2 t}{n_2+1}\right\}^2\right] \qquad (8.11)$$

$$L = \frac{c'}{2f} + s_1 + s_2 - \frac{1}{k'}\left[\arctan\left\{\left(1 + \frac{n_1 t}{B - n_1 t}\right)\left(1 + \frac{n_2 t}{R - n_2 t}\right)\tan(k' s_1)\right\} + \right.$$

$$\left. + \arctan\left\{\left(1 + \frac{n_1 t}{B - n_1 t}\right)\left(1 + \frac{n_2 t}{R - n_2 t}\right)\tan(k' s_2)\right\}\right] \qquad 8.12$$

As an example, the length L for a 20 kHz resonator of R = 150 mm having one slot in this direction ($n_2 = 1$) is calculated (see figure 8.10). The width B varies over a wide range, with 0 to 5 slots into it. The actual resonant length considerably differs from the half-wavelength. The length difference is ± 10-20 mm (10-15%!).
Figure 8.11 gives the results for a 40 kHz resonator. From these figures one can determine what number of slots is needed and what length L will be found.

The design of block-like resonators is more complicated as the results shown before would suggest. The resonant length L can be calculated, but the presence of spurious modes cannot be predicted. In appendix 1, the design of one specific block-like resonator is discussed to illustrate how spurious modes can be coupled to the longitudinal one, and how they can be eliminated on account of the measurement of resonance frequencies and vibrational modes.

In the following chapter the finite element method will be used, as an example, to study the effect of slot length variations on the vibrational characteristics of a blade-like resonator. With aid of mode charts that can be derived, one can predict the effect of changes in geometry on the presence of spurious modes, and how to eliminate them without influencing the "longitudinal" mode.

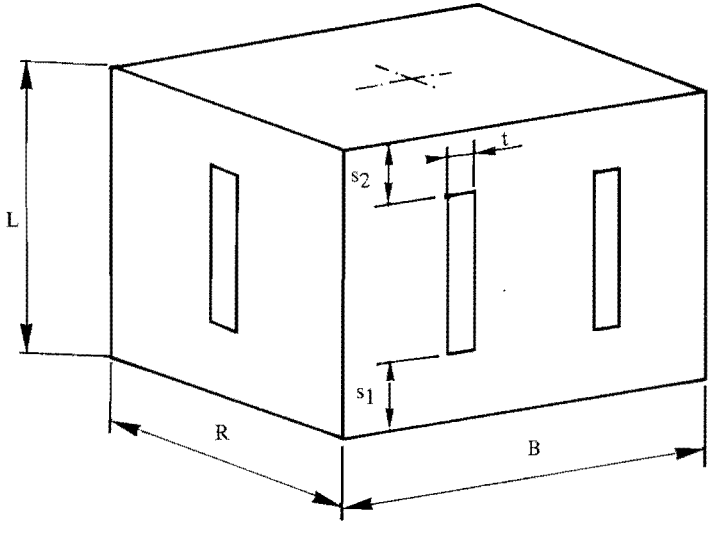

Fig. 8.9 A block-like resonator; width B, thickness R with $n_1 = 2$ and $n_2 = 1$ slots respectively.

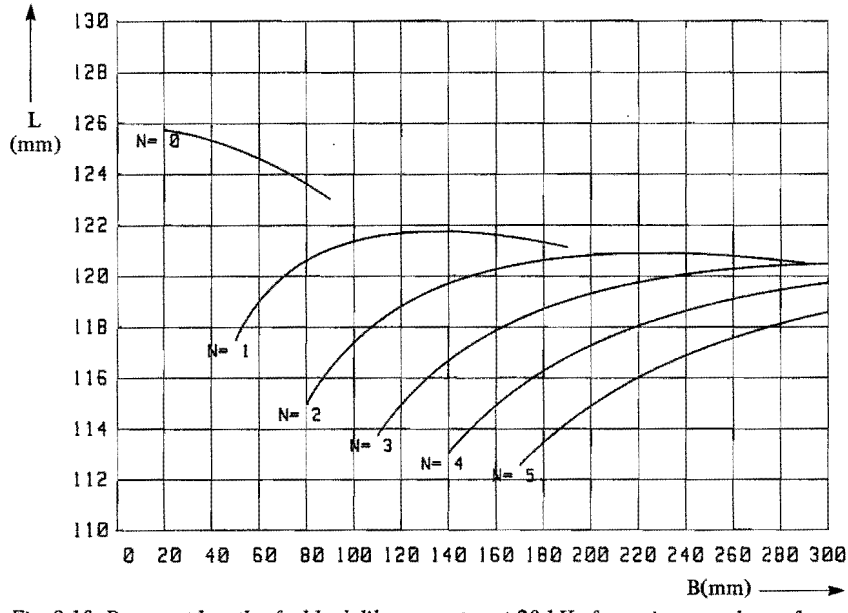

Fig. 8.10 Resonant length of a block-like resonator at 20 kHz for various numbers of slots as a function of its width B (R = 150 mm, n_2 = 1, t = 10 mm, s = 20 mm, c = 5200 m/s, ν = 0.335) (equation (8.12)).

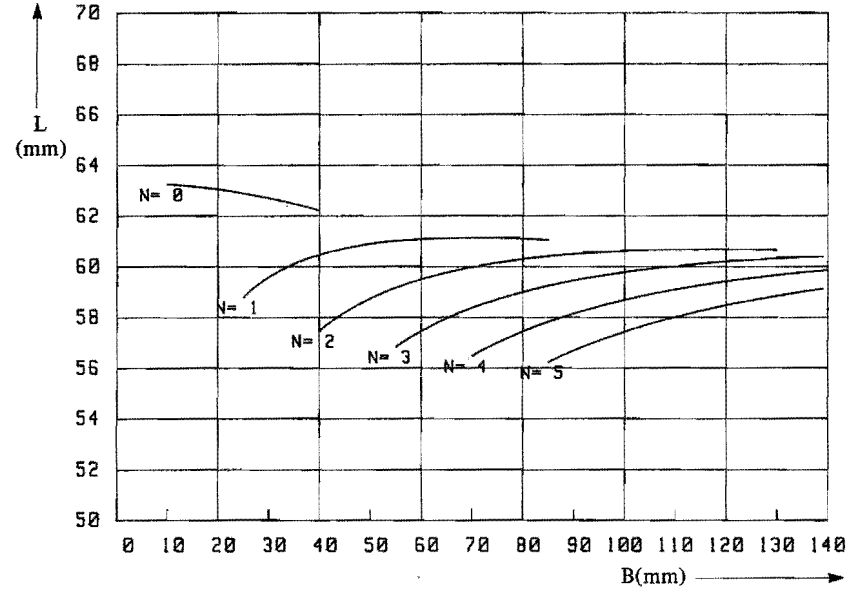

Fig. 8.11 Resonant length of a block-like resonator at 40 kHz for various numbers of slots as a function of its width B (R = 50 mm, n_2 = 1, t = 5 mm, s = 12 mm, c = 5200 m/s, ν = 0.335) (equation (8.12)).

8.4 The cylindrical-type resonator

Resonators of the cylindrical type are provided with slots in radial direction all over the diameter in a similar way as the other types. The number of slots is chosen such that the portions at the circumference, separated by the slots do not exceed $\lambda/4$. As shown in figure 8.12, the cross-section of the resonator is divided into n pie-elements of area A. By providing slots this area is reduced to A':

$$A' = \frac{\pi}{4} D^2 \left[\frac{1}{n} - \frac{1}{\pi} \arcsin\left(\frac{t}{D}\right)\right] - \frac{t.D}{4}\sqrt{1-\left(\frac{t}{D}\right)^2} + \frac{t^2}{4 \tan\left(\frac{\pi}{n}\right)} \qquad (8.13)$$

The propagation velocity of longitudinal waves into rods of quasi triangular cross-section is not easily calculated. As its dimensions are kept small as compared to the wavelength, it is assumed that the dispersion effect of the longitudinal wave can be estimated by using the Rayleigh correction in which the contribution of the cross-sectional area is taken rather than the actual shape (equation (6.5)). The resonant length again is calculated using the mechanical impedance transformation (equation (8.4)). The bridging elements are s_1 and s_2 high. Using equations (8.9), (8.13) it follows:

$$\frac{c'}{c} = 1 - \nu^2 \left(\frac{2\pi f}{c}\right)^2 \frac{A'}{4\pi} \qquad (8.14)$$

$$L = \frac{c'}{2f} + s_1 + s_2 - \frac{1}{k'}\left[\arctan\left\{\frac{A}{A'}\tan(k's_1)\right\} + \arctan\left\{\frac{A}{A'}\tan(k's_2)\right\}\right] \qquad (8.15)$$

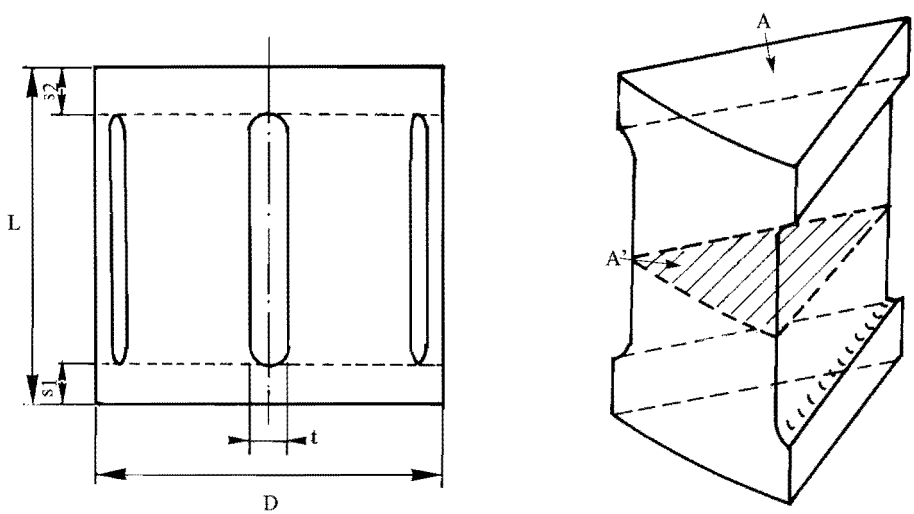

Fig. 8.12 Resonator of the cylindrical-type of diameter D and length L; the number of slots n is symetrically distributed along the circumference.

The minimum number of slots is n = 3, if the circumferential dimension of the elements is at least smaller than the diameter. It will be clear that the resonator diameter must not exceed 2 times $\lambda/3$ in order to guarantee any dimension of the cross-section being smaller than $\lambda/3$. At 20 kHz this implies a maximum diameter of ± 160 mm. Above this diameter the presence of the slots will not be sufficient to brake the Poisson coupling, unless other slots or cut-outs in the circumferential direction are provided. As an example figure 8.13 gives the length L for various diameters versus the number of slots.

The effect of variations of the length L on the resonance frequency for the longitudinal mode is seen in figure 8.14. This kind of relations can be very helpful to predict the effect of a length decrease when tuning up a specific resonator to raise its resonance frequency.

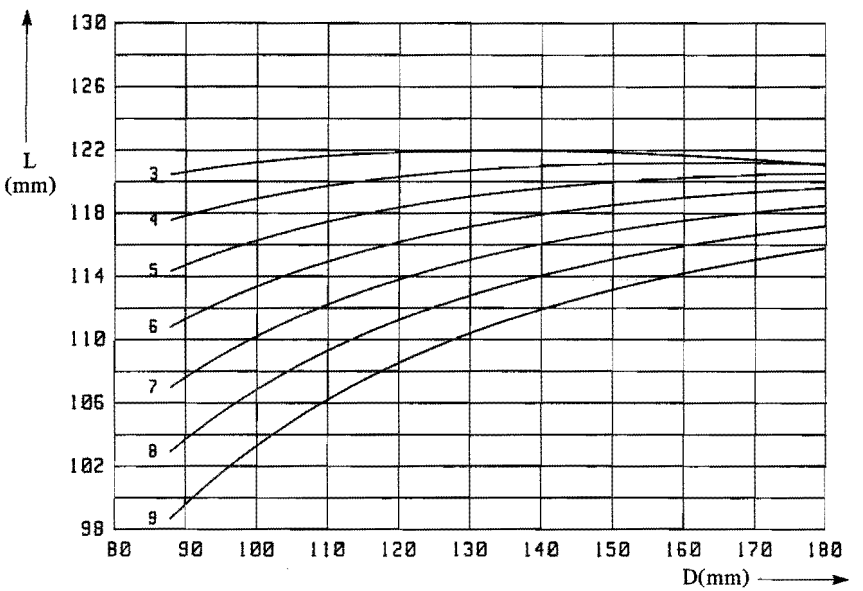

Fig. 8.13 Resonant length L of a 20 kHz cylindrical-type resonator for various number of slots (t = 10 mm, s = 20 mm, c = 5200 m/s, ν = 0.335) (equation (8.15))

8.5 Conclusions

The method described here to calculate the resonant length of wide-output resonators with slots, is very straightforward. However, comparison with some experiments showed the validity of this approximate theory. With the formula presented above one can determine how the resonator dimensions should be if a "longitudinal" vibrational mode must be possible at a given design frequency. Although the overall dimensions are correct for the "longitudinal" mode, it does not exclude the presence of spurious modes, as was shown in appendix 1 for a block-like resonator. However, the formula will be very helpful to predict how the change of some dimensions (to eliminate the spurious modes) will influence the resonance frequency of the "longitudinal" mode.

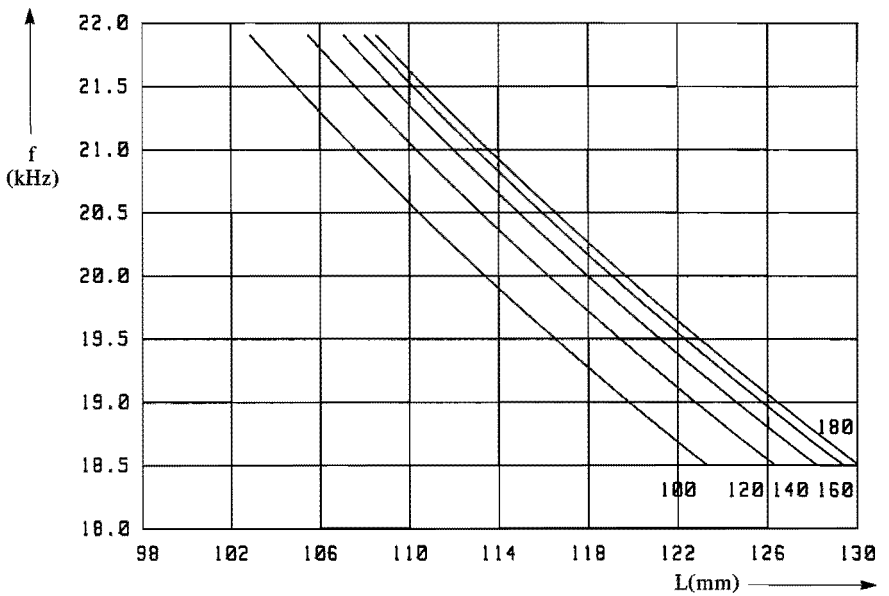

Fig. 8.14 The resonance frequency of a cylindrical-type resonator versus the length L for some diameters D (mm) (c = 5200 m/s, ν = 0.335, s = 20 mm, t = 10 mm, n = 6).

9. FINITE ELEMENT ANALYSIS OF THE EFFECT OF SHAPE VARIATIONS FOR SOME RESONATORS

9.1 Introduction

In the previous chapters a simplified model was presented to calculate the resonance conditions for three classes of wide resonators. Only the resonance frequency for the desired ("longitudinal") mode was chosen as a design parameter. By providing slots it was pursued to obtain a mode with a flat amplitude distribution at the output surface. However, the model is of no value to predict the optimum slot dimensions or locations with respect to the vibrational mode to be obtained. Neither can it be predicted when spurious modes will interfere with the desired one. In this chapter the effect of slot dimensioning for a blade-like resonator will be discussed with respect to the resonance frequencies, the shape of the "longitudinal" modes and the presence of spurious modes. Questions that will be answered are: does the "longitudinal" mode exist at all; are there critical slot dimensions; may the effect of slot length variations on the resonance frequency and the vibrational mode lead to contradictory requirements?

9.2 Two types of slots in a blade-like resonator

In chapter 6 the solid rectangular resonator was studied. When both width and length dimensions are in the order of the half-wavelength, the vibrational mode shows a strong distortion (see figure 6.8). Below such a resonator will be provided with two types of slots to compensate for the distortion. The first (A) as shown in figure 9.1, is identical with those discussed in chapter 8. The second (B) as shown in figure 9.2 is a slot with an open end at the output surface. This type has not been analyzed up to now, but it is often met with in practical resonators. Both will influence the resonance frequencies and the vibrational modes of the resonator. Of slot type A the effect of its length will be studied by variation of the thickness of the bridging element s (figure 9.1). For slot type B the variations of the length h will be studied (figure 9.2). In both cases the resonator is designed to resonate near 20 kHz in the "longitudinal" mode. The overall dimensions will be kept constant (length = 130 mm, width = 110 mm, thickness = 35 mm, slot width = 10 mm). The material is aluminium (see table 2.I).

9.3 Finite element analysis

A standard finite element package was used to anlayze the vibrational modes and corresponding resonance frequencies of the two resonator types described above. For reasons of symmetry, only part of the resonator needs to be analyzed (see figure 9.3) and in case of slot type B only half of the resonator is analyzed (see figure 9.4). By proper choice of the boundary conditions all modes which will occur in the total resonator can be calculated. The blade-like resonator will be considered as a two-dimensional problem (plain stress). No vibrational modes with motions perpendicular to the surface of drawing (see figure 9.3 and 9.4) will be calculated. It was demonstrated before that this assumption holds for practical resonator designs. Secondly, only those modes will be analyzed which do have an axis of symmetry coinciding with that of the resonator through the center of the input and output surface. In chapter 7 it was shown that modes which are not symmetrical with respect to this axis are not likely to be excited when the resonator is coupled to a transducer.

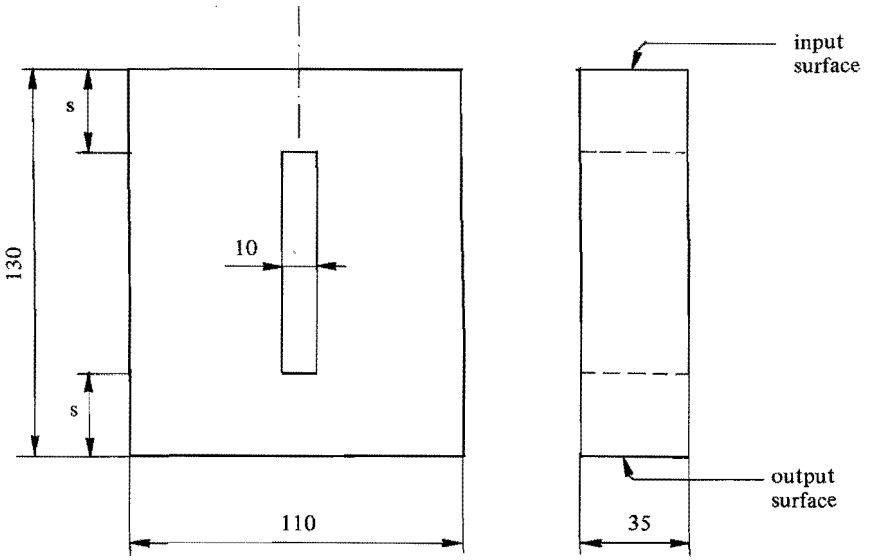

Fig. 9.1 Blade-like resonator of 110 mm width and 130 mm length with slot types A; thickness s of the bridging elements

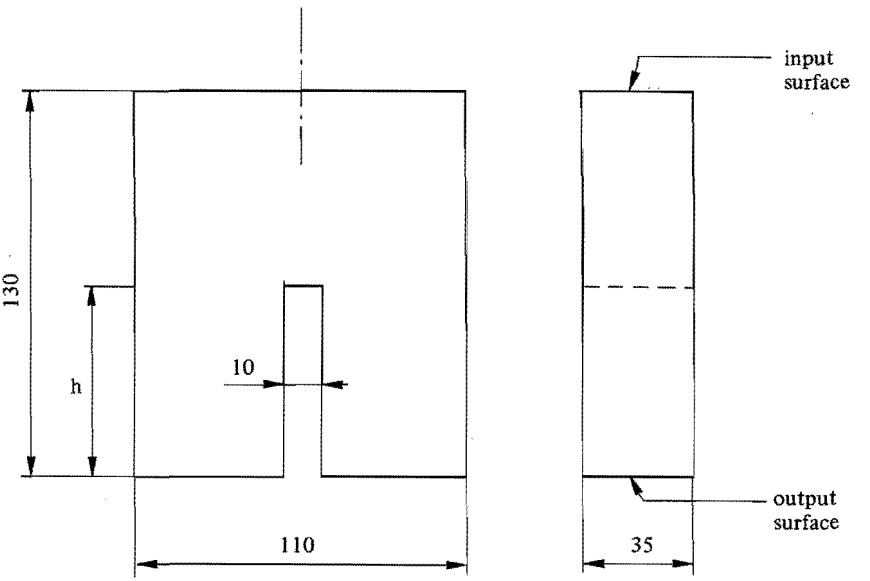

Fig. 9.2 Blade-like resonator of 110 mm width and 130 mm length with slot type B; of length h

Figure 9.3 and 9.4 show the division into elements. The number of element is so that at least 2 elements cover a half-wavelength of any mode to be calculated. In order to obtain valuable information from the calculations, all modes with a resonance frequency up to 30 kHz have to be calculated. In all cases the determination of the 10 lowest resonance frequencies was sufficient. The convergence of the solutions in solving the eigen value problem, generally was very fast, normally requiring only 4 iterations. The accuracy of the frequencies resulting from the finite element analysis was compared with experiments. In table 9.I the analysis of the solid rectangular resonator is summarized (see also chapter 6, table 6.I, no. 4), with the measurements of the resonance frequencies. The vibrational modes are shown in figure 9.5. Comparison of measurements and calculations yields a deviation of about 1%. As compared to the results discussed in table 7.I these results are somewhat less accurate, but still very well acceptable.

Frequencies (kHz)			
Mode	**Calculated**	**Measured**	**Deviation**
1	18.46	18.66	+ 1.06%
2	20.08	19.88	− 1.04%
3	21.94	21.81	− 0.64%

*Table 9.I Comparison of calculations and measurements for the solid rectangular resonator (resonator 110 * 130 * 35 mm³); the mode number is according to figure 9.5.*

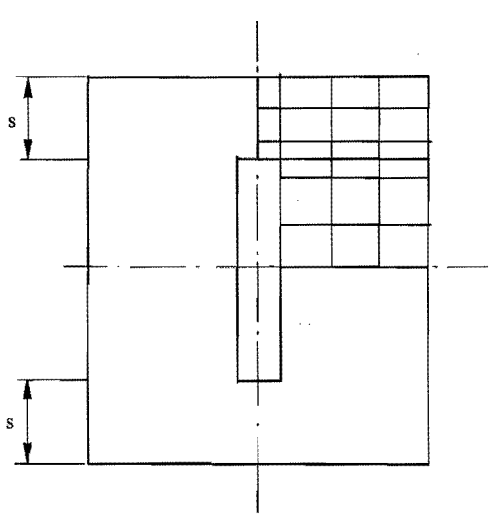

Fig. 9.3 Slot type A, division into finite elements (resonator of figure 9.1)

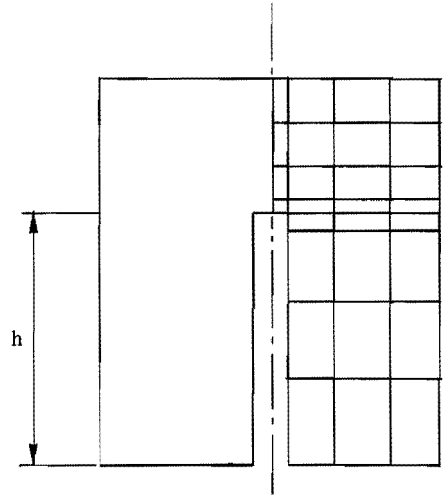

Fig. 9.4 Slot type B, division into finite elements (resonator of figure 9.2)

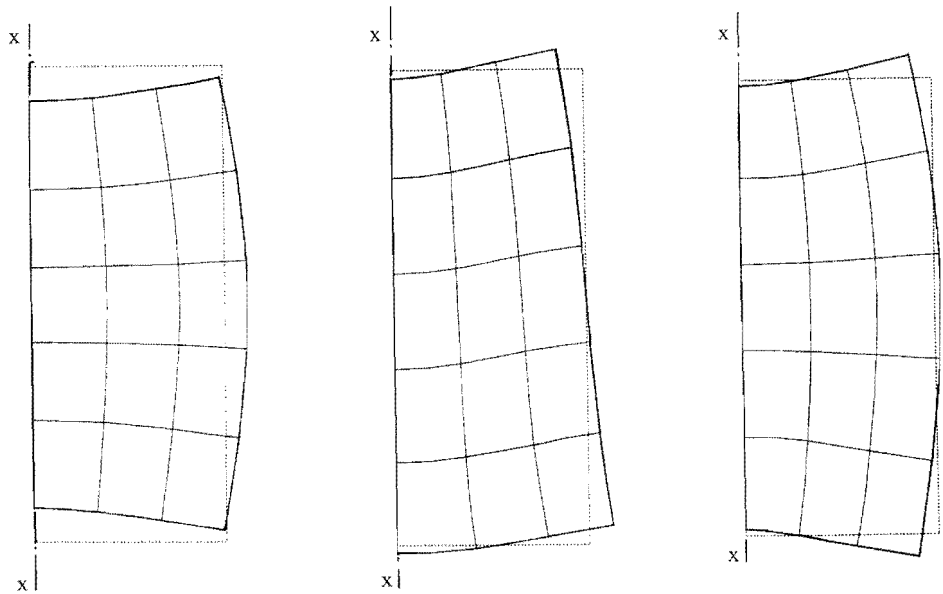

*Fig. 9.5 Vibrational modes of the solid rectangular resonator for the resonance frequencies near 20 kHz. All modes are symmetric to the axis x-x (only half of the resonator is shown, dimensions 110 * 130 * 35 mm³).*

9.4 Variation of the slot length of type A (figue 9.1)

The influence of the slot length of the resonator as shown in figure 9.1 and 9.3, is studied through the variation of the thickness s of the bridging elements. The case where there is no slot was shown in figure 9.5. The results of the finite element analysis are summarized in table 9.II. The lowest modes are presented, covering the frequency range from 0 to 35 kHz. There are always two or three frequencies near the design frequency of 20 kHz. The corresponding modes are shown in figures 9.6 to 9.9. In order to obtain the vibrational mode of the total resonator, the results have to be transformed according to the axis of symmetry. There are symmetric and anti-symmetric modes. From these modes the effect of slot length variations can be understood. As an example, the first three modes in figure 9.6 (s = 55 mm), are similar to those in figure 9.5. Clearly the small slot length hardly influences the mode shapes. The resonance frequencies of the first and third mode are lowered, while that of the second mode is increased. Finally, this small slot length does not improve the resonator so that a flat amplitude distribution near the output surface is obtained.

mode \ s	10	20	35	55	65
1	5.96	7.69	11.38	17.11	18.46
2	13.45	16.97	19.39	20.19	20.08
3	19.14	19.33	19.99	21.01	21.94
4	19.54	21.63	22.84	24.68	26.08
5	23.33	22.96	23.98	26.53	26.78
6	32.13	32.21	35.53	34.86	–
7	35.36	35.54	35.71	35.98	–

Table 9.II Calculated resonance frequencies (kHz) for the resonator of slot type A (see figure 9.1) as a function of the thickness s (mm) of the bridging elements for the 7 lowest modes (s = 65 mm corresponds to the solid rectangular resonator).

On account of the interpretation of the modes one can set up a frequency spectrum for the resonator, relating the resonance frequency of a specific mode shape as a function of the slot length. Figure 9.10 is such a frequency spectrum showing the branches for the 5 lowest modes.
Starting from the solid resonator (no slot) all frequencies decrease with increasing slot lengths. Only one mode has an almost stationary frequency for s = 10 up to s = 35 mm. Of very great importance is the observation that for some values of s two branches are crossing each other. In the frequency range of interest mode γ is crossing mode β three times! Near those crossing points clearly interferences of these modes can be expected when devicing a resonator. If no spurious modes are to be allowed in a 1 kHz bandwidth around the design frequency of 20 kHz, only a very limited choice of the slot length is possible.

Up to now no attention has been paid to what mode branch meets the design requirements for application as a welding tool. As a flat amplitude distribution at the output surface is desired, the choice of the slot length is restricted again. Close observation of the modes reveals that only three are found acceptable. These are marked in figure 9.10; for s = 35 mm, s = 20 mm and s = 10 mm respectively (all on mode branch γ). All slot lengths for values of $10 < s < 35$ mm will be a good choice. For $s > 35$ mm no acceptable mode shape if found. However, combination of the requirements of no spurious modes in a 1 kHz bandwidth and the latter results in a slot length range of $15 < s < 25$ mm.

Mode branch α (figure 9.10) for s = 65 mm corresponds to the longitudinal mode for the solid resonator. From the definition this mode is called the fundamental "longitudinal" mode (chapter 6). It has no flat amplitudes distribution at the output surface (in consequence of distortion due to Poisson's coupling). As can be seen in figure 9.10 those modes which have a uniform amplitude distribution at the output surface are on the γ branch. These are therefore not originating from the fundamental longitudinal mode in the solid resonator, but rather from a second order higher mode.

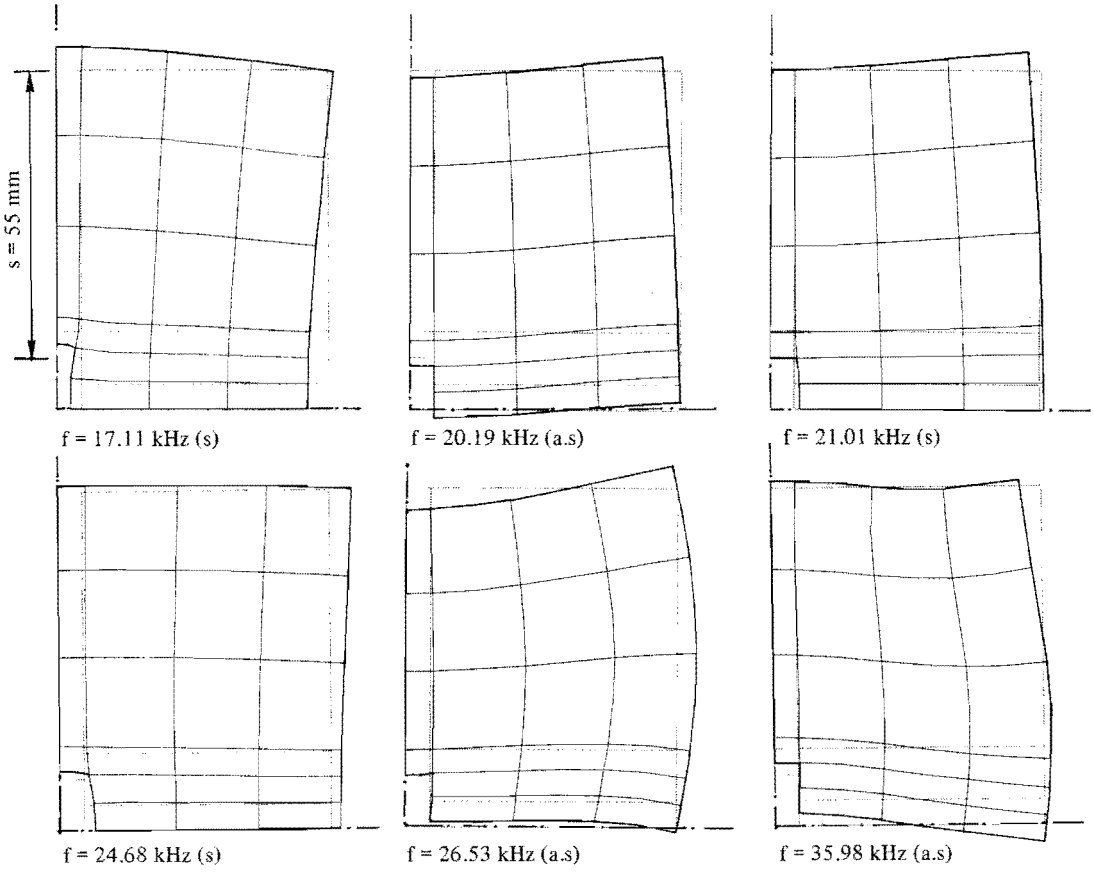

Fig. 9.6 Vibrational modes for the resonator of slot type A for s = 55 mm (see figure 9.3). (The axes of symmetry are shown; s = symmetric mode, a.s = anti-symmetric mode).

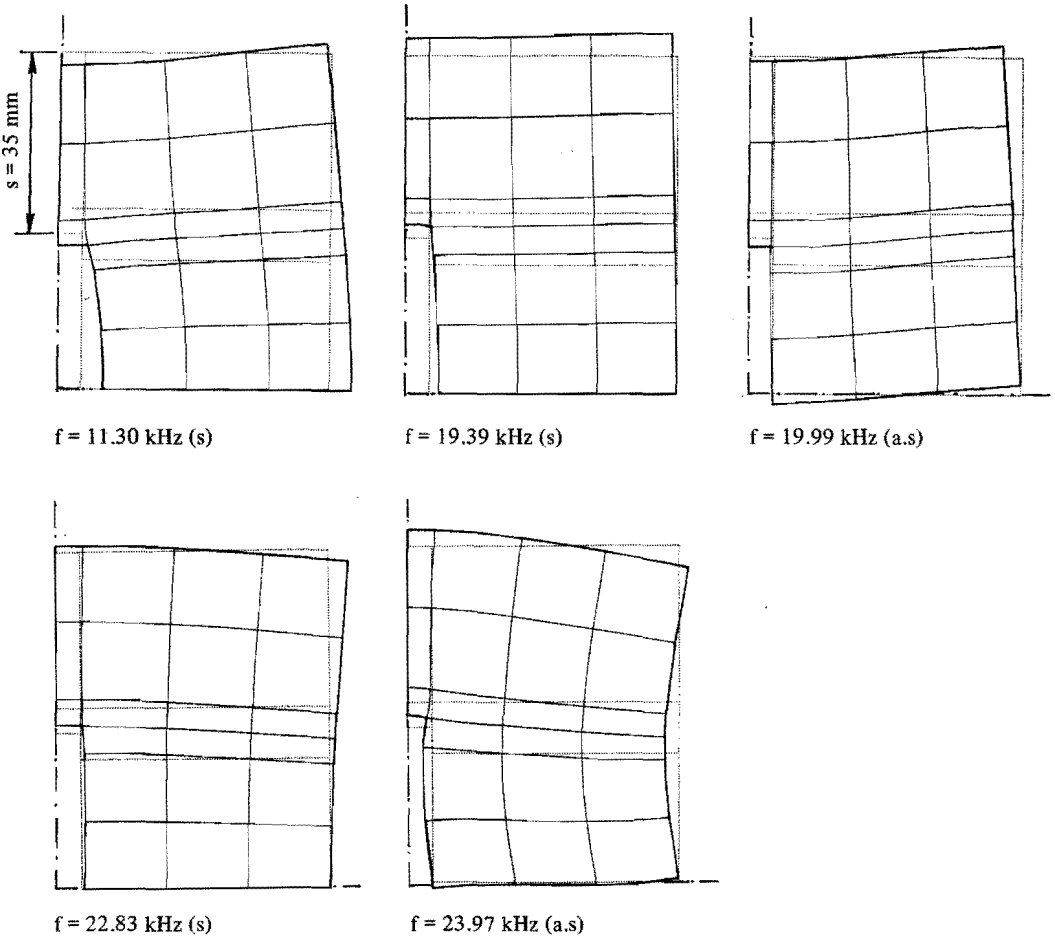

Fig. 9.7 Vibrational modes for the resonator of slot type A for s = 35 mm (see figure 9.3). (The axes of symmetry are shown; s = symmetric mode, a.s = anti-symmetric mode).

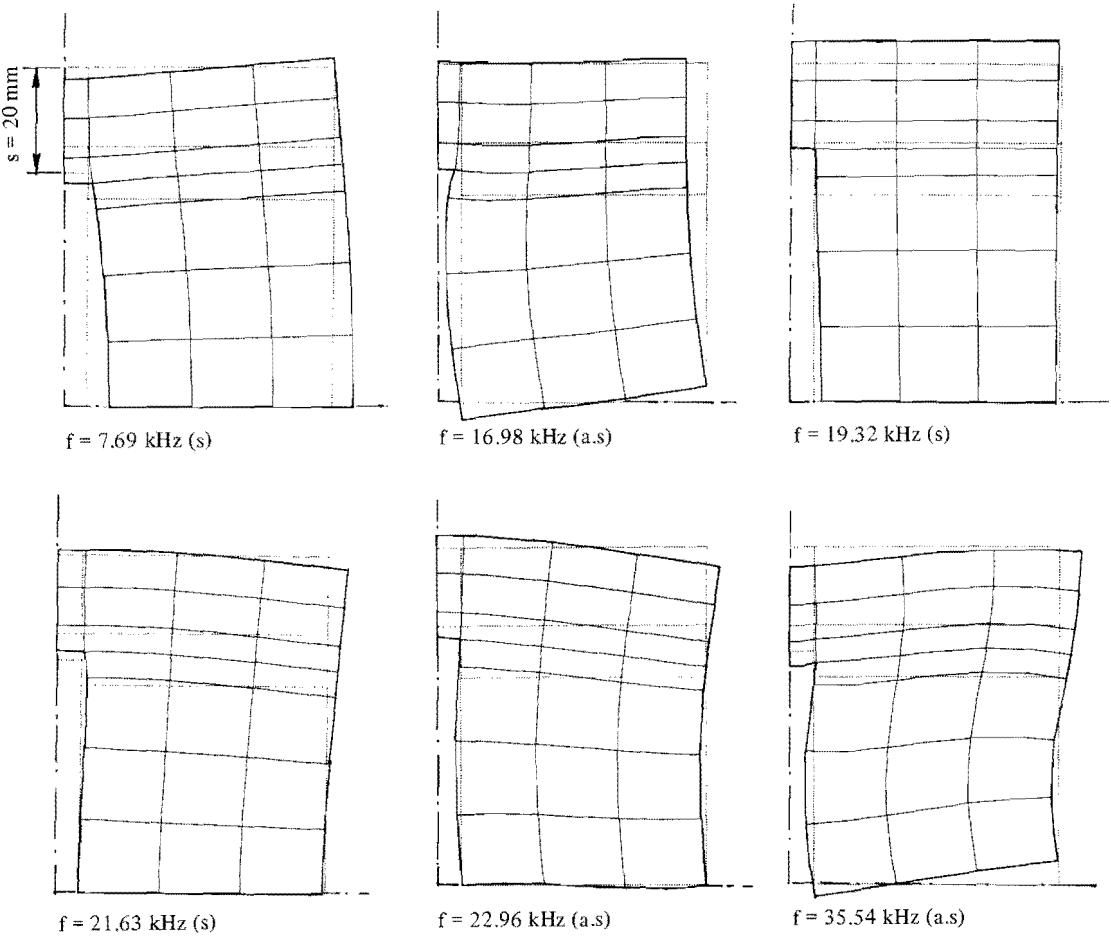

Fig. 9.8 Vibrational modes for the resonator of slot type A for s = 20 mm (see figure 9.3). (The axes of symmetry are shown; s = symmetric mode, a.s = anti-symmetric mode).

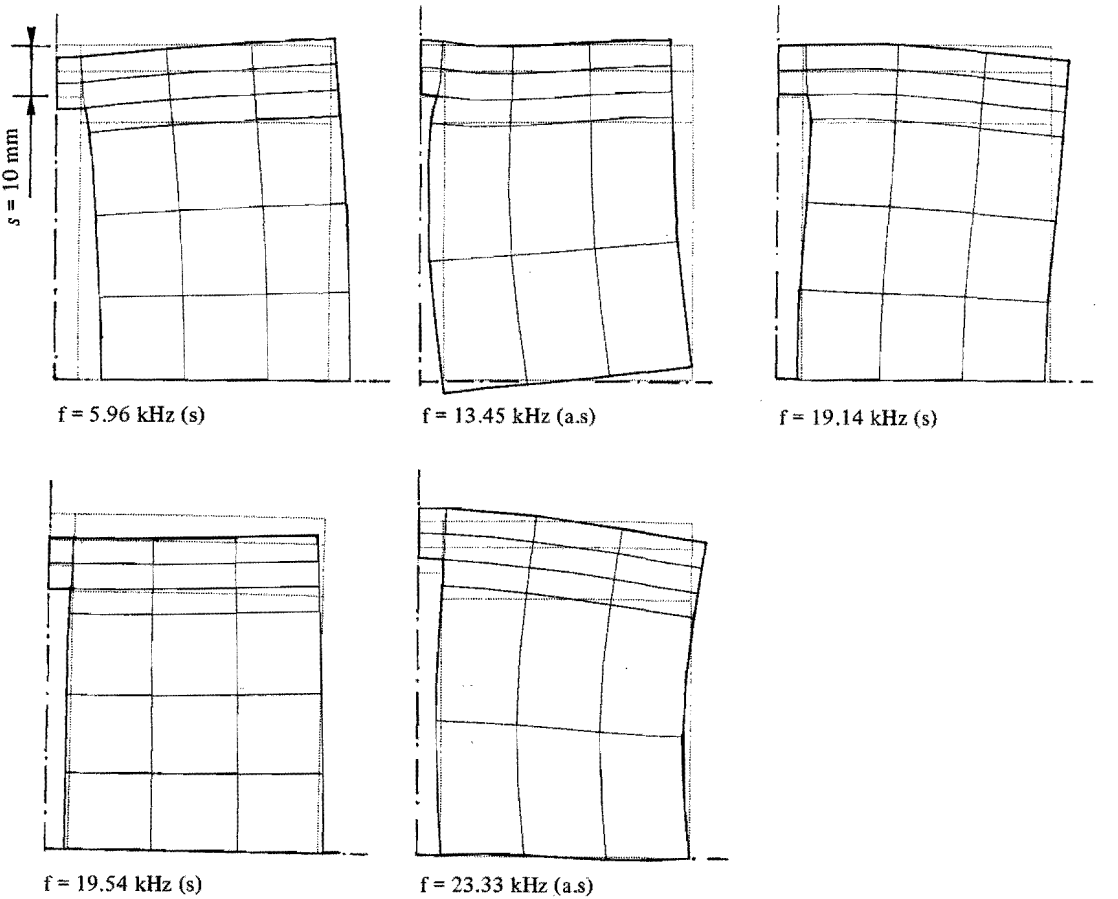

Fig. 9.9 Vibrational modes for the resonator of slot type A for s = 10 mm (see figure 9.3). (The axes of symmetry are shown; s = symmetric mode, a.s = anti-symmetric mode).

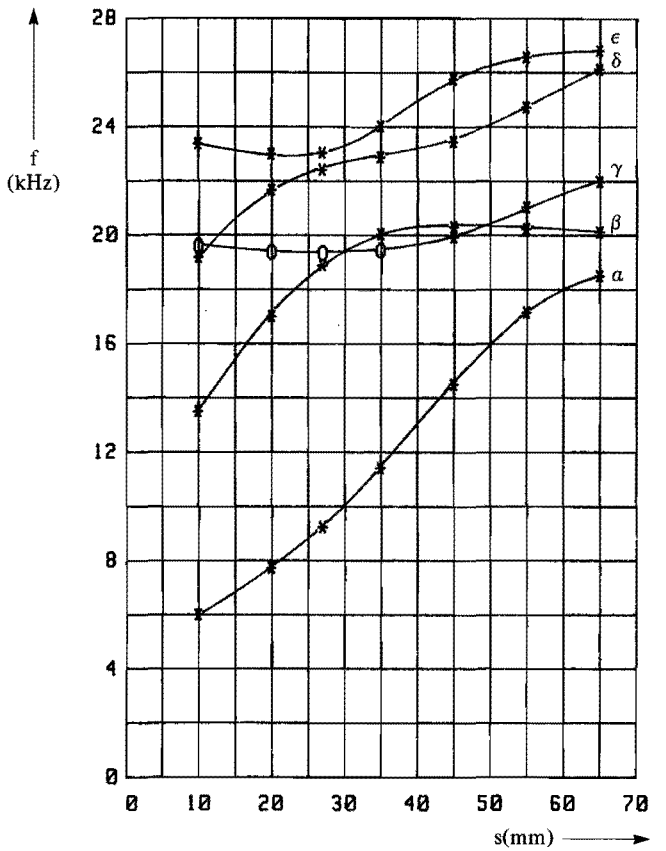

Fig. 9.10 Frequency spectrum of the resonator of slot type A (see figure 9.1) as determined from the finite element analysis (branches α through ε are according to figures 9.5 to 9.9); frequency f versus thickness s (denotes a calculated frequency; 0 denotes a mode with a constant output amplitude).*

For this reason it would be better not to use the description "longitudinal" mode for that desired mode with a uniform amplitude distribution at the output surface. One should preferably use the "mode with a flat output amplitude".

The blade-like resonator studied here was of 130 mm length. In order to raise the resonance frequency of the "constant output mode" to 20 kHz exactly, the length has to be shortened by about 3 mm. Other mode branches in the spectrum will also shift. However no striking effects are to be expected regarding the coupling to spurious modes in the range of $15 < s < 25$ mm.

9.5 Variation of the slot length of type B (figure 9.2)

As shown in figures 9.2 and 9.4, the second slot type B is characterized by an open end at the output surface. This slot type is often used to influence the mode shape when some distortion is present. As a function of the slot length h resonance frequencies and modes were calculated. The results are summarized in table 9.III. The case h = 0 corresponds to the solid resonator. In all cases the third and fourth mode are in the frequency range of interest.
Not all vibrational modes which have been calculated will be presented here. Figure 9.11 shows the second to the fifth mode for the resonator of slot length h = 110 mm. Clearly the fourth mode at f = 19.72 kHz corresponds to a "constant output mode", although the amplitude is not exactly constant. The third mode at f = 19.10 kHz has a flat amplitude distribution at the input surface and can therefore easily be excited when such a resonator is coupled to a transducer. However, this mode has zero output amplitude at the output surface near the center of the resonator and high amplitudes at the edges. It is of no value for welding applications. The frequency difference with the 19.72 kHz mode is about 600 Hz (~ 3%), which is generally too small for safe operation, due to the risk of interferences, or by an improper tuning procedure of the ultrasonic generator (tuning to the wrong mode).

A close study of all modes again reveals some similarities in the mode shapes. All modes are familiar to flexural vibrations in beams. Only few modes show an amplitude distribution at the output surface which would be acceptable for welding purposes. Figure 9.12 shows for all values of slot length h analyzed, those modes which do approximate the "constant output amplitude" requirements. The other modes have at least one nodal point at the output surface.

h / mode	0	20	40	60	90	100	110
1	18.46	12.90	7.34	4.50	2.17	1.54	0.95
2	20.08	18.71	18.53	16.50	11.65	10.35	9.22
3	21.94	21.14	20.99	20.09	19.45	19.40	19.10
4	26.08	25.20	23.41	21.94	21.63	21.09	19.72
5	26.78	26.85	26.25	26.08	23.89	22.84	22.82
6	–	34.87	34.88	35.18	33.30	32.98	32.53

Table 9.III Calculated resonance frequencies (kHz) for the resonator of slot type B (see figure 9.2) as a function of the slot length h (mm) for the 6 lowest modes. (h = 0 corresponds to the solid rectangular resonator).

The effect of a small slot length on the amplitude distortion of the fundamental longitudinal mode in the solid resonator is seen in figure 9.12. Up to h = 40 mm the effect is very small and can be neglected as a positive way to improve such a resonator. There is only a small increase in the resonance frequency. Up to h = 60 mm no modes are judged acceptable for devicing a good resonator for welding purposes. Only for h = 90 to h = 110 mm acceptable mode shapes are to be found.

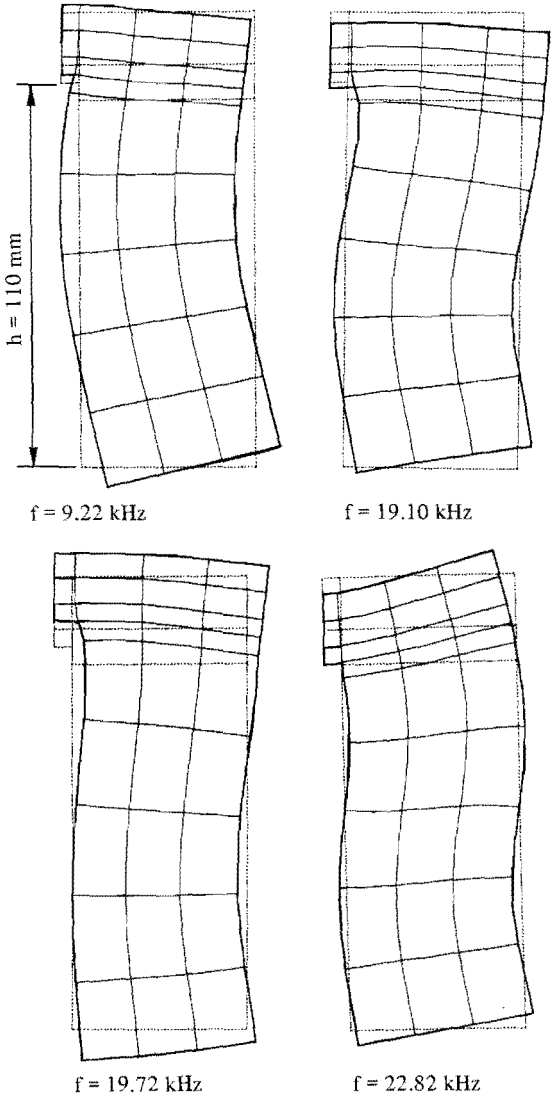

Fig. 9.11 Vibrational modes for the resonator of slot type B (see figure 9.4) for h = 110 mm (one axis of symmetry).

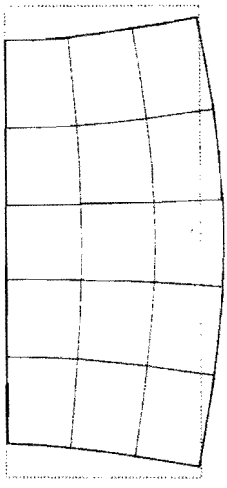

h = 0
f = 18.46 kHz

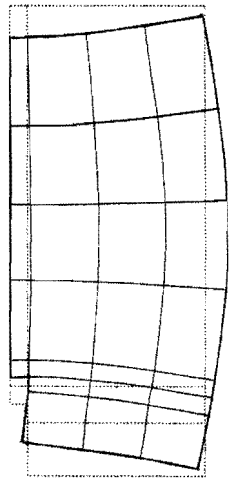

h = 20 mm
f = 18.71 kHz

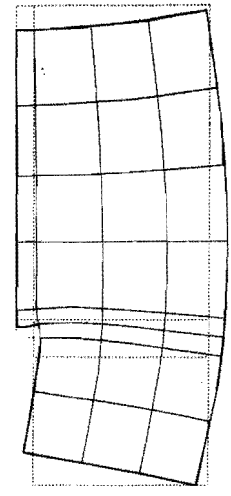

h = 40 mm
f = 18.52 kHz

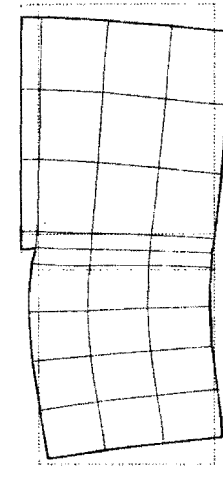

h = 60 mm
f = 20.09 kHz

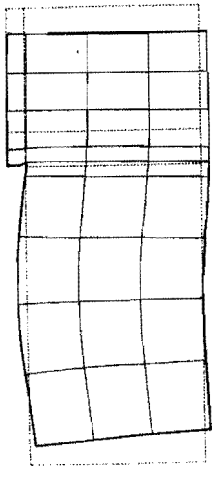

h = 90 mm
f = 19.45 mm

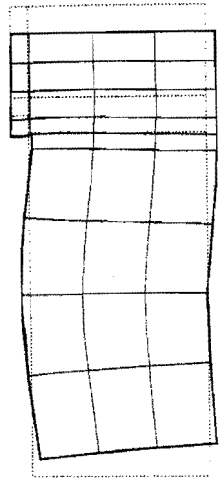

h = 100 mm
f = 19.40 kHz

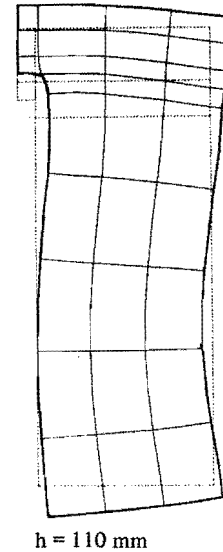

h = 110 mm
f = 19.72 kHz

Fig. 9.12 Vibrational mode of the resonator of slot type B (see figure 9.4) for various values of slot length h. Modes which approximate the constant output requirements (only one axis of symmetry)

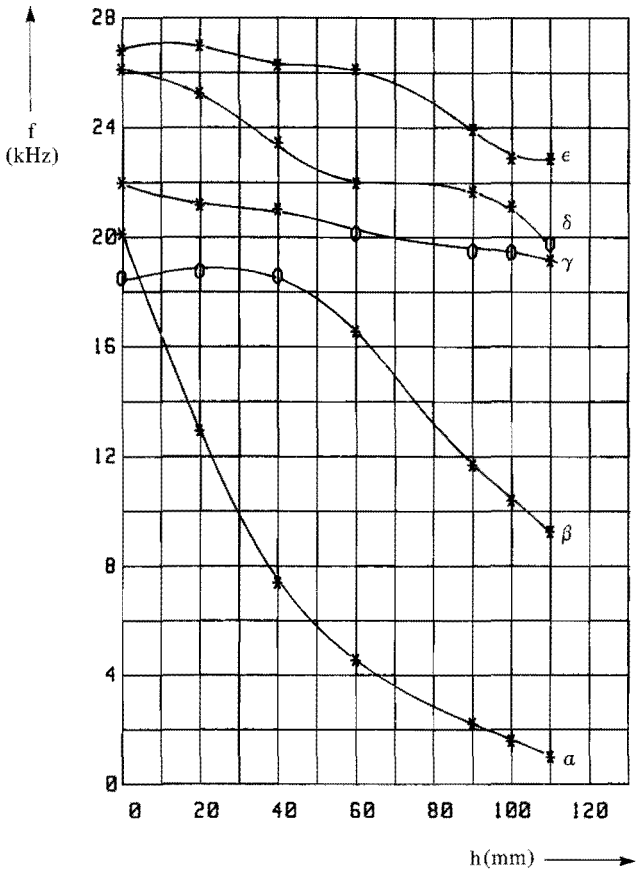

Fig. 9.13 Frequency spectrum of the resonator of slot type B (see figure 9.2) as determined from the finite element analysis (mode branches α to ε); frequency f versus slot length h. (denotes a calculated frequency; 0 denotes a mode which approximates the "constant output amplitude" requirements).*

From these results a frequency spectrum can be set up relating the resonance frequency of various modes to the slot length h. Five mode branches are shown in figure 9.13. All modes have a decreasing resonance frequency with an increasing slot length. The modes shown in figure 9.12 are marked in figure 9.13 by "0". Clearly they belong to three different branches.

Surprisingly their resonance frequencies are very close to the design frequency of 20 kHz. Only one branch crossing is found at h = 5 mm. Over a wide range of the slot length the frequency difference between the branches near 20 kHz is greater than 1 kHz. From the analysis it follows that resonators with slot type B can be used for slot lengths of $90 < h < 105$ mm.

From the frequency spectrum (figure 9.13) it follows again that the acceptable modes are on the γ or δ branch and are not originating from the longitudinal mode of the solid resonator (branch β).

Finally a striking effect is to be explained, which is often encountered when tuning a resonator on a trial and error base. Suppose one has deviced a resonator with a slot length h = 40 mm. From the mode shape (figure 9.12) it follows that at the outer portion of the output surface there is no motion. In order to improve the mode shape one would machine the resonator to enlarge the slot length to say h = 60 mm. Now some surprising observations can be made. Firstly the resonance frequency of the mode (β) will fall about 2 kHz (11%), and no improvement of the mode shape will result from it, but rather a deterioration (the new mode shape is not shown). The second observation would be that at a higher frequency a mode (branch γ) will be found of a shape very similar to that from the prior resonator (h = 40 mm). However, the mode shape now reveals a very small amplitude at the center portion of the output surface. No improvement will be reached as a result. Only a further increase of the slot length to about h = 90 mm will yield a better mode shape. Note that the resonance frequency of mode branch γ varies slowly with increasing slot length.

9.6 Stress analysis

In the present work no attention has been paid to the stresses in the resonator which greatly determine the toollife and the maximum attainable amplitude of vibration. In slender rod type resonators the stresses can be calculated analytically. In resonators of complex shape like the wide output resonators studied here stress concentrating factors such as slots and cut-outs are to be considered. Secondly, the stresses have to be determined for the loaded resonator when both static forces (needed to guarantee a good acoustical coupling between the resonator and the products to be welded) and the stresses resulting from the forced vibrations into it are present. Brinkmann (1971) already showed that the analysis of freely vibrating resonators not always provides realistic information with respect to the level and location of maximum stresses. However, there is no theoretical model available to describe the interaction of the welding process and the mechanical stresses in the resonator.

Being aware of the limitations we carried out some stress analysis for the freely vibrating resonator. The stress is calculated from the deflections of the resonator as calculated from the frequency analysis. As an example the resonator with slot type B is presented. In a slender rod with maximum amplitude $\bar{u}$, the maximum stress $\bar{\sigma}$ occurs in the nodal plane (chapter 2, equation 2.8). Taking the same input amplitude $\bar{u}$ for the resonators the locations and levels of the maximum stresses were determined. Figure 9.14 shows the results for slot lengths h = 60, h = 90 and h = 110 mm. As a conclusion, the slot length not only is crucial for obtaining an acceptable vibrational mode, but above all can result in high stress concentrations.

Clearly a slot length h = 110 mm will be too critical, because the stresses in the bottom of the slot are 1.45 times higher than those in the nodal plane. The slot length h = 60 mm was already excluded for reasons of the poor amplitude distribution. The stresses are far too high in this resonator. For slot length h = 90 mm, the maximum stress is $\bar{\sigma}$, identical to that in a slender-rod resonator. At the top of the slot, the maximum is only $0.85 * \bar{\sigma}$, so that this resonator would be acceptable regarding the stress-distributions in it.

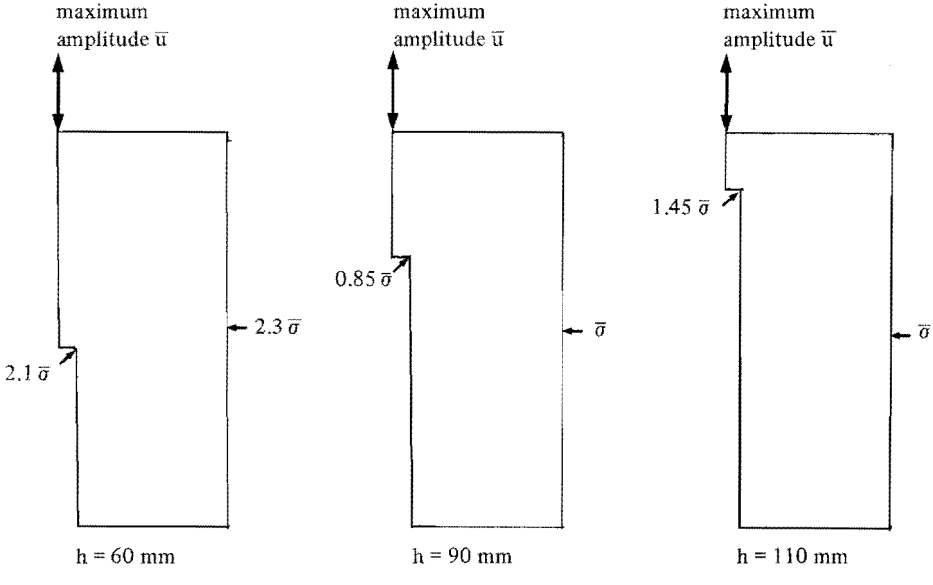

Fig. 9.14 Resonators of slot type B (see figure 9.2); locations of points of maximum stresses in the resonator with a maximum input amplitude $\bar{u}$ and with a vibrational mode as shown in figure 9.12 (the stress-level is referred to the slender rod stress amplitude $\bar{\sigma}$ at the same input amplitude $\bar{u}$).

9.7 Conclusions

The finite element analysis has shown that both slot types A and B are suited to design resonators having a nearly constant output amplitude. However, the freedom in choosing the slot dimensions is very limited. At first only for a specific range of slot dimensions an acceptable output amplitude distribution can be obtained. Secondly, this range is limited again by the presence of spurious mode within a 1 kHz bandwidth around the working frequency. Although not studied extensively, the mechanical stresses under load, will certainly imply other restrictions. The set-up of a frequency spectrum is an invaluable tool to understand the problems that can be expected in resonator design.

The predicted resonance frequencies of the modes which meet the design requirements coincide fairly well with the simplified model as presented in chapter 8.

Finally, it is suggested not to use the description "longitudinal" mode for the required one, but rather the "flat output amplitude mode".

In this chapter only the slot length variations were studied. Asymmetrical slots or slot width variations could also be studied. However, the present results showed that both slot types A and B do yield acceptable resonators, slot type A would be preferred regarding the uniformity of the output amplitude and a smooth output surface geometry.

10. MULTIRESONATOR SYSTEM FOR ULTRASONIC PLASTIC ASSEMBLY

10.1 Introduction

A very important application for wide output resonators will be discussed now. The use of resonators with wide output cross-sections in ultrasonic plastic welding, staking and rivetting makes it possible to transmit vibrational energy over large areas in one operating cycle. A higher throughput of welded area per welding machine is the result. However, there are restrictions with respect to height variations in the product parts to be joined. There is an interesting number of applications in which these resonators are employed as a "base" to transmit vibrational energy to a plurality of tools attached to it (Scotto (1974), see figures 4.8c and 10.1).

Reasons to choose these configurations are: multiple welding or staking operations in products at inaccessible places, at different height levels or across obstacles or jigs. Extra high vibrational amplitudes may be needed in some cases, which cannot be achieved in the large resonator itself due to high stress levels.

The most practical solution would be to attach the tools to the base resonator by screwing (fig. 10.1a); if so, the dimensions are limited by the inertia forces which would raise the mechanical stress levels in the screw well beyond the fatigue strength. As an example the dynamic stress amplitude in the coupling bolt for the case of a cylindrical tool attached to the base resonator will be:

$$\sigma_{bolt} = \frac{\frac{\pi}{4}\, d^2 . l . \rho . (2\pi f)^2\, u}{A_b} \qquad (10.1)$$

where d = tool diameter, l the length, ρ its material density, f the operating frequency of the resonator, u the output vibrational amplitude and A_b the effective cross area of the bolt. For a most practical application (where: f = 20 kHz, u = 25 μm, d = 25 mm, ρ = 7800 kg/m^3, a steel bolt M_{10} with A_b = 58 mm^2 and a dynamic fatigue strength σ = 200 N/mm^2) the maximum allowed tool length would be restricted to about $l \approx 8$ mm.
Furthermore any mass attached to the "base" will tend to decrease its resonance frequency (Young (1970)). The allowed frequency shift is small (± 1,5%), which will lead to practical problems when many tools are attached. Adding or leaving out a tool later on, once the system has been tuned, requires a retuning of the "base" to the working frequency. It will be obvious that in doing so the advantages of ultrasonic welding will be overruled by the costs of resonator design.

A more suitable solution is to use the tools in the form of a half-wavelength resonator (fig. 10.1b). For efficient operation each part has to be designed to resonate in the frequency corresponding with the optimum operating conditions of the transducer and base resonator assembly. The latter results into a low-stress coupling (only a prestress is used to assure good acoustical coupling between the resonating tool and the base). An inconvenience is that the tool length will mostly become much longer than necessary for most of the applications.

The design of the base resonator requires perhaps even more care than in the case of a resonator for welding only. The vibrational mode at the design frequency should be

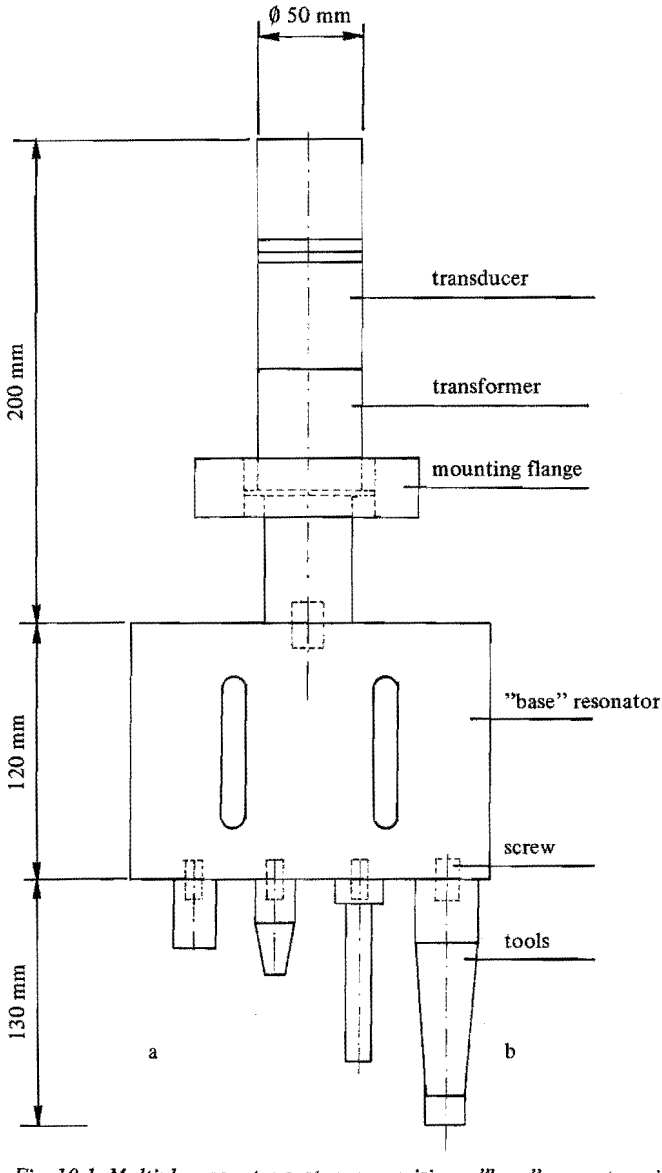

Fig. 10.1 Multiple resonator system comprising a "base" resonator with a plurality of tools attached to it;
a: small tools
b: resonating tools
(typical dimension for a 20 kHz system)

such that at the output surface, where the tools are attached, the amplitude of motion along the surface is as uniform as possible. In that case all attached tools will have an equal input amplitude. If the amplitude of the base is not uniform but distributed along the surface rather in a curved way, the attached tools will be excited in a combined longitudinal and flexural vibrational mode. In the worst case the tools may even become resonant in the flexural mode, generally causing failure of the clamping bolt due to excessive stresses.

Typical dimensions of a base resonator output surface are in the range of 60-200 mm^2 to 200-200 mm^2. For welding or staking up to 20 attached tools are used.

The designer of a multiple resonator system (as described above) will be asked to devise a resonator tool with a specified amplitude gain and with a predetermined length at a fixed operating frequency. Depending on the applications involved, some of the other dimensions like the diameter at the input or output end will be specified too. The resonator material will be specified too, e.g. low acoustical damping, high wear resistance, high fatigue strength. It will be clear that in all cases an optimization of the tool configuration is needed.

10.2 The funnel shaped resonator

Many publications are available in which the resonators geometry is optimized with respect to the stress distribution. There are conical, exponential, catenoïdal, stepped cylindrical, Fourier and Gaussian shaped resonators (Merkulov (1957)). The Gaussian bottleshaped, resonator is found to produce maximum output amplitude at minimum mechanical stress. The design of these thin halfwave length resonators requires the solution of the one-dimensional wave equation for the longitudinal motion (see chapter 2).
In ultrasonic engineering, however, most of these resonators although theoretically superior, are rarely used. Other reasons such as easy manufacturing, simple computer programming for design and easy tuning possibilities do explain the wide use of conical, exponential and stepped cylindrical shaped resonators. A resonator type which was found to be very suitable for application into a multi-resonator system will be described in more detail below.

None of the resonator shapes described above will give the designer enough freedom to easily produce tools with a predetermined length and predetermined amplitude gain at a given operating frequency. A three-element cylinder-cone-cylinder shaped resonator ("funnel-shaped", Neppiras (1977)) can be optimized such as to approach the properties of the Gaussian shaped one (see figure 10.2). Resonators of this type are easy to design and manufacture.

It is proposed here that these funnel shaped resonators give the designer enough freedom to satisfy more design conditions. By variation of the lengths and diameters of the cylindrical parts it is possible to satisfy the resonance condition for the half-wavelength longitudinal vibrational mode at a predetermined total length and a fixed amplitude gain. It will be clear that in this way the stress distribution cannot be kept as favourable as in the Gaussian resonator. For many applications, however, an acceptable compromise can be found, giving a resonator superior to the stepped cylindrical and conical shaped ones.

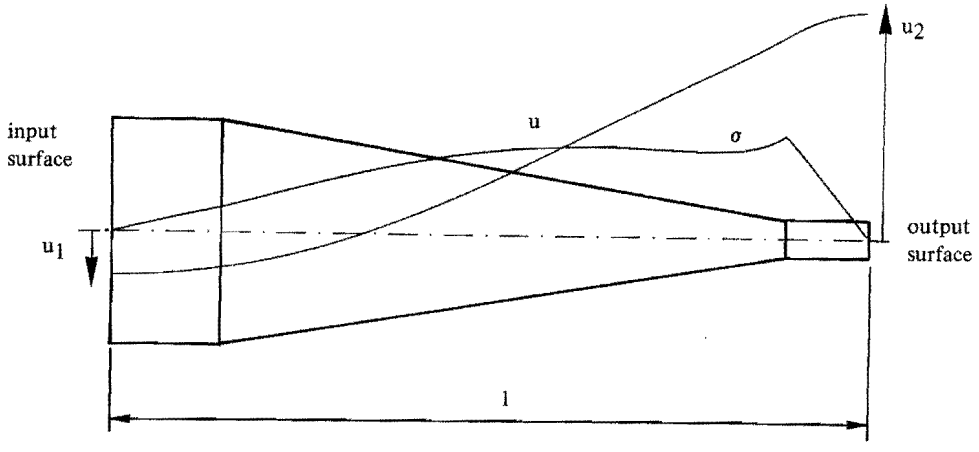

Fig. 10.2 Funnel-shaped resonator; amplitude u of the longitudinal vibrational mode and stress distribution σ (axial vibrations); amplitude gain $M = u_2/u_1$; total length l.

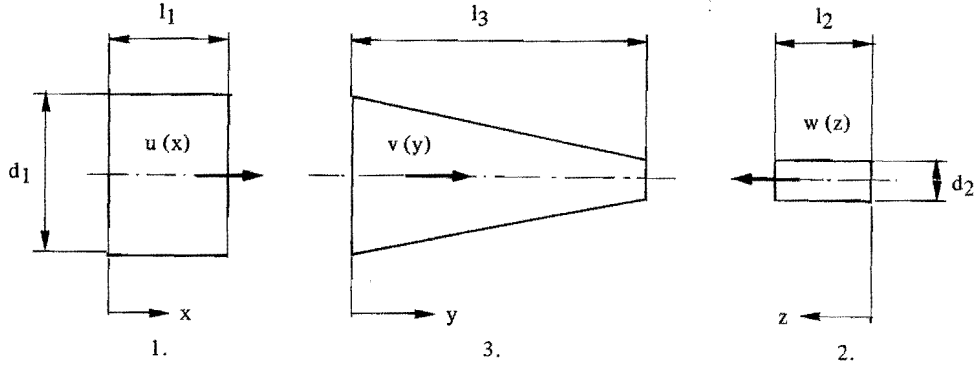

Fig. 10.3 Three separated sections of the funnel shapped resonator; definition of coordinates, dimensions and displacements (axisymmetric cross-sections). ($l = l_1 + l_2 + l_3$).

10.3 Frequency equation, amplitude gain and shape factor

The one-dimensional equation for the longitudinal motion in a resonator with variable cross-section written in terms of the motion amplitude u (x) along the axial ordinate x is as follows (it is an extension of equation (2.1)):

$$\left(\frac{d^2}{dx^2} + \frac{1}{A(x)} \frac{dA(x)}{dx} \frac{d}{dx} + k^2\right) u(x) = 0 \qquad (10.2)$$

As we deal with harmonic vibrations, the time-independent displacement functions u(x) can be considered only. A(x) is the area of the cross-section at distance x, k = wavenumber.

In figure 10.3 the three elements of the funnel shaped resonator are separated. In each section the solution of equation (10.2) can be found in terms of the displacement u(x), v(y) and w(z).
The boundary conditions and continuity of axial forces and axial displacements at the interfaces have to be satisfied. The displacement function in each of the elements 1, 2 and 3 can be written as follows:

$$u(x) = a_1 \cos(kx) + a_2 \sin(kx) \tag{10.3}$$

$$v(y) = \frac{m}{1-my} [a_3 \cos(ky) + a_4 \sin(ky)] \tag{10.4}$$

$$w(z) = a_5 \cos(kz) + a_6 \sin(kz) \tag{10.5}$$

where a_1, a_2, a_3, a_4, a_5 and a_6 are constants.

In equation (10.4) the factor m of the conical element (length l_3) equals:

$$m = \frac{1}{l_3} \cdot \frac{N-1}{N} \tag{10.6}$$

$$N = \frac{d_1}{d_2} \tag{10.7}$$

Where N is the ratio of the diameter of the cylindrical elements.

The desired vibrational mode is the fundamental longitudinal mode; therefore the input and output surfaces are stressfree, so:

$$\frac{du(x)}{dx}\Big/_{x=0} = 0 \text{ and } \frac{dw(z)}{dz}\Big/_{z=0} = 0 \tag{10.8}$$

Continuity of displacement between the elements 1 and 3, 2 and 3 follows:

$$\begin{aligned} u(x)\Big/_{x=1} &= v(y)\Big/_{y=0} \\ v(y)\Big/_{y=l_3} &= -w(z)\Big/_{z=l_2} \end{aligned} \tag{10.9}$$

Continuity of the forces at the interfaces can be satisfied when:

$$\begin{aligned} \frac{du(x)}{dx}\Big/_{x=l_1} &= \frac{dv(y)}{dy}\Big/_{y=0} \\ \frac{dv(y)}{dy}\Big/_{y=l_3} &= -\frac{dw(z)}{dz}\Big/_{z=l_2} \end{aligned} \tag{10.10}$$

The boundary conditions of equation (10.8), when applied to equations (10.3) and (10.5) give $a_2 = 0$ and $a_6 = 0$. When the input amplitude is defined as $u(x)/_{x=0} = u_1$ and the output amplitude $w(z)/_{z=0} = u_2$, we find:

$a_1 = u_1$ and $a_5 = u_2$ (see fig. 10.2 and 10.3)

Combination of equations (10.9) and (10.10) applied to equations (10.3), (10.4) and (10.5) will give the frequency equation. After some mathematical manipulation, it follows:

$$\left[\left(\frac{k}{m}\tan(kl_2) + \frac{1}{1-ml_3}\right]\left[\cos(k(l_1+l_3)) - \frac{m}{k}\sin(kl_3)\cos(kl_1)\right] =\right.$$

$$\frac{k}{m}\left[\sin(k(l_1+l_3)) + \frac{m}{k}\cos(kl_1)\cos(kl_3)\right] \qquad (10.11)$$

This is the so-called frequency equation. For a given resonator geometry (l_1, l_2, l_3, d_1 and d_2) from equation (10.11) the wavenumber k can be solved. In our case the resonance frequency is a design requirement, so one can choose the dimensions so as to satisfy the frequency equation.

The remaining constants a_3 and a_5 are found to be:

$$a_3 = u_1 \frac{\cos(kl_1)}{m} \qquad (10.12)$$

$$a_4 = -u_1\left[\frac{\sin(kl_1)}{m} + \frac{\cos(kl_1)}{k}\right] \qquad (10.13)$$

The amplitude gain in the resonator is given by $M = |\frac{u_2}{u_1}|$, being the ratio of the output amplitude to the input amplitude. M can be calculated from equations (10.3) through 10.13):

$$M = |\frac{u_2}{u_1}| = \frac{1}{\cos(kl_2)} \cdot \frac{1}{1-ml_3}\left[\cos(kl_1)\cos(kl_3) - \sin(kl_3)\sin(kl_1)\right.$$

$$\left. - \frac{m}{k}\sin(kl_3)\cos(kl_1)\right] \qquad (10.14)$$

The mechanical stress in the resonator can be determined from Hooke's law. The strain at any distance follows from the displacement functions, as given by equations (10.3), (10.4) and (10.5). In each of the resonator elements the stresses are:

$$\sigma_1(x) = -u_1 k.E \sin(kx) \qquad (10.15)$$

$$\sigma_3(y) = u_1 E \left(\frac{m}{1-my}\right)^2\left[\frac{\cos(kl_1)}{m}\cos(ky) - \left\{\frac{\sin(kl_1)}{m} + \frac{\cos(kl_1)}{k}\right\}\sin(ky)\right] +$$

$$+ u_1 Ek\left(\frac{m}{1-my}\right)\left[-\frac{\cos(kl_1)}{m}\sin(ky) - \left\{\frac{\sin(kl_1)}{m} + \frac{\cos(kl_1)}{k}\right\}\cos(ky)\right] \qquad (10.16)$$

$$\sigma_2(z) = -u_2 kE \sin(kz) \qquad (10.17)$$

In a cylindrical resonator, resonating in the fundamental longitudinal mode, the maximum stress $\bar{\sigma}$ occurs in the nodal plane and equals (see equation (2.8)):

$$\bar{\sigma} = \bar{u}\, k\, E \tag{10.18}$$

Where $\bar{u}$ is the maximum motional amplitude in the resonator, k is the wave number and E is Young's modulus.

The reason why in practical engineering the mechanical stresses are to be calculated, will be obvious. In general a tapered resonator will produce an output amplitude at a lower stress level than a cylindrical resonator does with the same output amplitude. The maximum possible output amplitude partly is limited by the dynamic fatigue strength of the resonator material. In order to evaluate the performance of the resonator shape chosen as compared to the cylindrical shape, the shape factor has been defined (Neppiras (1963), Scheibener (1971)).

$$\tilde{\Phi} = \frac{\bar{\sigma}}{\sigma_{max}} = \frac{\bar{u}kE}{\sigma_{max}} \tag{10.19}$$

Where σ_{max} is the maximum stress in the resonator to be evaluated with an output amplitude $\bar{u}$. The higher a shape factor, the better the performance of the resonator with respect to the cylindrical one. Practical values of $\tilde{\Phi}$ are between 1 (cylindrical) and 3,5 (Gaussian).
Typical values for some common resonator shapes are:

- cylindrical $\quad \Phi = 1$
- exponential $\quad \Phi = 1.5\text{-}2$
- conical $\quad \Phi = 1.5\text{-}2$
- Gaussian $\quad \Phi = 3.5$
- funnel-shaped $\quad \Phi = 2\text{-}2.5$

So, for a conical resonator up to 2 times higher output amplitudes can be used as compared to the cylindrical one. For the funnel-shaped resonator the shape factor has to be calculated numerically for each dimension specifically from equations (10.15), (10.16), (10.17) and (10.19).

10.4 Dimensioning of funnel-shaped resonators

The solutions of the frequency equation, the amplitude gain and the shape factor can be computed numerically. Normally one will calculate the resonator length l, the amplitude gain M and the shape factor, while the diameter ratio N and lengths l_1 and l_2 of the cylindrical parts, the design frequency f and the elastic properties of the material are given. It is of great advantage to represent the solutions graphically with non-dimensional parameters, useful for a broad range of the parameters.

All length dimensions can be normalized with respect to the length of the half-wave-length resonator of cylindrical shape ($l = \frac{c}{2f}$ or $l = \frac{\pi}{k}$) (see chapter 2).
In this way both material properties and frequency vanish.

In figures 10.4 and 10.5 the non-dimensional resonator length $\frac{k.l}{\pi}$ is shown versus the length of the second cylindrical part

$\frac{kl_2}{\pi}$ for various values of the diameter ratio N (N=1 to 8).

The length of the first cylindrical part $\frac{kl_1}{\pi}$ is kept constant.

In figure (10.4) $\frac{kl_1}{\pi} = 0.2$ and in figure (10.5) $\frac{kl_1}{\pi} = 0.35$.

In the same figures the amplitude gain M and the shape factor Φ are shown too. With the aid of these figures one can easily find the resonator dimensions in order to optimize the shape factor Φ. The resonator length and the amplitude gain can be chosen over a large range. It was found in practice that with only a few fixed values $\frac{kl_1}{\pi}$ the designer has enough freedom to find adequate resonator parameters for his application.

The maximum shape factor attainable is about $\emptyset = 2.6$, which confirms the superiority of the funnel-shaped over the cylindrical or stepped cylindrical shaped resonators.

10.5 Experimental verifications

To verify the calculations, a multiple resonator system was designed comprising 4 funnel-shaped resonators. Figure 10.6 shows these four resonators (material Aluminium c = 5200 m/s, frequency f = 20 kHz). The length and diameter of the first cylindrical part was kept constant, while the diameter ratio N and the length of the second cylindrical part were varied. The difference in length is up to 47 mm, while the amplitude gain of all of them is 4. The resonance frequency of these resonators was measured; the difference with respect to the design frequency can be explained by the presence of a threated hole at the input side, by means of which they are coupled to the base resonator (the shift was calculated to be about 800 Hz).

The measurements of the amplitude gain showed M = 4 for all resonators.

The results are summarized below (table 10.I).

Resonator	Diameter ratio (–)	Total length (mm)	Amplitude gain (–)	Shape factor $\emptyset$ (–)	Measured frequency (kHz)
1	3.75	160.0	3.94	2.0	20.77
2	3.0	153.3	4.04	1.82	20.91
3	2.31	134.6	4.05	1.12	20.69
4	2.31	113.0	4.05	1	20.65

Table 10.I Calculated length, amplitude gain and shape factor for 4 funnel-shaped resonators designed for 20 kHz application; the measured frequencies are listed.

The shape factor $\emptyset$ is between 1 and 2, indicating that it is not possible to optimize the resonator to meet the design requirements, and to keep the shape factor optimum too. The shape of resonator 1 allows twice as high amplitudes as the shape of resonator 4, with respect to the maximum mechanical stress.

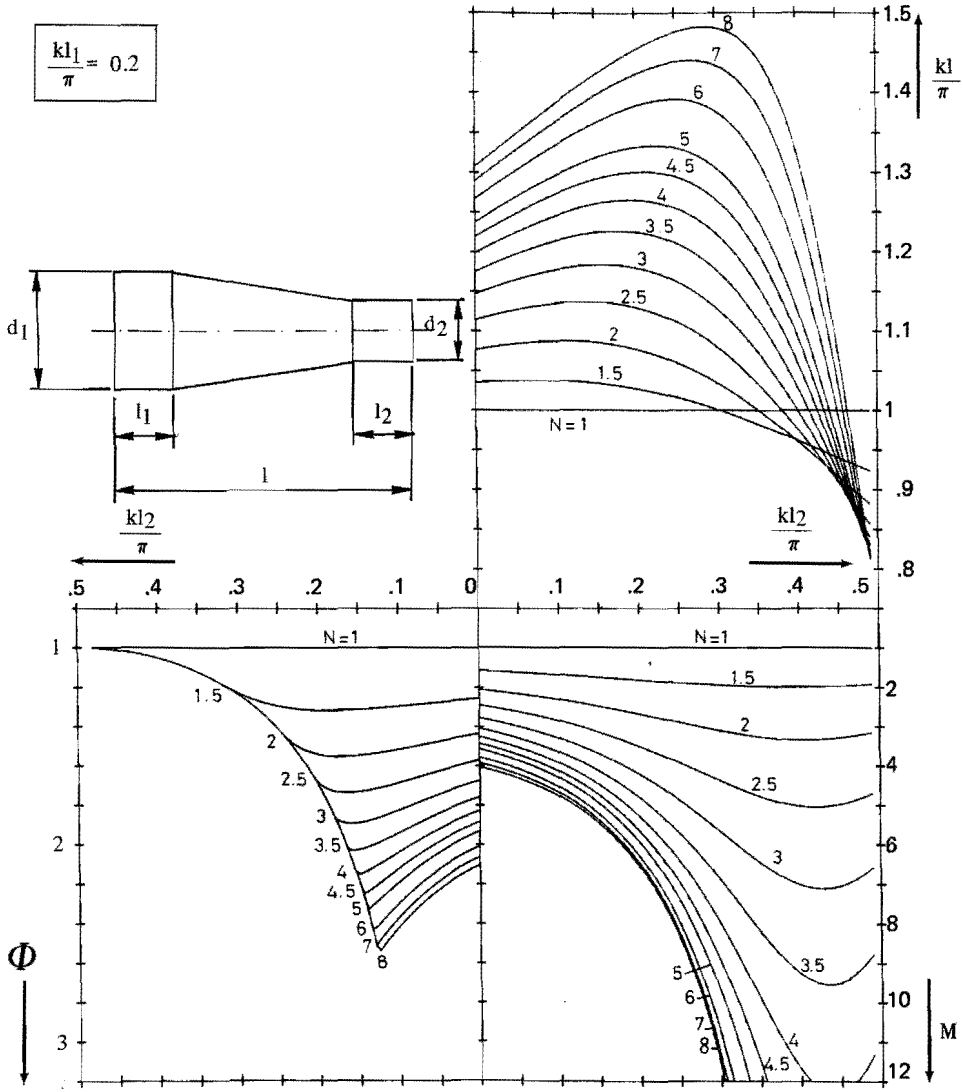

Fig. 10.4 Non-dimensional representation of the funnel-shaped resonator parameters for various values of the diameter ratio $N = \frac{d_1}{d_2}$. *The cylindrical part of length* l_1 *is kept constant:* $\frac{kl_1}{\pi} = 0.2$; *amplitude gain M and shape factor* $\bar{\Phi}$

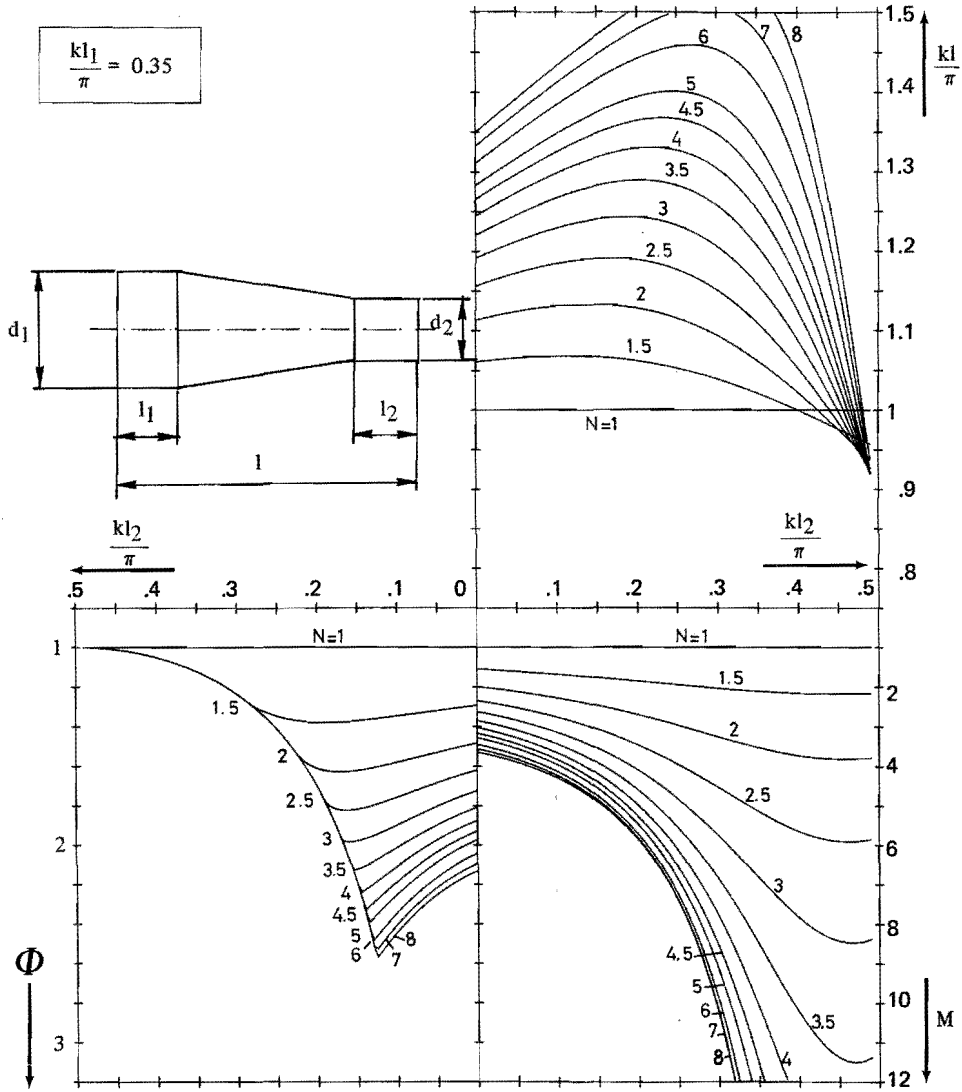

Fig. 10.4 Non-dimensional representation of the funnel-shaped resonator parameters for various values of diameter ratio $N = \frac{d1}{d2}$*; the cylindrical part of length* l_1 *is kept constant:* $\frac{kl1}{\pi} = 0.35$*; the amplitude gain M; shape factor* Φ

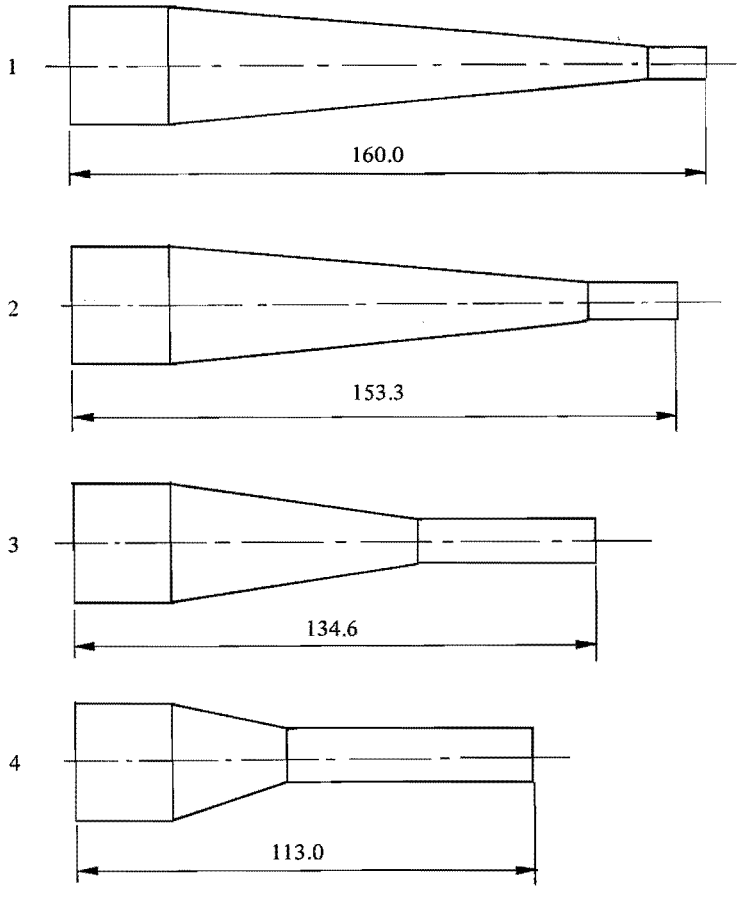

Fig. 10.6 Four resonators with different length (in mm) and equal amplitude gain (diameter d_1 = 30 mm and length l_1 = 25 mm for all; the length l_2 are: 15 mm, 24 mm, 43 mm and 63 mm respectively).

10.6 Additional tuning of the resonators

Finally, it is to be discussed how a resonator can be tuned once it has been made. Sometimes, the actual resonance frequency is below the operating frequency of the welding apparatus (whether by coincidence or by the designers choice). In other cases one wants to know what effect is to be expected when the resonator is shortened during the design or as a result of wear effects. Figure 10.7 shows the change in resonance frequency and amplitude gain when the cylindrical parts of the resonator are shortened by an amount Δl, as calculated from equations (10.11) and (10.14). Shortening of the cylinder with the smallest diameter results into the strongest frequency raise and decrease of the amplitude gain. Shortening of the cylinder with the large diameter hardly does change the amplitude gain, and has a much smaller effect on the frequency raise.

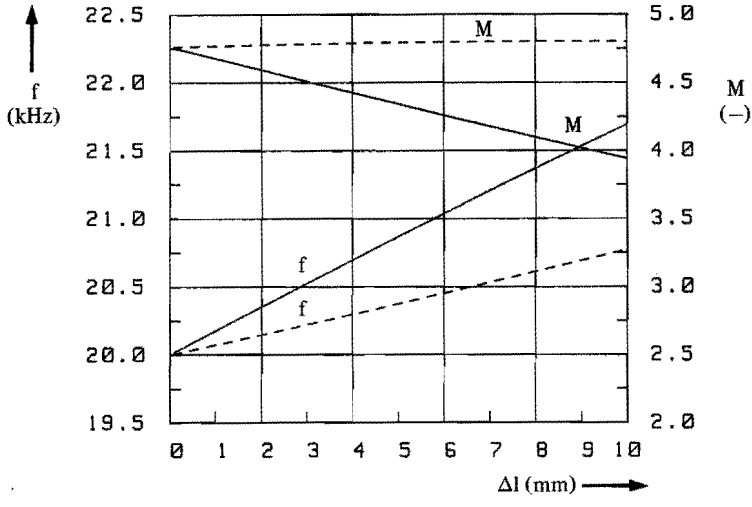

Fig. 10.7 Effect of shortening the cylindrical parts of the funnel-shaped resonator by an amount Δl on the amplitude gain M. (——): small cylinder (– – –): large cylinder. (Aluminium c = 5200 m/s, f = 20 kHz, l_1 = 30 mm, l_2 = 30 mm, d_1 = 40 mm, d_2 = 13 mm) (see figure 10.3).

10.7 Conclusions

The funnel-shaped resonator is very adequate for application in multiple resonator systems. Its geometry allows the designer enough freedom to meet the design requirements of specified frequency, length and amplitude gain. The results were presented graphically with non-dimensional parameters. The theory is accurate, so that no additional tuning of the resonators is required.

SUMMARY

Ultrasonic welding is a widely used technique for the assembly of thermoplastic product parts. A weld is created by local melting by the absorption of mechanical vibrations at an ultrasonic frequency (mostly 20 kHz) with amplitudes of 10 to 50 μm. A tool is used to transmit the vibrations from the transducer of a welding apparatus to the product parts. Tools are very often shaped as tapered rods and are designed to resonate in the length direction in the fundamental longitudinal mode of vibration (half-wavelength resonator). The design causes no problems if the lateral dimensions are small compared to the length. Usually, for cylinders the length to diameter ratio is L/D = 2.5 à 4, and the maximum productsize is then limited to 50-60 mm diameter. There is however, a great number of important applications that requires much larger tool dimensions, and then difficulties are encountered in designing tools properly.

It is the aim of the present work to study and describe the problems encountered in designing ultrasonic resonators with large dimensions (wide output cross-sections) and to elaborate design principles that can overcome at least part of the present limitations which prevent a full exploitation of the technique of ultrasonic plastic welding. Up to now resonators are almost always designed at a trial and error approach, and the results are not always very successful.

For an optimum operation a resonator has to meet the following design requirements. The shape of the products to be welded prescribes the dimensions of the output surface. The resonance frequency must coincide with the operating frequency of the welding apparatus. In order to transmit vibrational energy to the welding process adequately, the resonator must vibrate in a mode with a uniform amplitude along the output surface to guarantee a constant energy input (at least 90% uniformity is required). The same holds for the area of the input surface at which it is coupled to the transducer.

As appeared from the analysis of a large number of existing resonators, it followed that wide output resonators are typically not operated in the mode of vibration corresponding to the lowest resonance frequency. Mostly a very specific higher order vibrational mode will meet the design requirements and sometimes an acceptable mode does not exist at all. For reliable operation of the vibrating system, the resonance frequency of other modes should not be in a 1 kHz bandwidth around the operating frequency. If not, interferences of modes can occur and difficulties are met in tuning the ultrasonic generator to the operating frequency.

The wide variety of resonator geometry that is used, could be classified into three basical shapes: the blade-like, the block-like and the cylindrical type resonator. These shapes have been analysed in the present work.

To begin with, the vibrational characteristics of solid resonators of elementary shape (cylinder and rectangular block) have been studied to evaluate up to what dimensions they can be used as resonators that meet the design requirements. Approximate theories have been derived to calculate the resonance conditions for the fundamental longitudinal mode of vibration. At 20 kHz cylinders up to 70 mm diameter show a uniformity of the output amplitude of at least 90%. Above this dimension the resonator has to be provided with slots, bores or cut-outs to compensate for Poisson's coupling to obtain a uniform output amplitude.

For wide resonators various measures can be taken. As there is no literature available, patent publications have been reviewed. Valuable information can be derived from it on design principles and on how to improve the uniformity of the output amplitude.

To study the problems in designing a wide output resonator, the optimization of a 131 mm wide blade-like resonator has been described. On account of the interpretation of the measurements of resonance frequencies and modes of vibration, the resonator was optimized by providing slots and various cut-outs.
The effect of coupling the resonator to the transducer of a welding apparaturs, on the presence of unwanted (spurious) modes has been demonstrated.
A finite element analysis was used to optimize the same resonator, in order to study the practicalability of this method. Although the finite element analysis was in excellent agreement with the experiments (and finally resulted into a well-designed resonator), the success of it strongly depends on how good the first "shot" is to determine the overall dimensions of the resonator.

Therefore, formulae have been derived to calculate the resonance conditions for the desired mode of vibration in the wide output resonators of the three basical shapes. Experiments confirmed the validity of the approximate theory. Once the overall dimensions are determined, the finite element analysis must be used to calculate the resonance frequencies of other modes of vibration, close to the operating frequency. Results show that there are critical dimensions for the slots in a blade-like resonator. There is only a specific range of slot dimensions for which an output amplitude of acceptable uniformity can be obtained and for which the frequency of spurious modes is out of the 1 kHz range about the operating frequency.

Finally, an interesting field of applications for wide output resonators is discussed. They often are used to serve as a "base" to transmit vibrational energy to a plurality of tools (halfwavelength resonators of the slender rod type) attached to it. Mostly they are used for welding in products at different height levels or with different amplitudes. The so-called "funnel-shaped" resonator can be designed as a half-wavelength resonator with a specified amplitude gain and a specified length at a fixed resonance frequency. The results of the calculations have been presented graphically with non-dimensional parameters allowing use in a broad range of applications.

This study has demonstrated that the design of ultrasonic resonators with wide output cross-sections is of such a complexity that creating an efficient resonator at a trial and error approach will always be some kind of an art. The design, however, can be checked by calculation. Despite many unexpected problems encountered in resonator design, the phenomena always can be described in terms of resonance frequencies, modes of vibrations and mechanical stresses, no matter the complexity of the resonator geometry. With basic knowledge of the vibrations of bodies and the effect of coupling resonators to a transducer of a welding apparatus, the finite element method is an invaluable tool for designing resonators at an acceptable cost level.

SAMENVATTING

Het ultrasoon lassen van produktdelen uit thermoplastische kunststoffen wordt al twee decennia op industriele schaal toegepast. Een las wordt gevormd door locale verweking van de kunststof t.g.v. de absorptie van mechanische trillingen met een frequentie in het ultrasone gebied (meestal 20 kHz) en bij amplitudes tussen 10 en 50 μm. De mechanische trillingen worden gegenereerd in de transducer van een ultrasoon lasapparaat. Een speciaal gereedschap (meestal sonotrode of resonator genaamd) geleidt de trillingen van de transducer naar de te lassen produktdelen. Verreweg de meeste sonotrodes hebben de vorm van een taps uitlopende slanke staaf, welke in de lengterichting in the laagste trillingsvorm wordt aangestoten. De aanstootfrequentie is de resonantiefrequentie van deze trillingsvorm (de sonotrodes noemt men vaak halve-golflengte resonatoren). Het ontwerpen van sonotrodes levert geen problemen op wanneer de dwarsafmetingen klein zijn t.o.v. de lengte. Cylindrische sonotrodes hebben veelal een lengte-diameter verhouding L/D = 2 à 4, en de maximale diameter die nog bruikbaar is bedraagt 50 à 60 mm. Er is echter een groot aantal toepassingen waarvoor veel grotere sonotrode afmetingen vereist zijn. Juist het optimaal vormgeven van sonotrodes met grote dwarsafmetingen geeft veel problemen.

In dit proefschrift worden de problemen die kunnen optreden bij het ontwerpen van sonotrodes met grote dwarsafmetingen bestudeerd. Hierbij wordt er naar gestreefd om m.b.v. ontwerpregels in ieder geval een deel van de huidige beperkingen weg te nemen die een optimaal gebruik van het ultrasoon kunststoflassen in de weg staan. Tot op heden worden sonotrodes via trial and error ontworpen; dit leidt zelden tot een bevredigend resultaat.

Een optimale sonotrode moet aan de volgende ontwerpcriteria voldoen. De vorm van de te lassen produktdelen bepaalt de dimensies van het lasvlak van de sonotrode (uitgangsoppervlak). De resonantiefrequentie moet gelijk zijn aan die van de transducer van het lasapparaat. Voor een gelijkmatige overdracht van trillingsenergie van de sonotrode naar de te lassen produktdelen, moet de sonotrode resoneren in een eigentrillingsvorm waarvan de trillingsamplitude over het gehele lasvlak constant van grootte is (tenminste 90% uniformiteit is vereist). Ook aan het koppelvlak van de sonotrode met de transducer moet de sonotrode een vlakke amplitudeverdeling hebben.

Uit de analyse van een groot aantal bestaande sonotrodes kan worden geconcludeerd dat voor sonotrodes met grote dwarsafmetingen zelden de trillingsvorm wordt gebruikt die behoort bij de laagste resonantiefrequentie. Meestal voldoet slechts één zeer bepaalde hogere orde trillingsvorm aan de ontwerpcriteria en soms blijkt bij een gegeven sonotrodevorm geen geschikte trillingsvorm te bestaan. Het blijkt dat de stabiliteit van het ultrasoon resonerend systeem (transducer en sonotrode) gewaarborgd is wanneer de sonotrode geen andere resonantiefrequenties heeft binnen een bandbreedte van ± 1 kHz rond de werkfrequentie. Zo kan worden voorkomen dat trillingsvormen interfereren of moeilijkheden ontstaan bij het afstemmen van de ultrasone frequentiegenerator op de resonantiefrequentie van het resonerend systeem.

Er is een grote varieteit aan sonotrodevormen welke in drie basisvormen kunnen worden ingedeeld: de balk-vorm (blade-like), de blok-vorm (block-like) en de cylindrische vorm (cylindrical-type). Deze drie basisvormen worden in dit proefschrift besproken.

Zowel analytisch als experimenteel is uitvoerig onderzocht tot welke afmetingen sonotrodes met een cirkelvormige en rechthoekige doorsnede gebruikt kunnen worden in overeenstemming met de ontwerpcriteria. Er zijn benaderingsformules afgeleid waarmee de resonantiefrequentie voor de longitudinale trillingsvorm in deze sonotrodes kan worden berekend. Cilindrische sonotrodes geven tot een diameter van 70 mm bij een frequentie van 20 kHz, aan het lasvlak een uniformiteit van de trillingsamplitude van tenminste 90%. Voor grotere diameters moeten geometriewijzigingen aangebracht worden in de vorm van sleuven, gaten of zaagsnedes teneinde de trillingsvorm zodanig te beinvloeden dat een uniforme uitgangsamplitude verkregen wordt.

Diverse maatregelen kunnen getroffen worden om de trillingsvorm te beinvloeden. Aangezien over dit onderwerp géén literatuur bekend is, zijn patentpublicaties geanalyseerd. Hier kan bruikbare informatie worden afgeleid t.a.v. ontwerpmethodes.

Aan de hand van de optimalisatie van een 131 mm brede balk-vormige (blade-like) sonotrode, zijn de problemen die optreden bij het ontwerpen ervan uitvoerig beschreven. Op grond van de interpretatie van de gemeten resonantiefrequenties en de bijbehorende trillingsvormen, kon een goed werkende sonotrode gemaakt worden door het aanbrengen van sleuven en diverse zaagsnedes in het sonotrode oppervlak. Ook het effekt van het koppelen van een sonotrode aan een transducer van een las-apparaat op de aanwezigheid van ongewenste resonantiefrequenties in de buurt van de werkfrequentie is onderzocht. Met behulp van een eindige elementen analyse zijn van dezelfde sonotrode de frequenties en trillingsvormen berekend. Ofschoon de resultaten van de eindige elementen analyse zeer goed overeenstemden met de experimenten, en ofschoon ook hiermee uiteindelijk een optimale sonotrodevorm werd verkregen, is het succes van deze analyse er sterk afhankelijk van hoe goed men in eerste instantie er in slaagt de globale sonotrode afmetingen te bepalen.

Voor de drie basisvormen van sonotrodes met grote dwarsafmetingen zijn formules afgeleid waarmee de resonantiecondities voor de gewenste trillingsvorm voor een willekeurige werkfrequentie kunnen worden bepaald. Experimenten bevestigen de geldigheid van de gepresenteerde formules. Wanneer de hoofdafmetingen van de sonotrodes berekend zijn, moeten met een eindige elementen analyse de resonantie-frequenties van andere trillingsvormen worden bepaald om te kunnen beoordelen of deze te dicht bij de werkfrequentie liggen. Een analyse van de invloed van de sleuf-lengte in een balk-vormige sonotrode (blade-like) laat zien dat er kritische sleufafme-tingen zijn. Slechts voor enkele sleufafmetingen verkrijgt men een trillingsvorm met een uniforme uitgangsamplitude, waarbij bovendien de resonantiefrequenties van ongewenste trillingsvormen buiten de 1 kHz bandbreedte rond de werkfrequentie liggen.

Tenslotte wordt een belangrijk toepassingsgebied voor sonotrodes met grote dwarsafmetingen behandeld. Dergelijke sonotrodes worden vaak gebruikt als "moeder"-sonotrode (base), waaraan meerdere slanke sonotrodes gekoppeld zijn (halve-golflengte resonatoren). Deze worden gebruikt om te lassen in produkten waarin grote hoogteverschillen overbrugd moeten worden, of wanneer plaatselijk veel grotere trillingsamplitudes gewenst zijn. De zogenaamde "funnel-shaped" sonotrode biedt de mogelijkheid halve-golflengte resonatoren te construeren waarvoor de amplitude transformatie en de lengte voorgeschreven kunnen worden bij een gegeven werkfrequentie. De resultaten van berekeningen zijn grafisch weergegeven met daarin dimensieloze parameters, zodat deze geschikt zijn voor het dimensioneren van sonotrodes voor een breed toepassingsgebied.

Uit deze studie volgt dat het ontwerpen van sonotrodes met grote dwarsafmetingen zodanig complex is, dat het optimaliseren van een sonotrode op een trial and error benadering stellig als een niet overdraagbare vorm van vakmanschap kan worden beschouwd. Ondanks de vele onverwachte problemen die men tegenkomt bij het optimaliseren van grote sonotrodes, is het zeer wel mogelijk de verschijnselen te beschrijven in termen van resonantiefrequenties, trillingsvormen en mechanische spanningen, ongeacht de complexiteit van de sonotrodegeometrie.
Wanneer voldoende basiskennis aanwezig is over het trillingsgedrag van constructies waarvan de afmetingen in ordegrootte gelijk zijn aan de golflengte van de erin opgewekte trillingen, en over het effekt van het koppelen van een sonotrode aan de transducer van een lasapparaat is een analyse met behulp van de eindige elementen-methoden van grote waarde om sonotrodes te kunnen ontwerpen tegen acceptabele kosten.

APPENDIX 1

The design of a block-like resonator

As discussed in chapter 8, the resonance conditions for a block-like resonator, vibrating in a longitudinal mode, can be calculated from equation (8.12). The actual design and optimization of such a resonator will be discussed in more detail here. The product size requires a block-like resonator of about 100 mm thickness and 175 mm width. As it has to be designed for application at 20 kHz, the length will be about 120 mm (equation 8.12). In order to match the output surface to the shape of the product parts to be welded, a profile is needed, 5 mm high, 10 mm wide, along the circumference of the output surface, and with a total length of 500 mm. See figure A.1. The resonator will be machined starting from a block of 110 * 182 * 125 mm^3, provided with slots 12 mm wide and 71 mm long (two in the thickness direction, one in the width direction). The resonator is an aluminium alloy (see table 2.I).

The resonance frequencies of the resonator were measured with the aid of two vibration detectors, placed opposite to each other near the centre of the input and output surface respectively. In a 5 kHz range around 20 kHz, 4 frequencies are detected: f_1 = 17.14, f_2 = 19.18, f_3 = 21.20 and f_4 = 21.33 kHz.
The longitudinal mode is resonating at 19.18 kHz. When the profile at the output surface is machined, the mass of the removed material causes an increase of the frequency, which amounts to: ± (5.110.182 – 5.500.10)/(110.182.125) * 19.18 = 576 Hz.
The measurement showed: f_1 = 17.65, f_2 = 19.74, f_3 = 21.55, f_4 = 22.84 kHz. The increase of f_2 coincides fairly well with the predicted value.
When the resonator is coupled to the transducer of a welding apparatus of 20.3 kHz, again 4 resonance frequencies (measured at the electrical terminals of the transducer) can be detected: f_{1c} = 17.38, f_{2c} = 19.75, f_{c3} = 20.03 and f_{4c} = 21.90 kHz. Only f_{c2} = 19.75 kHz could be tuned to. At f_{3c} = 20.03 kHz the resonance is accompanied by a very high damping. Both f_{1c} and f_{4c} are out of the range of the generator.
In order to raise the longitudinal mode frequency close to 20 kHz the length was shortened by 1 mm (length = 119 mm). The frequencies became f_1 = 17.70, f_2 = 19.99, f_3 = 21.62 and f_4 = 22.82 kHz. Again, when coupled to the transducer, only the longitudinal mode could be tuned to; there are: f_{1c} = 17.48, f_{2c} = 19.86, f_{3c} = 19.98, f_{4c} = 21.88 kHz.
Although the resonance frequency f_{3c} = 19.98 kHz could not be tuned to, it has to be expected that it can influence the longitudinal mode because the frequency difference between the two is small. It certainly will determine the stability of the system during welding. For, in general, the system resonance frequency changes under the variable load and an interference can occur.

The vibrational mode of the longitudinal vibration at 19.86 kHz was measured optically with a Fotonic Sensor, while the resonator was activated at 10 μm input amplitude. This way of measurement gives only the components of the amplitude perpendicular to the surface. In order to visualize and facilitate the interpretation of the modes, they were calculated by interpolation between a limited number of measurements. Figure A.2 shows the vibrational mode of the three surfaces as measured. From the measurements it followed that in this case the amplitudes on the surfaces were symmetrical with respect to the axes of symmetry of the resonator.

The modes of figure A.2 can be used to compose the overall vibrational mode of the resonator. See figure A3. For convenience and better interpretation projections of this overall mode are shown in figure A.4. From this analysis one can conclude that the resonator is vibrating in a "longitudinal" mode indeed. However, there is some spurious mode coupled to it, resulting in the amplitudes observed on the side surfaces. At output surface 3 the amplitudes are not constant; the difference between the smallest and largest value is 40%, which is too high. At side 2 (figure A.2) a mode with a compressional phase and an extensional phase is observed, whereas at side 1, an almost completely compressional mode is present. These are not observed for a normal "longtudinal" mode. As the amplitudes are large as compared to the input amplitude (37% and 60% resp. for sides 1 and 2) this resonator is not acceptable for good operation.

As described above, the frequencies are measured using two vibration detectors, placed opposite to each other near the centre of the input and output surface. However it was demonstrated in chapter 7, that in this way some vibrational modes can be overlooked. In order to check the presence of more resonances, the resonator was suspended onto thin wires, while its frequency spectrum was measured with the vibration detectors placed at various locations on the input and output surface and on the lateral surfaces.

At some locations resonance frequencies did disappear, at others they were present and showed strong amplitudes. Now, frequencies could be detected at: f_1 = 17.70, f_2 = 18.13, f_3 = 19.52, f_4 = 19.80, f_5 = 19.99, f_6 = 20.98, f_7 = 21.62 kHz. Clearly, some frequencies had been overlooked in the previous analysis. Figure A.5 shows schematically what kind of modes correspond to the frequencies in the range of interest. Obviously the modes at f_4 = 19.80 and f_5 = 19.99 kHz do interfere when the resonator is coupled to the transducer at f = 19.86 kHz (compare figures A3 and A4 to A5).

The mode at f_4 = 19.80 kHz has no significant amplitudes of motion at the input surface, and therefore cannot be activated with the transducer as such (it can neither be detected by the vibration detectors when placed at the input and output surfaces). The same holds for f_3 = 19.52 kHz.

The next step in the tuning procedure was to eliminate the mode as shown in figure A.5b. Clearly its resonance frequency depends on the resonator thickness, as it is a compressional mode in this direction. At both width-sides 3.5 mm of material was removed. The thickness was reduced to 103 mm. The frequencies detected are: f_1 = 18.03, f_2 = 19.20, f_3 = 20.00, f_4 = 20.30, f_5 = 20.78 and f_6 = 21.43 kHz.
At f_3 = 20.00 kHz, the "longitudinal" mode is in resonance (figure A.5c).
At f_4 = 20.3 kHz a mode of complex shape is observed with no motion at the input surface, identical with that in figure A.5a. When coupled to a transducer, the frequency spectrum revealed no twin-resonances in the 18 to 22 kHz range; there are: f_{1c} = 19.96 kHz and f_{2c} = 21.19 kHz. Measurements of the overall mode at f_{1c} = 19.96 kHz at 10 μm input amplitude, only small amplitudes at theside surface could be measured (maximum 12% of the input amplitude). At the output surface the difference in amplitude was smaller than 20%. The mode at f_4 = 20.30 kHz did not couple to the one at f_3 20.00 kHz.

As a conclusion, by changing the thickness from 110 to 103 mm, the coupling of a spurious mode to the "longitudinal" one was eliminated, whilst the resonance frequency of the latter hardly changed, and other modes did not move towards this one.

In general the length dimensions of the resonator after tuning will fairly well coincide with those predicted from he elementary theory (chapter 8). The coupling of spurious modes however, depends on the overall dimensions and the presence of profiles and such. For each application individually, it has to be analysed how close spurious modes are to the "longitudinal" mode and what distortion of this mode is the result.

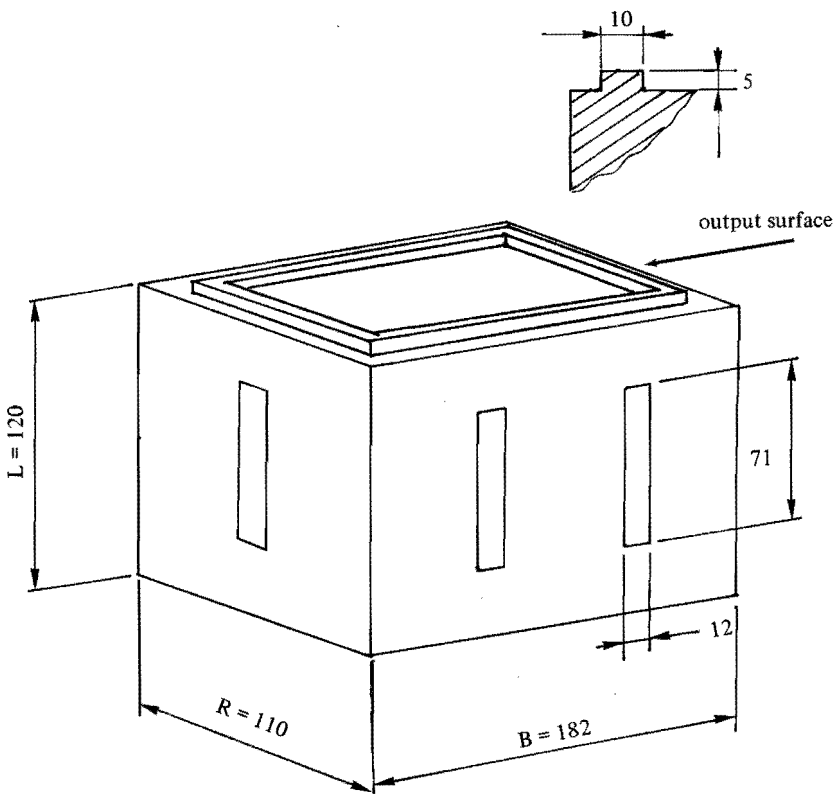

*Fig. A.1 A block-like resonator of 110 * 182 mm² output surface, with a profile, 5 mm high, 10 mm wide and 500 mm long. The slots are 12 mm wide and 71 mm high.*

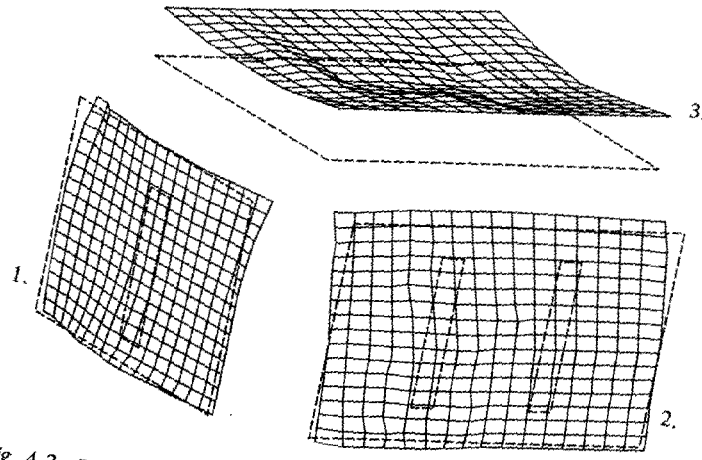

Fig. A.2 *The modes of vibration as measured on the surfaces (interpolation of the components of amplitudes perpendicular to the surfaces); actual maximum amplitude 10 μm.*

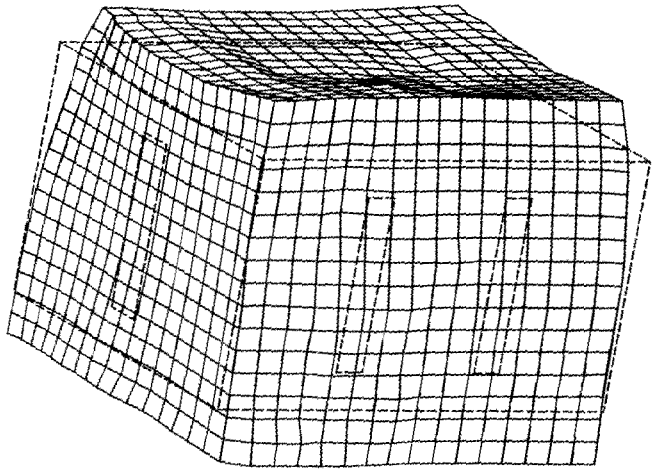

Fig. A.3 *Vibrational mode of the resonator at 19.86 kHz (composed of the modes shown in fig. A.2).*

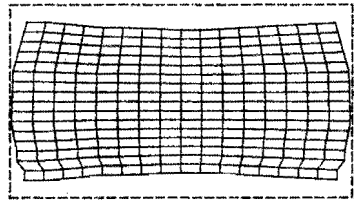

3.

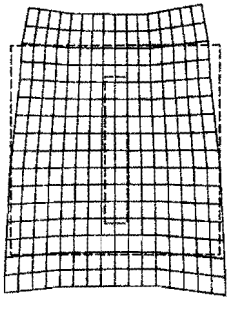

1.

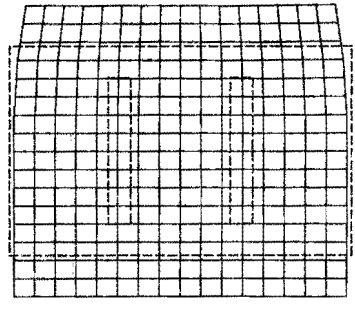

2.

Fig. A.4 Projections of the mode shape of the surfaces as determined from fig. A.3.

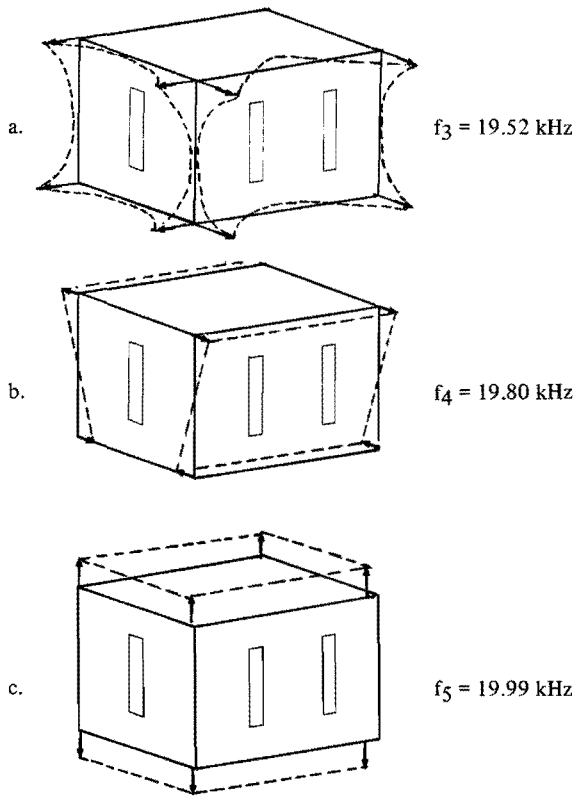

Fig. A.5 Modes of vibration for various resonance frequencies (schematically) obtained from a point by point analysis of the frequency spectrum of the resonator (the resonator overall dimensions are length L = 119 mm, width B = 182 mm, thickness R = 103 mm).

APPENDIX 2

Rayleigh's correction to the wave propagation velocity

The propagation of longitudinal waves in slender rods was explained in chapter 2. As long as the wavelength of the propagating wave is long as compared to the lateral dimensions of the rod, the finiteness of these dimensions are not taken into account. Lord Rayleigh presented a formula for the calculation of the wave propagation velocity which corrects for the effect of lateral motion. Due to Poisson's contraction the wave propagation is accompanied by lateral motion resulting into a decrease of this velocity. The derivation of the correction formula is presented here.

Rayleigh's energy method learns that the resonance frequency of a vibrating system can be approximated from the consideration that the total energy in the system remains constant. So the maximum kinetic energy and the maximum potential energy must be equal (in the case of the harmonic vibrations assumed for the vibrating rod):

$$\hat{U}_p = \hat{U}_k \tag{A2.1}$$

The kinetic energy stored in the vibrating rod as shown in figure (A2.I) (see also chapter 2) follows from the displacement function of the axial motion w(z).
The particle velocity in axial direction follows from w(z) by multiplification with the angular frequency ω.

The axial displacement equals (see equation 2.4):

$$w(z) = w_o \cos(kz) \tag{A2.2}$$

Where w_o is the maximum amplitude of motion. The maximum kinetic energy follows from integration over the rod:

$$\hat{U}_k = \int_0^l \int_0^{d/2} \frac{1}{2} \rho \, 2\pi r \, \omega^2 \, w^2(z) \, dr \, dz \tag{A2.3}$$

or:

$$\hat{U}_k = \frac{1}{16} \pi \rho \omega^2 \, d^2 \, l \, w_o^2 \tag{A2.4}$$

Identically it can be shown that the maximum potential energy equals:

$$\hat{U}_p = \frac{1}{16} \pi E k^2 \, d^2 \, l \, w_o^2 \tag{A2.5}$$

Equating (A2.4) and (A2.5) results into the well-known relation $k = \frac{\omega}{c}$.
We will now consider the contribution of radial motions to the kinetic and potential energy.
The radial stresses σ_r in the vibrating rod of radius $\frac{d}{2}$ and length l (figure A2.I) are neglectable compared to the axial stresses σ_z. From Hooke's law it follows that at distance z the radial strain $\epsilon_r(z)$ is related to the axial strain $\epsilon_z(z)$ by:

$$\epsilon_r(z) = -\nu \, \epsilon_z(z) \tag{A2.6}$$

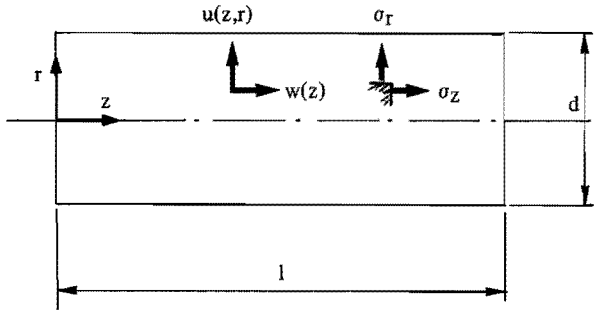

Fig. A2.1 Slender rod resonator of constant cross-section of diameter d and length l

The radial displacement u(z,r) at distance z and radius r can be approximated by:

$$u(z,r) = \epsilon_r(z) \cdot r \tag{A2.7}$$

So, in radial direction the motion does contribute to the kinetic energy of the vibrating rod. Because of the zero radial stress, there is no contribution to the potential energy. The displacement in radial direction can be calculated from (A2.2), (A2.6) and (A2.7).

$$u(z,r) = -\nu\, r\, k\, w_o \sin(kz) \tag{A2.8}$$

The contribution of the radial motion to the kinetic energy $d\hat{U}_k$ follows by integration over the rod:

$$d\hat{U}_k = \int_0^l \int_0^{d/2} \frac{1}{2} \rho\, 2\, \pi\, r\, \omega^2\, u^2(z,r)\, dr\, dz \tag{A2.9}$$

or

$$d\hat{U}_k = \frac{1}{128} \rho\, \pi\, \nu^2\, \omega^2\, k^2\, d^4\, l\, w_o^2 \tag{A2.10}$$

By equating the potential and kinetic energy ($\hat{U}_p = \hat{U}_k + d\hat{U}_k$), the angular frequency ω' can be calculated from (A2.4), (A2.5) and (A2.10):

$$\omega'^2 = \frac{E\, k^2}{\rho + \frac{1}{8} \rho\, \nu^2\, k^2\, d^2} \tag{A2.11}$$

Clearly the radial motion results into a decrease of the resonance frequency of the vibrating rod. For a given rod of length l, the relation between angular frequency ω, wave propagation velocity c and length l are (equations 2.3 and 2.5):

$$\omega = \frac{\pi c}{l} \tag{A2.12}$$

A decrease of the resonance frequency is physically identical to a decrease of the velocity c. The corrected velocity c' due to radial motion in the vibrating rod follows from (A2.11) and (A2.12) (using $k = \frac{\omega}{c}$ and $c = \sqrt{\frac{E}{\rho}}$):

$$\frac{c'}{c} = \frac{\omega'}{\omega} = \sqrt{\frac{1}{1 + \frac{1}{8}\nu^2\, k^2\, d^2}} \tag{A2.13}$$

This equation can be linearized by the fact that $\frac{1}{8}\nu^2\, k^2\, d^2$ is small for the half-wavelength resonator ($d \ll l$). So, (A2.13) can be re-written:

$$\frac{c'}{c} = 1 - \frac{1}{16}\nu^2\, k^2\, d^2 \tag{A2.14}$$

This equation gives the Rayleigh correction to the wave propagation velocity of longitudinal waves in rods.

APPENDIX 3

Wide output resonator according to Stepanenko (1979)

A very wide output resonator of the blade-like type as described by Stepanenko, is shown in the figure below. The resonators consist of a number of half-wavelength resonators of width b = ± 100 mm, and of length l = ± 120 mm. The resonators are coupled through bridging elements at both free ends, and in the midplane where the lateral motion is maximum. Each resonator is provided with a transducer, the locations of which are shown in the figure below. A total width of ± 800 mm was achieved.

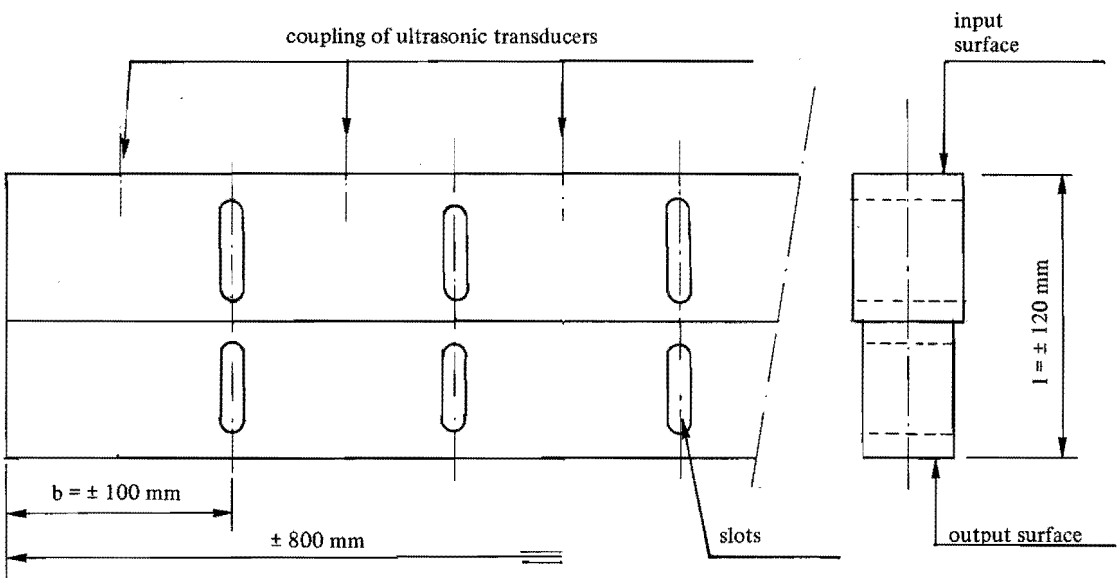

Fig. A3.1 Resonator for generating longitudinal vibrations, with a very wide output cross-section (typical dimension for f = 20 kHz); transducers are placed as shown over the entire input surface.

REFERENCES

1. Allik H., Webman K.M. (1974)
   Vibrational response of sonar transducers using piezoelectric finite elements.
   Journal Acoust. Soc. Am., Vol. 56, Dec. 1974, pp. 1782-1800.

2. Bancroft D. (1941)
   The velocity of longitudinal waves in cylindrical bars.
   Physical Review, Vol. 59, April 1941, pp. 588-593.

3. Balamuth L. (1966)
   Method and apparatus for joining sheet materials.
   U.S. Patent 3.254.402.

4. Becker K., Pungs L., Lamberts K. (1973)
   Uber die Vorgänge beim Ultraschall-Schweissen Thermoplastischer Kunststoffe.
   Kunststoffe 63 (1973), pp. 100-106.

5. Biro T. (1971)
   Ultrasonic vibration transmitting member
   US Patent 3.733.238.

6. Brinkmann R. (1971)
   Beanspruchung und Betriebsverhalten von Ultraschallkonzentratoren bei Belastung.
   Frequenz, 25 (1971) 5, pp. 128-137.

7. Coy J.J., Tse F.S. (1974)
   Synthesis of solid elastic horns.
   Journal of Engineering for Industry, May 1974, pp. 627-632.

8. Crawford A.E., (1969)
   High power ultrasonics in industry – A Review.
   Industrial Ultrasonics, Sept. 1969, pp. 1-8, Loughborough University of Technology.

9. Davis P. (1978)
   Ultrasonic horn.
   US Patent 4.131.505.

10. Daniels, H.P.C. (1965)
    Ultrasonic welding.
    Ultrasonics, October 1965, pp. 190-196.

11. Denys B. (1967)
    Etude de l'outillage pour la soudure ultrasonique des plastiques.
    Plastiques et Elastomères, April 1967, pp. 84-88.

12. Eisner E. (1963)
    Design of sonic amplitude transformers for high magnification.
    Journal of Acoust. Soc. of America, Vol. 35, No. 9, September 1963, pp. 1367-1377.

13. Elbert E. (1982)
Ultraschallschweissgerät.
German patent specification, "Patentschrift" DE 3032241.

14. Finer M. (1978)
Ultrasonc welding of plastics.
Engineering, June 1978, pp. 1-8.

15. Fitzgerald K.R. (1980)
The latest in ultrasonic plastics assembly equipment.
Design News 46 (1980), pp. 46-63.

16. Gladwell G.M. (1967)
The vibrations of mechanical resonators: rings, discs and rods of arbitrary profiles.
Journal of Sound and Vibrations, 1967, 6, pp. 351-364.

17. Gladwell G.M., Vyay D.K. (1975)
Vibration analysis of axysymmetric resonators.
Journal of Sound and Vibrations, 1975, 42 (2), pp. 137-145.

18. Graff K.F. (1977)
Ultrasonics; historical aspects.
Proceedings of 1977 Ultrasonics Symposium, Graz, pp. 1-10.

19. Grgach F. (1976)
Ultrasonic welding and cutting apparatus.
US Patent 3.939.033.

20. Holze E.P. (1982)
Resonator exhibiting uniform motional output.
US Patent 4.363.922.

21. Hulst A.P. (1972)
Macrosonics in industry. 2. Ultrasonic welding of metals.
Ultrasonics, November 1972, pp. 252-261.

22. Hulst A.P. (1973)
On a family of high power transducers.
Proceedings of Ultrasonics International 1973 Concference
pp. 285-294. IPC Guildford.

23. Hutchinson J. (1972)
Axisymmetric vibrations of a free finite length rod.
Journal Acoust. Soc. Am., Vol. 51, no. 1, pp. 233-240.

24. Hutchinson J. (1980)
Vibrations of solid cylinders.
Journal of Applied Mechanics, Vol. 47, 1980, pp. 901-907.

25. Hutchinson J., Zillmer S.D. (1983)
Vibrations of free rectangular parallelepipeds.
Journal of Applied Mechanics, Vol. 50, 1983, pp. 123-130.

26. Itoh K., Mori E. (1971)
Experimental study on directional convertors of ultrasonic vibration.
Seventh International Congress on Acoustics, Budapest 1971, pp. 644-651.

27. Jakubowski M. (1972)
Ultrasonic horn design: translating an art into sound design principles.
Electromechanical design, April 1972, pp. 30-36.

28. Kleesattel C. (1968)
Uniform stress contours for disk and ring resonators vibrating in axially symmetric radial and torsional modes.
Acustica, Vol. 20, 1968, pp. 2-13.

29. Kleesattel C. (1970)
Eine einfache Methode zum Entwurf von Schall-leitern und Resonatoren mit vorgewählten Eigenschaften.
Acustica, Vol. 23, 1970, pp. 63-72.

30. Kleesattel C. (1963)
Ultrasonic vibration generator.
US Patent 3.113.225.

31. Kröbl K. (1980)
Besser Fügen mit Ultraschall
Technische Rundschau, Bern, 42 (1980), p. 42.

32 Kynch G.J. (1957)
The fundamental modes of vibration of uniform beams for medium wavelengths.
British Journal of Applied Physics, Vol. 8, 1957, pp. 64-73.

33. Leissa A., Zhang Z. (1983)
On the three-dimensional vibrations of the cantilevered rectangular parallelepiped.
Journal. Acoust. Soc. Am. 73 (6), June 1983, pp. 2013-2021.

34. Long D. (1973)
Apparatus for vibration welding of sheet materials.
US Patent 3.733.238.

35. Makarov L.O. (1964)
Method of design of rod-type exponential ultrasonic concentrators.
Soviet Progress in Applied Ultrasonics, 1964, Vol. 1, pp. 160-171.

36. Maropis N. (1969)
The design of high power ceramic transducer assemblies.
IEEE Trans. on Sonics and Ultrasonics, Vol. 16, No. 3, July 1969, pp. 132-136.

37. McMahon G.W. (1964)
Experimental study of the vibrations of solid, isotropic, elastic cylinders.
Journal Acoust. Soc. of Am., Vol. 36, No. 1, 1964, pp. 85-92.

38. McNiven, Perry D. (1962)
Axially Symmetric Waves in finite, elastic rods.
Journal Acoust. Soc. of Am., Vol. 34, No. 4, 1962, 00. 433-437.

39. Merkulov L.G. (1957)
Design of ultrasonic concentrators.
Soviet Physics – Acoustics, 3, 1957, pp. 246-255.

40. Mori E., Ithoh K., Imanuza A. (1977)
Analysis of a short column vibrator by apparent elasticity method and its application.
Ultrasonics International, 1977, conf. papers, pp. 262-266.

41. Morse R.W. (1950)
The velocity of compressional waves in rods of rectangular cross-section.
Journal Acoust. Soc. of Am., Vol 22, No. 2, 1950, pp. 219-223.

42. Neppiras E.A. (1960)
Very high energy ultrasonics
British Journal of Applied Physics, Vol. 11, 1960, pp. 143-150.

43. Neppiras E.A. (1973)
The pre-stressed piezoelectric sandwich transducer.
Ultrasonics International 1973 Conference Proceedings, pp. 295-302.

44. Neppiras E.A. (1977)
A simple efficicient mechanical transformer for high intensity ultrasonic applications.
Ultrasonics International 1977 Conference Proceedings, pp. 96-102.

45. Potente H. (1971)
Untersuchung der Schweissbarkeit thermoplastischen Kunststoffe mit Ultraschall.
Dissertation, Aachen, 1971.

46. Rayleigh, Lord (1926)
Theory of Sound, MacMillan & Co., London (1926), Vol 1, pp 252 et seq.

47. Redwood M. (1960)
Mechanical Waveguides, Pergamon Press.

48. Rasband S. (1975)
Resonant vibrations of free cylinders and discs.
Journal Acoust. Soc. of Am., Vol. 57, No. 4, 1975, pp. 899-905.

49. Rumerman M. (1971)
Natural frequencies of finite circular cylinders in axially symmetric longitudinal vibration.
Journal of Sound and Vibration, (1971), 15 (4) pp. 529-543.

50. Scheibener H. (1971)
Auslegung von Hochleistungsrüsseln für die Ultraschall bearbeitung.
Dissertation T.U. Hannover, 1971.

51. Scotto J.P. (1977)
Vorrichtung zur Erzeugung von Ultraschallwellen.
German Patent Application, "Offenlegungschrift" 27 11 305.

52. Scotto J.P. (1974)
Perfectionnement aux appareils pour la production d'ultrasons
French Patent Specification "Brevet d'Invention", No. 2.203.295.

53. Scotto J.P. (1974)
Ultraschallerzeuger, insbesondere für Ultraschallschweissgeräte.
German Patent Application "Offenlegungsschrift", 2 355 333.

54. Shoh A. (1975)
Industrial Applications of ultrasound – A review I. High power ultrasound.
IEEE Transactions on Sonics and Ultrasonics, Vol. 22. No. 2, March 1975, pp. 60-71.

55. Skimin H. (1964)
Ultrasonic Method of measuring the mechanical properties of liquids and solids.
Physical Acoustics, chapter 4, Academic Press New York.

56. Stafford R.D. (1979)
High power ultrasonic equipment for assembling rigid thermoplastic components.
Industrial Ultrasonics, Sept. 1973, pp. 9-26.

57. Stepanenko A.V. (1979)
Theory and calculation of an ultrasonic waveguide with a wide output cross-section.
Russian Ultrasonics, Jan. 1979, pp. 178-182.

58. Thews H. (1975)
Leistungsbestimmung beim Ultraschall-Schweissen und Nieten von Kunststoffen.
Maschinenmarkt, Heft 45, June 1975.

59. Thews H. (1978)
Fügen von Formteilen aus thermoplastischen Kunststoffen.
Verbindungstechnik, Heft 2, Febr. 1978.

60. Tuschak P.A., Allaime R.A. (1975)
Axisymmetric vibrations of a cylindrical resonator measured by Holographic Interferometry.
Experimental Mechanics, 1975, pp. 81-88.

61. Vetter T. (1966-1968)
Das Werkstattgerechte Bemessen von Bohrrüsseln zum Ultraschall bearbeiten
VDI-Zeitschrift 108 (1966), no. 11, pp. 459-462
108 (1966), no. 12, pp. 512-515
110 (1968), no. 9 , pp. 349-351

62. Young M., Winsper C., Sansome D. (1970)
Radial mode vibrators for oscillatory metal forming.
Applied Acoustics, Vol. 3, 1970, pp. 299-308.

63. Young M., Winsper C., Sansome D. (1970)
The effect of tool attachment on the resonant characteristics of ultrasonic waveguides.
Applied Acoustics, Vol. 3, 1970, pp. 217-224.

Additional information

64. Applications des Ultrasons aux thermoplastiques
Private communication Mécasonic France, 1979.

65. Holografische Untersuchung von Sonotroden
Private Communication Walter Herrmann, 1982.

66. ASKA, User's Reference Manual, Stuttgart, 1971.

67. Fotonic Sensor, Mechanical Technology Incorporation New York.

68. Hulst A.P. private communication, 1975.

CURRICULUM VITAE

Naam	:	Piet Derks
Geboren	:	18 januari 1955 te St. Setiers (Frankrijk)
Opleidingen	:	Gymnasium β te Venray 1967-1973 Technische Hogeschool te Eindhoven 1973-1978 opleiding tot werktuigbouwkundig ingenieur.
Stages	:	Brown-Boveri te Baden (Zwitserland), juli-augustus 1976 D.S.M. te Geleen, september 1977 - mei 1978
Werkzaamheden	:	Sinds augustus 1978 werkzaam bij de Nederlandse Philips Bedrijven B.V. te Eindhoven als projectleider Ultrasone Technieken bij het Centrum voor Fabricage Technieken.

Met dank aan de directie van het Centrum voor Fabricage Technieken (C.F.T.) van de Nederlandse Philips Bedrijven B.V. te Eindhoven, voor de toestemming tot het publiceren van de onderzoekresultaten die beschreven worden in dit proefschrift.

STELLINGEN

behorende bij het proefschrift

The design of ultrasonic resonators with wide output cross-sections

Eindhoven, 16 november 1984

P.L.L.M. Derks

1. De laszijde van een ultrasoon lasgereedschap moet (ten behoeve van een optimale werking) over het gehele gebruikte oppervlak een amplitude hebben die nagenoeg constant van grootte is en in fase. De aanduiding "longitudinale" trillingsvorm voor de hierbij behorende toestand is uiterst misleidend, wanneer dit gereedschap grote dwarsafmetingen heeft. Veel logischer is de aanduiding "trillingsvorm met een uniforme uitgangsamplitude".

Dit proefschrift, hoofdstuk 9

2. De door Stepanenko voorgestelde methode om sleuven aan te brengen in een ultrasoon lasgereedschap met grote dwarsafmetingen is principieel ongeschikt om een uitgangsamplitude te verkrijgen die constant van grootte is over het gehele oppervlak.

Stepanenko, A.V.: Russian Ultrasoncis, 1979, pp. 178-182

3. Bij het ultrasoon metaallassen maakt men vaak gebruik van een lasgereedschap dat in een buigtrillingsvorm wordt aangestoten. In tegenstelling tot hetgeen noodzakelijk is bij het ultrasoon kunststoflassen, dient bij deze vorm van metaallassen het lasgereedschap bij voorkeur *niet* in één van de resonantie-frequenties te worden aangestoten.

Derks, P.: Tool design for ultrasonic metal welding, Seminar Welding Inst., Coventry, 1982

4. De conclusie van Potente, dat zeer dunne kunststoffolies ($< 100\ \mu m$) alleen goed ultrasoon lasbaar zijn, indien tussen de folie en het ondersteunend gereedschap (lasmal) een dempende laag aangebracht wordt, is in zijn algemeenheid onjuist.

Potente, H.: Untersuchung der Schweissbarkeit thermoplastischer Kunststoffe mit Ultraschall, Dissertatie, Aachen, 1971

5. De overeenkomst tussen het tunen van een ultrasoon lasgereedschap en het tunen van een klok houdt niet in dat het resultaat even mooi klinkt.

Perrin, T. and Charnley, T.: Normal modes of the modern English church bell, Journal of Sound and Vibration, 90 (1983) 1, pp. 29-40.

Calon, G.: Afstudeerverslag, HTS Eindhoven, 1984

6. Dit proefschrift heeft ertoe bijgedragen dat ultrasone lasgereedschappen op een efficientere wijze kunnen worden ontworpen, dan volgens deze variant op Wyskowski's tweede wet: "Any resonator can be made to work, if you fiddle with it long enough".

Arthur Bloch: Murphy's law and other reasons why things go wrong (1983)

7. Bij het reinigen van produkten op industriële schaal is de keuze voor een ultrasoon reinigingssysteem geen excuus voor een gebrek aan kennis van het reinigingsprobleem zelf.

8. Uit historisch oogpunt is het onjuist water-, wind- en zonne-energie aan te duiden als alternatieve energiebronnen.

9. Een weggebruiker is zinvoller geïnformeerd over de ellende bij een verkeersknooppunt door een schatting van de tijd die extra nodig is om dat punt te passeren dan door de lengte van de file.

Dagelijkse verkeersinformatie